CONFIDENTIAL

Copy 5
RM L52J21

NACA

RESEARCH MEMORANDUM

STATIC AEROELASTIC PHENOMENA OF M-, W-, AND Λ-WINGS

By Franklin W. Diederich and Kenneth A. Foss

Langley Aeronautical Laboratory
Langley Field, Va.

CLASSIFIED DOCUMENT

NATIONAL ADVISORY COMMITTEE
FOR AERONAUTICS

WASHINGTON
February 9, 1953

CONFIDENTIAL

CONTENTS

NATIONAL ADVISORY COMMITTEE FOR AERONAUTICS

RESEARCH MEMORANDUM

STATIC AEROELASTIC PHENOMENA OF M-, W-, AND Λ-WINGS

By Franklin W. Diederich and Kenneth A. Foss

SUMMARY

Spanwise lift distributions, lift coefficients, spanwise centers of pressure, shifts in aerodynamic center, coefficients of damping in roll, aileron rolling-moment coefficients, and rates of steady roll per unit aileron deflection have been calculated for nine M-, W-, and Λ-wings, as well as for comparable ordinary sweptforward, unswept, and sweptback wings. Although the calculations are too specific to permit any quantitative conclusions which are generally applicable, certain qualitative conclusions are drawn concerning the plan forms most suitable from the aeroelastic point of view. In general, there is reason to believe that certain M and W plan forms exist which are superior aeroelastically and structurally to ordinary swept wings.

INTRODUCTION

The use of M- and W-wings has been suggested as a means of alleviating the static aeroelastic problems of swept wings, such as the shift of aerodynamic center and the loss of lateral control. The obvious, but not necessarily most economical, remedy for these static aeroelastic difficulties consists in stiffening these wings. The advantage of an M- or W-wing over an ordinary swept wing is that, inasmuch as in the M- or W-wing the over-all effects of bending and torsion deformations tend to oppose each other, a more flexible structure may be acceptable. The concept of alleviating static aeroelastic difficulties by such a balancing process is not new. In reference 1, for instance, means are discussed for achieving this balance organically with a swept wing, and in reference 2 an artificial balancing device (an auxiliary lifting surface mounted on a boom of the tip of a sweptback wing) is analyzed.

In the appendix of the present paper a method based on those of references 3 and 4 is presented for analyzing the static aeroelastic phenomena of M-, W-, and Λ-wings, such as change in aerodynamic loading, lift-curve slope, and aerodynamic-center shift due to aeroelastic effects,

divergence, loss of lateral control, and change in damping in roll due to aeroelastic effects, as well as aileron reversal.

This method has been used to calculate the foregoing aeroelastic phenomena for three M-, three W-, and three Λ-wings (including one inverted Λ-wing). The results of these calculations are discussed with particular regard to the problem of selecting optimum plan forms for the minimization of the adverse effects of static aeroelastic phenomena. Similar calculations have also been made for a sweptback, a sweptforward, and an unswept wing to afford a basis of comparison of the static aeroelastic phenomena of the M-, W-, and Λ-wings with those of the more conventional wings. The calculated aeroelastic phenomena of the M-, W-, and Λ-wings are discussed in the light of these comparisons.

SYMBOLS

A	aspect ratio, b^2/S
a	distance of section aerodynamic center from leading edge, fraction of chord
$\bar{a}$	position of wing aerodynamic center measured from leading edge of mean aerodynamic chord $\left(\frac{1}{4} - \frac{C_m}{C_L}\right)$
$\Delta\bar{a}$	wing aerodynamic-center shift $(\bar{a} - \bar{a}_0)$
b	wing span
b_a	span of both ailerons
b'	span of exposed wing $(b - w)$
C_B	bending moment (semispan rolling-moment) coefficient, $4M_{\mathcal{L}}/qSb$
C_L	lift coefficient, L/qS
C_{L_α}	lift curve slope
C_{l_d}	rolling-moment coefficient for a linear antisymmetrical angle-of-attack distribution with a tip angle of one radian, $-C_{l_p}$

[redacted]

C_{l_p}	damping-in-roll coefficient
C_{l_δ}	rolling-moment coefficient due to a unit aileron deflection
C_m	pitching-moment coefficient, $M_p/qS\bar{\bar{c}}$
c	chord of wing (measured parallel to air stream)
c_a	chord of aileron
c_l	section lift coefficient, l/qc
$c_{\mathbb{C}}$	chord at airplane center line
$\bar{c}$	average chord, S/b
$\bar{\bar{c}}$	mean aerodynamic chord, $\dfrac{\int_0^{b/2} c^2 dy}{\int_0^{b/2} c\, dy}$
d	span of part of wing, fraction of $b/2$
EI	bending stiffness in planes perpendicular to elastic axis
e	distance of elastic axis from leading edge, fraction of chord
e_1	dimensionless moment arm $(e - a)$
e_2	distance of center of pressure due to aileron deflection behind elastic axis, fraction of chord
GJ	torsional stiffness in planes perpendicular to elastic axis
L	lift on total wing span
l	lift per unit distance along span
M	accumulated bending moment about axes parallel to air stream

[redacted]

M_Λ accumulated bending moment about axes perpendicular to elastic axis

$M_{\mathcal{L}}$ accumulated single-wing rolling moment about fuselage center line

M_p total wing pitching moment about quarter-chord point of mean aerodynamic chord, positive nose up

$\frac{pb}{2V}$ wing-tip helix angle due to roll

Q_{φ_T}, Q_{φ_M}, Q_{Γ_T}, Q_{Γ_M} root-rotation constants defined in equations (33), (34), and (36), respectively

q dynamic pressure

$\tilde{q}$ dimensionless dynamic-pressure parameter, $\frac{qC_{L_{\alpha_0}}c_r\left(\frac{b}{2}\right)^3}{(GJ)_r}$

S wing area

T accumulated torque about axes perpendicular to plane of symmetry

T_Λ accumulated torque about elastic axis

t running torque in planes parallel to air stream (le_1c)

w width of fuselage at wing root

w_e distance defined in figure 1

x streamwise distance of a section aerodynamic center aft of an unswept reference line through the quarter-chord point of the mean aerodynamic chord

y lateral ordinate (see fig. 1)

y^* dimensionless lateral ordinate, $\frac{y}{b/2}$

$\bar{y}^*$ dimensionless position of lateral center of pressure

[redacted]

α	angle of attack measured in planes parallel to air stream
α_δ	angle of attack equivalent to unit aileron deflection, $\frac{dc_l/d\delta}{dc_l/d\alpha}$
Γ	local dihedral angle (in a plane through elastic axis) due to wing deformation along elastic axis
δ	aileron deflection measured in planes parallel to air stream
Λ	angle of sweepback at elastic axis
λ	taper ratio, $c_t/c_{\text{℄}}$
φ	angle of twist in planes perpendicular to elastic axis

Subscripts:

B	at point of wing break (point of spanwise discontinuity of angle of sweep)
℄	at center line of airplane
D	at divergence
f	that portion of wing covered by fuselage
g	geometric (built in or due to airplane attitude)
i	inner part of wing, not including that part covered by fuselage
o	outer part of wing, from wing break to wing tip
R	at aileron reversal
r	wing root (located at intersection of elastic axis and fuselage side)
s	structural (due to structural deformation)
w	wing alone (not including that portion covered by fuselage)
0	pertaining to rigid wing ($\tilde{q} = 0$)

[redacted]

Matrix Notation:

Note: Specific matrices are defined where they first occur.

$\| \|$ rectangular matrix

$[]$ square matrix

$\lfloor \rceil$ diagonal matrix

$\{\}$ column matrix

$\lfloor \rfloor$ row matrix

DESCRIPTION OF THE CALCULATIONS

Method of the Calculations

The method used to perform the calculations of static aeroelastic phenomena of M-, W-, and Λ-wings is presented in the appendix to this paper; it is based on the method of references 3 and 4 and consists, like those methods, in integrating by means of numerical and matrix techniques the differential equations which describe the static aeroelastic phenomena.

Assumptions

The spanwise lift distribution is assumed to be given by suitable aerodynamic influence coefficients and the local centers of pressure of the lift due to angle of attack and due to aileron deflection are assumed to be invariant with angle of attack and aileron deflection. Both of these assumptions imply small angles of attack and aileron deflection.

A straight elastic axis is assumed to exist in both parts of the wing, and the wing is assumed to be mounted flexibly at an effective root perpendicular to the elastic axis through the intersection of the elastic axis and the fuselage (see fig. 1) so that the root triangle imparts rigid-body rotations to the wing, the rotations being proportional to the root bending moment and the root torque. On the other hand, the outer part of the wing is assumed to be attached rigidly to

[redacted]

the inner part, so that, if the inner part were rigid, no rigid-body rotations would be imparted to the outer part of the wing. All deformations beyond those due to the rigid-body rotations imparted by the root triangle are then assumed to be given by the elementary theories of bending and of torsion along the elastic axis.

The angle between the aileron and the wing is assumed to be constant along the span of the aileron. This assumption implies that the aileron and wing twist the same amount.

Scope of the Calculations

The M-, W-, and Λ-wing plan forms for which calculations have been made are listed in table 1 as wings 1 to 9. Wings 1 to 3 are M-wings; wings 4 to 6 are W-wings; wings 7 and 8 are Λ-wings and wing 9 is an inverted Λ-wing. For the sake of comparison, calculations have been made also for three conventional plan forms - a sweptforward wing, an unswept wing, and a sweptback wing - listed in table 1 as wings 10, 11, and 12, respectively. All wings have a taper ratio of 0.5; all have angles of sweep of either zero or $\pm 45^\circ$, and all have an aspect ratio of 6. Three values of the spanwise position of discontinuity in sweep, hereinafter referred to as the "break," are included in this series of plan forms, namely, $y^* = 0.3$, 0.5, and 0.7. All wings were considered to be mounted on a fuselage of width equal to 0.1 of the span.

For all plan forms, symmetrical lift distributions were calculated for one subsonic and one supersonic flow condition at values of the aeroelastic parameter $\tilde{q}$ equal to 3.0, and for most plan forms for $\tilde{q} = 6.0$ as well. Lift distributions were calculated for unit geometric angle of attack across the span, for linear antisymmetric geometric angle of attack with unit angle at the tip; and for unit effective angle of attack due to the deflection of an outboard aileron. These lift distributions were integrated to obtain total lifts, rolling moments, and positions of the wing center of pressure.

For subsonic speeds the lateral-control parameters were calculated for 20-percent-chord, 50-percent-span outboard ailerons, with some additional calculations for all-movable wing tips extending over the outer 30 percent of the semispan (which may be considered to be 100 percent-chord ailerons). For supersonic speeds lateral-control calculations were made for 20-percent-chord, 30-percent-span outboard ailerons, with some additional calculations for 50-percent-span ailerons. (See table 2.)

Basic Data

The spanwise stiffness distributions used in this paper are given in figure 2. These stiffnesses are based on the constant-stress analysis in reference 1 (with modifications occasioned by the wing break), except

[redacted]

that the stiffnesses were taken proportional to the fourth power of the chord from $y = 0.7$ to 1.0 so that there would be finite stiffness at the wing tip. Other structural parameters (including the root-rotation constant) are given in table 1; the values of the stiffness ratio given $\left(\frac{(GJ)_r}{(EI)_r} = 0.794\right)$ and of the elastic-axis location ($e = 0.45$) are typical of wings of conventional thin-skin construction, having a thickness ratio of about 10 to 12 percent.

For subsonic speeds aerodynamic influence coefficients were calculated by the method of reference 5; the manner in which this method was modified to apply to M-, W-, and Λ-wings is discussed in the appendix. The rigid-wing subsonic lift distributions used to compute the aerodynamic influence coefficients were taken from reference 6, in which they were calculated for incompressible flow by simplified lifting-surface theory.

For supersonic speeds strip theory was used because no suitable means (such as aerodynamic influence coefficients) were available for calculating lift distributions for angle-of-attack distributions which are not initially known, although lift distributions can be calculated for any given angle-of-attack distribution by linearized supersonic theory. (See, for instance, the methods of refs. 7 and 8.) The development of such coefficients solely for the purpose at hand was not considered justified principally because M-, W-, and Λ-wings are intended primarily for flight at subsonic and transonic speeds. Also, the results of the calculations of the present paper can be interpreted as flexibility corrections to the aerodynamic characteristics of the rigid wings; if the corrections are relatively small the corrected results will be relatively insensitive to the assumptions made in calculating the corrections. The resulting flexible-wing characteristics are then, of course, no better than rigid-wing characteristics to which the corrections are applied. Inasmuch as in the present paper the aeroelastic increments are of primary interest, the rigid-wing characteristics were estimated by strip theory for the sake of simplicity.

The subsonic local aerodynamic-center positions were also taken from reference 6; and the corresponding dimensionless section moment arms, $e_1 = \bar{e} - a$, are plotted in figure 3. For convenience, the local aerodynamic centers for supersonic flow were assumed to lie along the 45-percent-chord line, so that they coincide with the elastic axis; thus e_1 is 0 along the entire span.

For subsonic speeds the values of the dimensionless section moment arm due to aileron deflection, e_2, were calculated from the two-dimensional values by assuming that the difference between the two and three-dimensional lifts acts at the section aerodynamic center as

[redacted]

described in references 4 and 9. The values of e_2 obtained in this manner are plotted in figure 3. For the wings with rotating tip panels the values of e_2 were assumed to be equal to $(-e_1)$. For supersonic speeds the center of pressure due to aileron deflection was assumed to be at 90 percent of the chord; consequently, a value of $e_2 = 0.45$ was used for all wings.

The quarter-chord point of the mean aerodynamic chord is used as a reference for pitching moments. Unlike the case of an ordinary wing the longitudinal location of the mean aerodynamic chord does not coincide with that of the chord at the station which corresponds to the centroid of area of the wing. An expression for the distance of the quarter-chord point of the mean aerodynamic chord rearward of the intersection of the quarter-chord line and the plane of symmetry is given in equation (10) of reference 6; however, attention is called to the fact that in reference 6 the angle of sweepback refers to the quarter-chord line rather than the elastic axis.

Results of the Calculations

Spanwise lift distributions.- The spanwise lift distributions for the nine M-, W-, Λ-, and three ordinary wings are presented in figures 4 to 15 for two or three dynamic pressures including 0 (the rigid-wing case) and for subsonic as well as for supersonic speeds. The top parts of the figures show the lift distributions due to a unit airplane or root angle of attack represented by the coefficient $\frac{cc_l}{\bar{c}C_{L_{\alpha_0}}}$, the lift coefficient $C_{L_{\alpha_0}}$ being that of the given wing for $\tilde{q} = 0$. The bottom parts of the figures show the lift distributions due to unit effective aileron deflection ($\alpha_\delta \delta$) represented by the coefficients $\frac{cc_l}{\bar{c}C_{l_{d_0}}}$, that is, the loading coefficients $\frac{cc_l}{\bar{c}}$ divided by the damping coefficient of the rigid wing. The coefficient $\frac{cc_l}{\bar{c}C_{l_{d_0}}}$ can also be construed as the product of the coefficients $\left(\frac{cc_l}{\bar{c}C_{l_0}}\right)$ and $\left(\frac{\frac{pb}{2V}}{\alpha_\delta \delta}\right)_0$; the first of these coefficients represents the loading coefficient per unit rolling moment of the rigid wing and is analogous to the coefficient $\left(\frac{cc_l}{\bar{c}C_{L_{\alpha_0}}}\right)$ used for

[redacted]

the lift distribution due to angle of attack, whereas the second coefficient is the wing-tip helix angle per unit effective aileron deflection of the rigid wing.

The calculations made in reference 6 which form the basis for the aerodynamic information used for the subsonic calculations in the present paper pertain to a Mach number of 0, and hence, so do the calculated results. However, the lift distributions may be expected to be substantially unchanged (for small angles of attack) throughout the subsonic region and, except locally near the fuselage and the wing break and except for the unswept and Λ-wings through the transonic region as well. The lift distributions for supersonic speeds were estimated by strip theory and are, therefore, independent of Mach number.

If the rigid-wing lift distributions are independent of Mach number so are the flexible-wing lift distributions. However, inasmuch as the rigid-wing lift-curve slope $C_{L_{\alpha_0}}$ enters into the definition of $\tilde{q}$ the lift distributions for a given value of q correspond to different values of $\tilde{q}$ if $C_{L_{\alpha_0}}$ changes with Mach number.

Aerodynamic parameters associated with the spanwise lift distribution.- The quantities C_L/C_{L_0}, $\bar{y}^*$, $\bar{a}$, $C_{l_\delta}/C_{l_{\delta_0}}$, $C_{l_p}/C_{l_{p_0}}$, and $pb/2V$ are presented in table 2 and the quantities C_L/C_{L_0}, $\bar{a}$, $C_{l_\delta}/C_{l_{\delta_0}}$, and $pb/2V$ are also plotted in figures 16 to 22 against the dimensionless dynamic pressure $\tilde{q}$ for several of the M-, W-, and Λ-wings as well as for the unswept and sweptback wings. The values of C_L/C_{L_0} and $\bar{a}$ given in table 2 were extrapolated to the large values of $\tilde{q}$ represented in figures 16 to 22 by the use of the approximate formulas in reference 1. The values of the coefficients C_L, C_{l_p}, and C_{l_δ} for dynamic pressures other than 0 can be determined from the ratios C_L/C_{L_0}, $C_{l_p}/C_{l_{p_0}}$, and $C_{l_\delta}/C_{l_{\delta_0}}$, since the rigid-wing values C_{L_0}, $C_{l_{p_0}}$, and $C_{l_{\delta_0}}$ are presumably known. The values of $C_{L_{\alpha_0}}$ and $C_{l_{d_0}}$ are given in table 1; C_{L_0} can be obtained from $C_{L_{\alpha_0}}$ for any value of the airplane angle of attack, and $C_{l_{\delta_0}}$ is equal to the product of $(pb/2V)_0$ and $C_{l_{d_0}}$. (The values of $(pb/2V)_0$ are the values of $pb/2V$ given in table 2 for $\tilde{q} = 0$.)

[redacted]

The rigid-wing values of C_{L_α} and C_{l_d} given in table 1 for subsonic speeds are those calculated in reference 6 for $M = 0$; in principle they can be corrected for subsonic compressibility effects by the three-dimensional Prandtl-Glauert rule, but calculations must be available for M-, W-, and Λ-wings with many different sweep angles and aspect ratios before this correction can be effected. The correction for $C_{l_{p_0}}$ can be used for $C_{l_{\delta_0}}$ as well; within this approximation $\left(\frac{pb}{2V}\right)_0$ is then unaffected by compressibility at subsonic speeds.

The rigid-wing values of C_{L_α} and C_{l_d} given in table 1 for supersonic speeds are estimated on the basis of the Ackeret theory for $M = 2$ and are intended for qualitative comparisons only. For quantitative purposes they can be calculated by linearized supersonic theory not only for $M = 2$ but for any supersonic Mach number which is not too large nor too close to 1. For ordinary wings the results of such calculations are presented in references 10, 11, 12, and 13, for instance.

In considering figures 16 through 22 the fact should be kept in mind that the abscissa is subject to compressibility effects to the extent that, as previously mentioned, for a given value of q a change in $C_{L_{\alpha_0}}$ implies a change in $\tilde{q}$. Apart from this effect the results presented in these figues are independent of compressibility effects provided the lift distributions (within a given speed region) are substantially unaffected by Mach number.

The dynamic pressures at divergence and at reversal.- The values of the dimensionless dynamic pressure $\tilde{q}$ at divergence and at aileron reversal are given in table 2. From these values the corresponding values of q can be calculated from the definition of $\tilde{q}$. In cases for which the lowest (in absolute magnitude) dynamic pressures required to diverge the wing were found to be negative, the next higher critical dynamic pressures were calculated by using the method outlined in this paper; these values are also presented in table 2. For the wings with rotating tips the lowest (in absolute magnitude) dynamic pressures required to reverse lateral control were found to be complex.

DISCUSSION

Comparison of the Aeroelastic Properties of the Various Wings

Spanwise lift distributions.- The rigid-wing lift distribution of the unswept wing is approximately elliptical at subsonic speeds, and the

effects of sweepforward and sweepback on the spanwise lift distribution are to shift the load inboard and outboard, respectively. As pointed out in reference 6, the rigid-wing lift distributions calculated therein for these compounded plan forms at subsonic speeds are similar to those that could have been estimated qualitatively from the knowledge of the characteristics of the lift distributions of the ordinary swept wings of which the compounded plan forms may be considered to be composed. In the case of the M-wing represented in figure 4, for instance, the inner part of the wing behaves aerodynamically like a sweptforward wing with the characteristic peak in the lift distribution near the plane of symmetry, (see fig. 13), whereas the outer part behaves like a sweptback wing with the characteristic loading up of the wing tip (see fig. 15).

As previously mentioned, for supersonic speeds strip theory was used to estimate the rigid-wing lift distributions as well as the aeroelastic increments to these distributions. The rigid-wing lift distributions are therefore identical for all wings.

At subsonic speeds the effect of aeroelasticity on the unswept wing is to increase the lift, particularly near the tip, in the symmetric case, and to decrease the lift in the aileron-deflected case. (See fig. 14.) At supersonic speeds aeroelasticity has no effect on the symmetric lift distribution because the center of pressure was assumed to be in a position which coincides with the elastic axis. The decrease in lift in the antisymmetric case is quite pronounced, however, due to the fact that the moment arms e_2 (or, more to the point, the sums of the moment arms $e_2 + e_1$) are relatively large.

The symmetric lift distributions on the sweptforward wing (fig. 13) at subsonic speeds exhibit an even larger increase in lift due to aeroelastic effects than do those of the unswept wing. At supersonic speeds there is also a large increase in lift on the sweptforward as compared to the unswept wing; this increase is due entirely to the bending of the wing, inasmuch as the moment arm e_1 is zero as for the unswept wing. The lift due to aileron deflection is increased as a result of aeroelasticity because in the case of the sweptforward wing the bending effects which tend to increase the lift due to aileron deflection predominate over the torsion effects which, as in the case of the unswept wing, tend to decrease this lift.

On the sweptback wing (fig. 15) the effect of the bending deformations also predominates over the torsion deformations but causes a decrease in lift in the symmetric case and augments the effect of the torsional deformations in the aileron-deflected case as $\tilde{q}$ increases to produce a large loss of lift.

The effects of aeroelastic action on the lift distribution of the compounded plan forms are qualitatively as may be expected from a

knowledge of the aeroelastic effects on the lift distributions on the constituent parts of the wing. In the case of the M-wing 1 (fig. 4), for instance, the large sweptback outer part of the wing results in aeroelastic effects which are similar to those of a sweptback wing in that they decrease the lift both in the symmetrical case and in the aileron-deflected case, both at subsonic and supersonic speeds. The aeroelastic effects on the lift distribution on the sweptforward inner part of the wing are in the opposite direction but not large enough to result in an increase in lift but merely to decrease the loss in lift caused on the inner part of the wing by the aeroelastic action of the outer part of the wing.

The aeroelastic effects on the lift distribution of wing 2 (see fig. 5) are similar to those on the lift distribution of wing 1, but due to the large relative size of the sweptforward inner part of the wing an increase in lift is actually noted in the symmetric case on the inner part of the wing. As a result of this increase there is a tendency for the aeroelastic effects on the symmetric lift distribution to cancel. If the inner part of the wing were slightly larger still, the lift and center of pressure would probably be substantially unaffected by aeroelastic action. The loss in lateral control due to aeroelastic action is less than that of wing 1, but still quite large.

In the case of wing 3 (fig. 6) the position of constant lift and center of pressure has been passed; the aeroelastic characteristics of the large sweptforward inner part of the wing dominate the aeroelastic behavior of the wing in the symmetric case, although in the supersonic case the opposite aeroelastic characteristics of the sweptback outer part are sufficiently large to cancel the increase in lift resulting from the aeroelastic behavior imparted to the whole wing by its inner part, at least near the tip. In the aileron-deflected case the aeroelastic behavior of the inner part dominates that of the outer part and results in an increase in lift at subsonic speeds. At supersonic speeds, however, the outer part of the wing dominates the inner part to the extent that the loss in lift is only slightly smaller than that noted for wings 1 and 2.

The W-wings 4 and 5 (see figs. 7 and 8) have large sweptforward outward parts which completely dictate the aeroelastic behavior of the entire wings; the sweptback inner parts are capable only of reducing slightly and locally the increase in lift imposed everywhere on the wing as a result of the aeroelastic action of the outer part of the wing.

The W-wing 6 (see fig. 9) is close to an over-all aeroisoclinic condition, that is, a condition of over-all cancellation of the effects of bending and torsion deformations. In the subsonic symmetric case the lift, and in the supersonic symmetric case the center of pressure, are substantially unaffected by aeroelastic action as a result of the balance

between the aeroelastic tendencies of the inner and outer parts of the wing. There is an outboard shift of the center of pressure in the subsonic case, as for wings 4 and 5, but a decrease in lift in the supersonic case, which is opposite to the behavior of wings 4 and 5. In the antisymmetric case, both at subsonic and supersonic speeds, the aeroelastic behavior of the large sweptback inner part of the wing dominates that of the whole wing and results in a loss in the lift due to aileron deflection.

In the case of the A-wing 7 (see fig. 10) as in the case of W-wings 4 and 5, the behavior of the outer part dominates that of the sweptback inner part except in the supersonic symmetric case, for which the outer part is largely inactive as far as aeroelastic behavior is concerned so that the aeroelastic behavior of the sweptback inner part results in a small decrease in lift. On the other hand, in the case of A-wing 8 (see fig. 11) the large sweptback inner part of the wing dominates its aeroelastic behavior. The aeroelastic action of the unswept outer part only serves to reduce the resulting loss of lift locally to a small extent. Similarly, the large sweptforward inner part of the inverted A-wing 9 (see fig. 12) largely dominates the aeroelastic behavior of that wing, except that at supersonic speeds the twist of the outer part resulting from the large moment arm e_2 of the lift due to aileron deflection is so large that it overshadows the bending effects of the inner part of the wing and results in a small loss in the lift due to aileron deflection.

In general, the effects of aeroelasticity on the spanwise lift distributions may be seen to be much less for certain compounded plan forms (wing 6, for example) than for ordinary swept wings.

Inasmuch as strip theory was used in the calculations for supersonic speeds the results for supersonic speeds cannot be expected to be as accurate as those for subsonic speeds. If more realistic values of the lift distributions are desired for supersonic speeds the increments due to aeroelastic action shown in figures 4 to 15 can be applied to rigid-wing lift distributions calculated by linearized supersonic theory. These increments are probably quite accurate, because the integrating matrices used in the present paper have the effect of rounding off any lift distribution to which they are applied; the aeroelastic effects would have been overestimated slightly if strip theory had been used rigorously.

Aerodynamic parameters associated with the lift distributions.- The lift and aerodynamic center are determined by the symmetrical spanwise lift distributions; similarly, the rolling-moment coefficient due to aileron deflection and wing-tip helix angle per unit aileron deflection are determined by the corresponding antisymmetric lift distributions. The effects discussed in this section are therefore direct consequences of those discussed in the preceding section.

[redacted]

The effects of aeroelasticity on some of the aerodynamic properties of the unswept wing are shown in figure 21. They result in an increase in lift and a loss in the rolling power and rate of roll at subsonic speeds; the rate at which lateral control is lost, slowly at first and then more rapidly, is typical of wings for which q_R/q_D is positive, as discussed in reference 9. At supersonic speeds the lift is unaffected, but the losses in lateral control and rolling velocity are even greater than at subsonic speeds. The rate at which the control is lost with increasing $\tilde{q}$ is constant, a phenomenon typical of wings with infinite q_D.

Although the lateral control of the sweptforward wing is improved by aeroelastic action, the increase in lift and the outboard shift in center of pressure are so large (see table 2) as to make this type of plan form undesirable. The sweptback wing 12 (fig. 22), on the other hand, experiences a loss in lateral control which is even greater than that of the unswept wing. The rate at which control is lost is rapid at first, then slower; as is typical of wings with q_R/q_D negative. The sweptback wing loses some lift and its center of pressure moves inboard as a result of aeroelastic action. This movement of the center of pressure is accompanied by a shift of the aerodynamic center forward and, hence, a loss in the static-stability margin. The loss of control and the shift of the aerodynamic center are disadvantages of the sweptback wing from the aeroelastic point of view and the aim of this analysis is to determine whether there are compounded plan forms which are substantially superior to the sweptback wing in this respect.

As noted in the preceding section, there are among the nine compounded plan forms considered some which exhibit little or no loss in lift due to aileron deflection and little shift in spanwise center of pressure as a result of aeroelastic actions. (Of course, the fore-and-aft movement of the center of pressure varies with the spanwise shift in a more complicated manner than in the case of the ordinary swept wings as a result of the complicated geometry of the compounded wings.) As shown in figures 16, 18, and 20, the aerodynamic-center shift of wings 1, 6, and 8 is smaller than for that of the sweptback wing (fig. 22), and the shift for wings 2 and 7 (figs. 17 and 19) is practically nil. However, the loss of lateral control of wings 1 and 2 is only slightly less, and that of wing 8 is actually slightly greater, than that of the sweptback wing. At low dynamic pressures ($\tilde{q}$ less than 6) wings 6 and 7 suffer relatively little loss of control. These five wings are typical of the others, as may be seen from table 2, except that the other wings actually experience a gain in lateral control. However, this gain is purchased at the price of greater shift of aerodynamic center (all but wing 5) or low divergence speed (particularly wings 4, 5, and 9) with the resulting tendency to general aeroelastic instability. Thus, although some of the compounded plan forms have

[redacted]

generally more favorable aeroelastic characteristics than does the sweptback wing, some show little improvement and others are actually inferior to the sweptback wing from the aeroelastic point of view.

Dynamic pressures at divergence and at reversal.- For ordinary unswept wings the dynamic pressure is usually primarily of interest as a reference quantity which serves as an index for the severity of static aeroelastic pheonomena. Only for sweptforward wings does the divergence speed have any physical significance, and for these wings it is likely to be so low as to rule out the use of the wings because stiffening the wings would require a prohibitive amount of structural material. On the other hand, the dynamic pressure required to diverge sweptback wings is negative, so that its only significance is as a reference parameter.

The significance of the dynamic pressures listed in table 2 can be assessed by the fact that a sweptforward wing is likely to diverge at relatively low dynamic pressures. (See refs. 3 and 14, for instance.) Therefore, a value of $\tilde{q} = 6$ may be expected to be attained by a fighter-type airplane at about Mach number 1 at low altitudes. This value of $\tilde{q}$ is seen to be close to the value of divergence for some of the W-wings and the inverted A-wing; the sweptforward wing would diverge at an even lower value of $\tilde{q}$. Similarly, at a value of $\tilde{q} = 6$ several of the M-wings would experience aileron reversal at supersonic speeds. However, more definite statements cannot be made unless the physical parameters that enter into the definition of $\tilde{q}$, that is, the dynamic pressure of operation as well as the geometric and structural properties of a given wing, are known.

An interesting use of the dynamic pressure as a reference parameter was pointed out in reference 1. As the sweep of an ordinary wing is varied from unswept to sweptback, or as the stiffness-ratio GJ/EI or the elastic-axis location of a sweptback wing is varied, the dynamic pressure required for divergence goes to infinity and then reverses sign at a particular combination of structural, geometric, and aerodynamic parameters. For this combination of parameters the bending and torsion deformations lead to forces which tend to cancel each other; in other words, the aerodynamic loads give rise to deformations which do not give rise to any further aerodynamic loads. This phenomenon is referred to as aeroisoclinicism, and its significance is that under these conditions the lift and center of pressure are substantially invariant with dynamic pressure. As pointed out in references 1 and 9, there are certain disadvantages attached to this condition; the lateral-control properties of such a wing are not likely to be superior and the dynamic characteristics may well be inferior to those of a wing which is not operating at aeroisoclinic conditions. For the ordinary wings represented in table 2, for instance, interpolation (on the reciprocals of the dynamic pressure at divergence) indicates that a wing with about 12° sweepback would be substantially aeroisoclinic at subsonic speeds; at supersonic

speeds the unswept wing is aeroisoclinic. That the unswept wing at supersonic speeds and probably also the wing with 12° sweepback at subsonic speeds are subject to large losses of lateral control can be seen from table 2.

Some of the compounded wings represented in table 2 appear to be close to an over-all type of aeroisoclinicism because their dynamic pressure at divergence is very high. However, as a result of the more complicated geometry and the consequently more complicated structural properties of the compounded wings the fact that the dynamic pressure at divergence is approaching infinity is no longer a certain indication that the wing is approaching an aeroisoclinic condition. This subject will be discussed in some detail in the next section.

In contrast to the compounded wings with very high values of $\tilde{q}_D$, some of the compounded wings have dynamic pressures at divergence which are sufficiently low to be of concern, particularly plan forms of wings 4, 5, and 9. These plan forms, and probably plan form 3 also, must therefore be considered to be impractical from the aeroelastic point of view.

In contrast to the dynamic pressure at divergence the dynamic pressure at aileron reversal is almost always of physical significance; unswept and particularly sweptback wings designed for high-speed flight are usually designed with resistance to reversal as one of the major structural design requirements. The dynamic pressure at reversal also serves as an index for the aeroelastic effects on the lateral control of a wing, but in itself it is only a crude index; for instance, although the wing represented in figure 17 has a higher subsonic reversal speed than the one represented in figure 18, it has much less control power in the dynamic pressure range of primary concern (below $\tilde{q} = 6$). As mentioned previously this phenomenon may be predicted qualitatively from the ratio of the dynamic pressure at reversal to that at divergence. If, however, more complete information concerning the dependence of the rolling power and the maneuverability on the dynamic pressure is available, the dynamic pressure at reversal loses most of its significance.

In view of the foregoing considerations no quantitative deductions should be made from the values of $\tilde{q}_R$ given in table 2. On the other hand, one conclusion may be drawn from them: Whereas the value of $\tilde{q}_D$ given in table 2 vary from -134 to $+\infty$, the values of $\tilde{q}_R$ vary from 11.7 to 20.3 in the subsonic case and from 5.11 to 11.07 in the supersonic case; these numbers indicate that although the aeroelastic effects on the aerodynamic properties associated with level flight can be changed radically by a suitable compounding of the plan form the aerodynamic properties associated with rolling can be varied only within certain limits. That this is true for the process of balancing the effects of

bending and torsion deformations in general has been noted in references 1, 2, and 9. However, this conclusion must not be taken too literally; the limits within which the lateral control power can be varied by compounding are sufficiently wide to permit the selection of a satisfactory configuration in many cases.

Extension of the Calculated Results to Other Plan Forms

The process of compounding plan forms gives rise to two new geometrical parameters - the angle of sweep of the outer part of the wing and the position of the wing break - in addition to the three parameters which define the geometry of the more conventional plan forms, namely, the angle of sweep, the taper ratio, and the aspect ratio. Although the 9 compounded plan forms considered in this paper are typical of such plan forms, they fall short of the minimum number required to represent adequately all such plan forms that may be of interest. An attempt is made in this section to deduce the static aeroelastic characteristics of some related plan forms.

The values of the parameters C_L/C_{L_0}, $\Delta\bar{a}$, $C_{l_\delta}/C_{l_{\delta_0}}$, and $\left(\frac{pb}{2V}\right)_{\delta=1}$ at a value of $\tilde{q} = 3$ are plotted in figure 23 as functions of the spanwise position of the break and as functions of the angle of sweepback of the outer panel in figure 24. Also plotted are the lowest and second lowest (in absolute magnitude) values of $\tilde{q}_D$.

The series represented in figure 23(a) consists of plan forms which vary from a sweptback wing $(y^*_B = 0)$ through a range of M-wings with $\Lambda_1 = -\Lambda_0 = -45^\circ$ and varying positions of the break to a sweptforward wing $(y^*_B = 1.0)$. At $\tilde{q} = 3.0$ the shift in aerodynamic center $\Delta\bar{a}$ is seen to be 0 at both subsonic and supersonic speeds for the wing with $y^*_B = 0.55$, and the loss in the lateral control power at subsonic and supersonic speeds is zero for the wings with $y^*_B = 0.68$ and 0.84, respectively. For all these wings $\tilde{q}_D$ is positive, but for the wings with $y^*_B = 0.55$ and $y^*_B = 0.68$ it is sufficiently high to be of no concern. (The second-lowest value of $\tilde{q}_D$ for subsonic speeds and for small values of y^*_B is too large to be represented in the figure; it decreases from -80 to -120 as y^*_B increases from 0 to 0.3.) The rate of roll or lateral maneuverability is affected only slightly by a change in y^*_B, as a result of the fact that changes in the rolling power are accompanied by almost equal changes in the damping roll.

The series represented in figure 23(b) consists of plan forms which vary from a sweptforward wing $(y^*_B = 0)$ through a range of W-wings with $\Lambda_i = -\Lambda_o = 45^\circ$ and varying positions of the break to a sweptback wing $(y^*_B = 1.0)$. When y^*_B is about 0.6 the shift in aerodynamic center and the loss or gain in the lateral control power are almost zero at $\tilde{q} = 3.0$. However, the speed required to diverge this wing is relatively low. For wings with y^*_B less than 0.6 there is a gain in the lateral-control power due to aeroelastic action, but $\tilde{q}_D$ is even lower; for wings with y^*_B greater than 0.6 the dynamic pressure required to diverge the wings is higher, but there is some loss in control power. Again, the rate of steady roll is affected only slightly by a variation of y^*_B.

The series represented in figure 23(c) consists of plan forms which vary from an unswept wing $(y^*_B = 0)$ through a range of Λ-wings with $\Lambda_i = 45^\circ$, $\Lambda_o = 0$ and varying positions of the break to an ordinary sweptback wing $(y^*_B = 1.0)$. The aerodynamic-center shift is very small when y^*_B is less than 0.5, but this result is due to the fact that one-half or more of the wings is unswept. There is some loss in lateral-control power for all of these wings but the loss is very small when y^*_B is less than 0.3. The dynamic pressure at divergence is positive for most of the wings represented in figure 23(c) but sufficiently large to be of no concern. The rate of roll is substantially constant for y^*_B less than 0.4 and does not vary much for greater values of y^*_B.

A series of Λ-type wings with $\Lambda_i = 45^\circ$, $y^*_B = 0.3$ and varying Λ_o is represented in figure 24(a); when Λ_o is 0, they reduce to a Λ-wing with $\Lambda_i = 45^\circ$; when Λ_o is positive they are intermediate between a Λ-wing and an ordinary sweptback wing; and when Λ_o is negative, they are intermediate between a Λ-wing and a W-wing. At subsonic speeds the wing with $\Lambda_o = -10^\circ$ has no shift in aerodynamic center nor loss in lateral control; at supersonic speeds the wing with $\Lambda_o = 0$ has no shift in aerodynamic center, and the wing with $\Lambda_o = -25^\circ$ has no loss in control. The divergence speed of all three wings is probably sufficiently high not to be of concern. The rolling speed does not vary much between the various wings represented in this figure.

The wings represented in figure 24(b) differ from those represented in figure 24(a) only in that their break is at 70 percent rather than 30 percent of the semispan. The condition of zero aerodynamic-center shift can be achieved only at subsonic speeds in this series (with $\Lambda_o = -22^\circ$) and the condition of no loss of lateral control power, not

[redacted]

at all. The rate of roll is about the same for all the wings represented in figure 24(b) and only little lower than that of the wings represented in figure 23 and in figure 24(a). The divergence speed is sufficiently high for all the wings represented in figure 24(b) not to be of concern.

A series of inverted Λ-type wings is represented in figure 24(c); the wings differ from those represented in figure 24(b) only in that their inner parts are sweptforward rather than sweptback. The condition of zero aerodynamic-center shift is not attained by any of these wings, and although their lateral-control power is more than adequate, their divergence speed is so low as to rule out most of these wings for practical purposes.

The relation between the behavior of $\tilde{q}_D$ and the achievement of the aeroisoclinic condition can now be considered on the basis of figures 23 and 24. In the case of ordinary swept wings the higher values of $\tilde{q}_D$ (corresponding to the higher modes) are much larger in absolute value than the lowest; a case where the two lowest values coincide in absolute magnitude does not appear to arise for most ordinary swept wings. Consequently, if for these ordinary swept wings $\tilde{q}_D$ is plotted as a function of the angle of sweepback or, more generally, as a function of the parameter k defined in references 1, 3, 4, and 9 (or the parameter d/a of ref. 14), which contains the stiffness ratio GJ/EJ, the aspect ratio and the moment arm e_1 in addition to the angle of sweepback, there is only one value of the parameter for which $\tilde{q}_D$ goes to infinity.

For the compounded wings, however, the two lowest values of $\tilde{q}_D$ frequently have the same absolute magnitude. For instance, in figure 23(a) the lowest value of $\tilde{q}_D$ is negative at subsonic speeds for all values of y^*_B less than 0.59 and the second lowest value is positive for values of y^*_B greater than about 0.35 and less than 0.59. At $y^*_B = 0.59$ the two values of $\tilde{q}_D$ coincide in absolute magnitude, and at values of y^*_B greater than 0.59 the lowest value of $\tilde{q}_D$ is positive and the second lowest value is negative. Consequently, the lowest value of $\tilde{q}_D$ never approaches infinity; it merely jumps from negative to positve at $y^*_B = 0.59$. The same phenomenon occurs at supersonic speeds at $y^*_B = 0.71$. The second lowest value of $\tilde{q}_D$ goes to infinity twice, at $y^*_B = 0.35$ and 0.75 at subsonic speeds and $y^*_B = 0.50$ and 0.87 at supersonic speeds.

[redacted]

For the family of wings represented in figure 23(a) the aerodynamic-center shift was noted to be 0 at $y^*_B = 0.55$ for both subsonic and supersonic speeds. The change in lift-curve slope due to aeroelastic action is 0 for $y^*_B = 0.53$ for subsonic speeds and $y^*_B = 0.63$ at supersonic speeds. The conditions of either zero aerodynamic-center shift or zero lift increase may be considered to define the over-all aeroisoclinic condition. Inspection of figures 23 and 24 indicates that the jump of the lowest value of $\tilde{q}_D$ from negative to positive tends to occur when the wing is close to an over-all aeroisoclinic condition, but more definite conclusions cannot be drawn.

The values of $\tilde{q}_D$ shown in figure 24(a) vary with the angle of sweep of the outer part of the wing in much the same manner as they do for ordinary swept wings with the angle of sweep of the entire wing. The lowest value of $\tilde{q}_D$ goes to infinity at $\Lambda_o = 12^\circ$ and -2° at subsonic and supersonic speeds, respectively. These values of Λ_o are also the angles at which the change in the lift and the shift of the aerodynamic center are zero, although at subsonic speeds the aerodynamic-center shift is also zero at $\Lambda_o = -18^\circ$. On the other hand, the values of $\tilde{q}_D$ shown in figures 24(b) and 24(c) vary with Λ_o in an entirely different manner. The lowest values of $\tilde{q}_D$ never change sign; the second lowest values of $\tilde{q}_D$ go to infinity at $\Lambda_o = 21^\circ$ and $\Lambda_o = -6^\circ$ at subsonic and supersonic speeds, respectively, in figure 24(b) and at $\Lambda_o = 33^\circ$ and 0, respectively, in figure 24(c). However, these values of Λ_o have no significance insofar as the lift, aerodynamic-center shift, and lateral control power are concerned, as may be seen from figures 24(b) and 24(c). Consequently, any deductions concerning the aeroelastic phenomena of interest can be drawn only from the behavior of the lowest value (in absolute magnitude) of $\tilde{q}_D$.

The Optimum Compounded Plan Form

On the basis of the preceding discussion the problem of the selection of an optimum compounded plan form can now be broached, the term optimum being used in the sense of most favorable aeroelastic characteristics at the least sacrifice in aerodynamic and structural performance. In view of the relatively small number of plan forms considered in this paper and inasmuch as no dynamic aeroelastic calculations have been made, the following discussion can shed light on only a few aspects of the problem.

The desired static aeroelastic characteristics.- The desired static aeroelastic characteristics are, approximately in the order of their importance:

[redacted]

(1) The shift of the aerodynamic center should be small if it is forward, as it is in almost all cases of practical interest.

(2) There should be no loss in the rate of roll nor in the lateral control power.

(3) There should be no appreciable change in the lift-curve slope.

(4) The dynamic pressure required for divergence should be either negative or, if positive, at least 25 percent higher than the highest expected dynamic pressure in the given speed range.

In the case of airplanes designed to fly occasionally at high supersonic Mach numbers (say 2 or greater) these conditions should be satisfied as much as possible at those Mach numbers as well as at subsonic speeds.

The selection of a plan form possessing some of these characteristics can now be discussed on the basis of a union effected between the three series of plan forms represented in figure 23 with those represented in figure 24, a process which gives rise to plan forms of which the inner part is either swept back or swept forward at an angle of 45°, but of which both the outer part and the position of the wing break are arbitrary. In considering all these combined results the fact must be kept in mind that they still apply to a quite restricted class of wings. The aspect ratio of all wings is 6, the taper ratio 0.5, and the angle of sweep 45° or -45°, the span of the outboard aileron is 50 percent of the wing span (unless another aileron configuration is specified), and the structures are of a certain kind, namely the stiffness distributions vary substantially as dictated by constant-stress considerations (as outlined in ref. 1), and $GJ/EI = 0.794$. The conclusions reached in this section may not be valid for any wing with taper ratio, aileron configuration (in the case of conclusions concerning lateral-control properties), stiffness ratio, and variation of the stiffnesses GJ and EI (particularly near the wing tip) which differ greatly from the values used in the calculations described in this paper.

The information pertinent to this discussion is summarized in figures 25 and 26. The plan forms represented in figures 25(a) and 26(a) have an inner part sweptback 45°, and those represented in figures 25(b) and 26(b) have an inner part which is sweptforward 45°. The location of the break and the angle of sweepback of the outer part are arbitrary and constitute the coordinates of these figures. The curves shown are the loci of the points representing plan forms which have a zero aerodynamic-center shift at $\tilde{q} = 3.0$ (in the case of fig. 25) and no loss in lateral control at $\tilde{q} = 3.0$ (in the case of fig. 26). The aerodynamic-center shifts for all wings represented in figure 25 are negative, except that those represented by points on or between the two lines for zero shift

have a zero or a very small positive shift, respectively. The rolling-moment ratio is less than 1 in the region above and greater in the regions below the lines of no loss of lateral control shown in figure 26.

A comparison of figure 25 with figure 26 indicates that a wing with the inner part swept forward 45° must have the break at 72 percent span and the outer part swept back 60° in order to have no shift in aerodynamic center nor loss in lateral control at subsonic speeds. No wing with the inner part swept forward 45° can satisfy both of those conditions at supersonic speeds. When the inner part of the wing is swept back, however, almost all the wings represented by the line for subsonic speeds in figure 26(a) should be satisfactory at subsonic speeds because they have no loss in lateral control and only a small forward shift of the aerodynamic center. Of this group of wings those on the lower part of the curve (y^*_B greater than 0.55 or Λ_o less than -40°) should be satisfactory at supersonic speeds as well as subsonic speeds because they should have only a small rearward shift of the aerodynamic center and only a small loss in the lateral control. Probably the optimum wings among those considered here are the ones with $y^*_B = 0.58$ to 0.60 and corresponding values of Λ_o from -40° to -45°.

The number and range of geometric and structural variables covered by the calculations described in this paper is insufficient to permit any generalization of the figures cited in the preceding paragraph. In a given case sufficient calculations should be made to permit the preparation of charts similar to those of figures 25 and 26 for several values of the sweep angle of the inner part of the wing and, unless they are decided upon beforehand, for several aspect and taper ratios. Also, if the stiffness-ratio GJ/EI can be varied without increasing the structural weight, several values of the ratio should be considered. Furthermore, inasmuch as the simultaneous achievement of zero aerodynamic-center shift and zero lateral-control loss at both subsonic and supersonic speeds in an aerodynamically acceptable wing is unlikely, it would be desirable to plot on charts of the type represented by figures 25 and 26 lines of constant aerodynamic-center shift and lines of constant lateral-control loss, respectively, in addition to lines of zero shift and zero loss in order to facilitate the selection of an optimum compromise plan form. (The number of plan forms for which calculations have been made is insufficient to permit the plotting of such contour lines on figs. 25 and 26.) This procedure implies a great number of calculations, despite the fact that many plan forms with obviously undesirable aerodynamic characteristics can be eliminated from consideration beforehand, as will be pointed out in a subsequent section.

The no-shift and no-loss requirements can, of course, also be satisfied simultaneously by choosing a wing with zero aerodynamic-center shift and equipping it with an all-movable wing tip. This procedure has the

advantage of providing greatly increased rigid-wing rolling performance, particularly at supersonic speeds, in addition to the decreased loss in this performance as a result of aeroelastic action. However, this advantage is offset to a large extent by the mechanical and flutter problems which beset such a configuration. Only if the wing under consideration has its break far outboard, say 85 percent or more of the semispan, and the lateral control provided by rotating the portion of the wing outboard of the break is sufficient is this configuration likely to be practical.

The desired dynamic aeroelastic characteristics.- The desired dynamic aeroelastic characteristics are, substantially,

(1) That the inertia effects on the aerodynamic center and the lateral control should be small or in such a direction as to oppose any adverse static aeroelastic effects

(2) That the flutter speed be higher than any expected flying speed at all altitudes

(3) That the dynamic response of the wing to atmospheric excitation give rise to no excessive stresses

The inertia effects on the aerodynamic-center shift will be small if the wing weight represents a small fraction of the airplane weight, and the inertia effects on the lateral-control power are not likely to be important because the rate of steady roll (which is independent of inertia effects) is usually considered to be more important than the control power (which is an index of the attainable rolling acceleration).

The flutter and dynamic-response characteristics of wings designed on the basis of a balance of torsion and bending deformations may well be inferior to that of an ordinary swept wing because they are likely to be more flexible. Careful flutter studies must therefore be made in each case. When necessary, however, it may be possible in some cases to raise the flutter speed at relatively low weight penalty by taking advantage of the large moment arms available for mass balancing. A high wing-flutter speed (relative to the highest flying speed at the given altitude) usually implies satisfactory dynamic-response characteristics, provided the airplane as a whole is stable.

The desired structural characteristics.- For the purposes of this discussion the desirable structural characteristics are that the weight of the structure of a compounded wing be no higher than that of a comparable ordinary swept wing. The break requires locally a certain amount of material not needed in an ordinary wing, and the large torques near the root of an M- or W-wing require additional torsion-resisting material. However, the bending moments are much smaller than for an

ordinary wing, and the saving in flexure-resistant material may be so large as to compensate for the aforementioned increases in structural material. Thus the weight of a compounded wing may be little, if any, higher than that of an ordinary wing.

The desired aerodynamic characteristics.- Within the scope of this discussion the desired aerodynamic characteristics are that the drag and the stability characteristics of the compounded wing be no worse and better, respectively, than those of a comparable sweptback wing. A few tests have shown that the stability characteristics of M- and W-wings can, indeed, be superior to those of ordinary swept wings. The drag of a compounded wing is likely to be higher than that of an ordinary swept wing, as has been shown by tests at subsonic, transonic, and supersonic speeds (see ref. 15, for instance) and as may be inferred from calculations for ordinary swept wings at supersonic speeds (see refs. 16 and 17, for instance). The whole question of whether to use M- and W-wings thus hinges primarily on the problem of whether the saving in structural weight afforded by these configurations in achieving the desired stability and control characteristics is worth the drag penalty.

The additional drag of a compounded wing as compared to an ordinary sweptback wing arises from three sources: the fact that part of the wing may have a relatively low sweep angle, the fact that in the case of an M-wing the inner part of the wing may be sweptforward (giving rise to fuselage interference drag), and the fact that in the case of a W-wing the break itself is the source of a certain amount of interference drag.

When the results of static aeroelastic analyses of a variety of plan forms are summarized on charts similar to figures 25 and 26 some of the plan forms brought to light by these charts can be eliminated because they are likely to be subject to one or more of the aforementioned types of drag. In figures 25 and 26, for example, the plan forms represented by points within the wedge-shaped regions labeled "aerodynamically undesirable" have too much of their area swept at too low an angle to compete with a completely swept wing. (These regions are based on qualitative estimates and are shown primarily for illustrative purposes.)

Similar reasoning may be employed in connection with the interference drag. In figures 25(a) and 26(a), the plan forms represented by points above the wedge-shaped regions are likely to have higher drag than do those represented by points below this region, because the difference in sweep angle between the inner and outer portions of the wing is much greater for the former than for the latter. The reverse is true for figures 25(b) and 26(b). Also, the plan forms represented by points in figures 25(a) and 26(a) are likely to have less drag than those represented by points in figures 25(b) and 26(b) because the

interference drag caused by the break of a W-wing is likely to be less than that caused by the root of an M-wing as a result of the smaller chords involved, particularly if the break of the W-wing is near the tip.

Finally, experimental or theoretical drag studies must be used to decide which, if any, of the remaining plan forms may be suitable for any given purpose, the theoretical studies being useful primarily for supersonic speeds. If there are any satisfactory compounded plan forms, these studies should be followed by further studies aimed at reducing the drag of these wings. For instance, there is a possibility that the interference drag at subsonic speeds may be reduced by using fences. Also, the drag caused by the region of the wing which has a relatively low sweep angle can be reduced by resorting to thinner airfoil sections in that region; the resulting weight penalty should be very small, because that region is likely to contain only a small part of the wing area and be in a region where the stresses are relatively low. Thus, when large adverse static aeroelastic effects are anticipated, as for wings with low wing loading designed for low load factors and intended for high-speed low-altitude flight, compounded plan forms may well constitute the best solution.

CONCLUDING REMARKS

Calculations have been made of the static aeroelastic characteristics of nine M-, W-, and Λ-wings by using the best available aerodynamic and structural information. Although the number of plan forms considered is too small and the calculations too specific to permit of quantitative conclusions which are generally applicable, certain qualitative conclusions have been drawn. The question of the plan form with the optimum static aeroelastic characteristics has been discussed on the basis of these conclusions. In general, there is reason to believe that by suitable compounding plan forms can be obtained which are superior aeroelastically and structurally to ordinary swept wings.

Langley Aeronautical Laboratory,
National Advisory Committee for Aeronautics,
Langley Field, Va.

[redacted]

APPENDIX

METHOD OF CALCULATING STATIC AEROELASTIC PHENOMENA OF M-, W-, AND Λ-WINGS

Symmetrical Flight Conditions

The aerodynamic influence coefficients.- In keeping with the assumptions concerning the aerodynamic properties of the wing, the lift on sections parallel to the air stream is given by

$$\left\{\frac{cc_l}{c_r}\right\}_w = C_{L_{\alpha_0}}\left[Q\right]\left\{\alpha\right\}_w \tag{1}$$

where $\left[Q\right]$ is an aerodynamic influence-coefficient matrix. A method of calculating such a matrix from known rigid-wing additional lift distributions is given in reference 5. The matrix obtained in this manner is

$$\left[Q\right] = \frac{\bar{c}}{c_r}\left[\frac{cc_l}{\bar{c}C_L}\right]_{w_0}\left[k_1\left[1\right] + \frac{w}{b}\left[I\right]_f\left\{\frac{cc_l}{\bar{c}C_L}\right\}_{f_0}\left[1_r\right] + \right.$$

$$\left.(1 - k_1)\frac{b'}{b}\left\{1\right\}\left[I'\right]_w\left[\frac{cc_l}{\bar{c}C_L}\right]_{w_0}\right] \tag{2}$$

where $\left[1\right]$ is a unit matrix, $\left[1_r\right]$ is a square matrix defined by

$$\left[1_r\right] = \begin{bmatrix} 1 & 0 & \cdots & 0 \\ 1 & 0 & \cdots & 0 \\ \cdot & \cdot & \cdots & \cdot \\ \cdot & \cdot & \cdots & \cdot \\ 1 & 0 & \cdots & 0 \end{bmatrix} \tag{3}$$

[redacted]

and $\{1\}$ is a column matrix, each element of which is unity. The row matrix $\lfloor I' \rfloor$ serves to integrate the lift distribution and is based on Simpson's rule with a modification which assumes that the lift goes to zero with infinite slope at the wing tip. (See ref. 3.) The parameter k_1 is given in reference 5 in terms of the plan-form parameter

$$F \equiv \frac{A}{\frac{c l_\alpha}{2\pi} \cos \Lambda}$$

by the relation

$$k_1 = \frac{F\sqrt{1 + \frac{4}{F^2}} + 2}{F\sqrt{1 + \frac{36}{F^2}} + 6} \tag{4}$$

For M-, W-, and Λ-wings this method requires some modification. For the purpose at hand the expression for $[Q]$ (eq. (2)) can be written as

$$[Q] = \frac{\bar{c}}{c_r}\left[\frac{cc_l}{\bar{c}C_L}\right]_{w_0}\left[k_1 K[1] + \left(1 - K + \frac{w}{b}[I]_f \left\{\frac{cc_l}{\bar{c}C_L}\right\}_{f_0}\right)[1_r] + \right.$$

$$\left.(1 - k_1)K \frac{b'}{b}\{1\}[I']_w\left[\frac{cc_l}{\bar{c}C_L}\right]_{w_0}\right]$$

In reference 5 the factor K (which may be considered to be the ratio of the lift coefficient due to a unit symmetrical twist to the dimensionless lateral center of pressure of the additional lift distribution) and the related factor K' used for antisymmetrical lift conditions are shown to be 1 according to lifting-line theory, and the method of calculating approximate aerodynamic influence coefficients presented in reference 5 is based on the assumption that these factors are 1. The calculations made in reference 6 have shown, however, that these factors are not 1 for M-, W-, and Λ-wings. The values of K and K' are therefore

[redacted]

obtained from the spanwise lift distributions and associated aerodynamic parameters presented in reference 6. They are introduced in the matrix $[Q]$ (respectively the matrix $[Q_a]$ in the antisymmetric case) in such a way (see eq. (2)) as to yield the correct spanwise lift distribution for any angle-of-attack distribution which consists of a linear superposition of a constant angle of attack and a linear twist in the symmetric case, and of a linear twist and a 50-percent-semispan outboard-aileron deflection in the antisymmetric case. Specifically,

$$K = \frac{\left(C_{L_0}\right)_{\alpha=y^*}}{C_{L_{\alpha_0}} \int_0^1 y^* \left(\frac{cc_l}{\bar{c}C_L}\right)_0 dy^*} \tag{5}$$

Also, inasmuch as the plan-form parameter F is a function of the cosine of the sweep angle, there is some question as to which value should be chosen in the case of a Λ-wing or of an M- or W-wing with angles of sweep in the inner and outer parts of the wing which differ in absolute magnitude. For the calculations made by the method of the present paper an average value of $\cos \Lambda$ deduced by

$$\overline{\cos \Lambda} \equiv \int_0^1 \cos \Lambda \, \frac{c}{\bar{c}} \, dy^*$$

has been used.

This procedure is believed to furnish results with sufficient accuracy for the purpose intended, because the values of the lift distributions calculated by the matrices $[Q]$ and $[Q_a]$ are not very sensitive to the value of F. Since, when K and K' are 1, the matrices $[Q]$ and $[Q_a]$ reduce to those presented in reference 5, which are valid for all angle-of-attack distributions, there is reason to believe that the matrices $[Q]$ and $[Q_a]$ used in the present paper yield lift distributions for angle-of-attack distributions other than the aforementioned ones with sufficient accuracy for the purpose intended. A few calculations by means of the method used in reference 6 and of the matrices of the present paper for parabolic symmetric and antisymmetric twists have yielded results in excellent agreement with each other.

[redacted]

If strip theory is used, as has been done in the calculations for supersonic flow, the aerodynamic influence-coefficient matrix is

$$\left[Q\right] = \left[\frac{c}{c_r}\right] \tag{6}$$

The aeroelastic equation.- The running load on each part of the wing can be written as

$$\left\{l\right\} = qc_r\left\{\frac{cc_l}{c_r}\right\} \tag{7}$$

and the running torque in planes parallel to the air stream for uncambered wing sections is

$$\left\{t\right\} = qc_r^2\left[\frac{e_l c}{c_r}\right]\left\{\frac{cc_l}{c_r}\right\} \tag{8}$$

The subscripts i and o used on the matrices of equations (7) and (8) in the following analysis refer, respectively, to the inner and outer parts of the wing.

The single and double integrations required to obtain the accumulated torques and bending moments from the running torques and loads are performed by means of integrating matrices $\left[I\right]$ and $\left[II\right]$, respectively. These matrices are based on Simpson's rule and are similar to those described in reference 3. When a modification is made at the wing tip which takes into account the infinite slope of the spanwise lift distribution at the wing tip at subsonic speeds, this fact is described by adding a prime mark to the matrices. For the sake of definiteness the matrices $\left[I'\right]$ and $\left[II'\right]$ appropriate for subsonic speeds will be used in the following derivation.

The integrating matrices used in the calculations described in the present paper are given in table 3. They pertain to the stations used in the calculations, namely:

For ordinary wings: $y^* = 0.1, 0.25, 0.4, 0.55, 0.7, 0.85$

For wings with $y^*_B = 0.3$: $y^* = 0.1, 0.2, 0.3, 0.44, 0.58, 0.72, 0.86$

For wings with $y^*_B = 0.5$: $y^* = 0.1, 0.2333, 0.3667, 0.5, 0.625, 0.75, 0.875$

For wings with $y^*_B = 0.7$: $y^* = 0.1, 0.25, 0.4, 0.55, 0.7, 0.8, 0.9$

[redacted]

In the calculations of the aerodynamic influence coefficients, stations were taken at $y^* = 0$, 0.05, and 0.1 on the part of the wing covered by the fuselage for all wings. The matrices $\left[I_f\right]$ and $\left[II_f\right]$ are not shown in table 3; they are the same as the matrices $\left[I_1\right]_i$ and $\left[II_1\right]_i$ for the wings with $y^*_B = 0.3$, except that when used as matrices $\left[I_f\right]$ and $\left[II_f\right]$ they refer to the stations $y^* = 0$, 0.05, and 0.1 rather than the values given in table 3, namely $y^* = 0.1$, 0.2, and 0.3.

The accumulated bending moment M about axes parallel to the air stream can then be obtained directly by using the matrix $\left[II'\right]$ to perform the indicated double integration. Similarly, at a given section parallel to the air stream the accumulated torque about an axis which passes through the shear center of that section and is perpendicular to the plane of symmetry can be found by performing a single integration by means of the $\left[I'\right]$ matrix of the running torque and then subtracting from this result the product of the accumulated bending moment at the section and the tangent of the angle of sweepback outboard of the section.

Thus

$$\left\{M'\right\}_i = d_i^2\left(\frac{b}{2}\right)^2\left[II\right]_i\left\{l\right\}_i \tag{9}$$

$$\left\{M\right\}_o = d_o^2\left(\frac{b}{2}\right)^2\left[II'\right]_o\left\{l\right\}_o \tag{10}$$

$$\left\{T'\right\}_i = d_i\,\frac{b}{2}\left[I\right]_i\left\{t\right\}_i - \tan\Lambda_i\left\{M'\right\}_i \tag{11}$$

$$\left\{T\right\}_o = d_o\,\frac{b}{2}\left[I'\right]_o\left\{t\right\}_o - \tan\Lambda_o\left\{M\right\}_o \tag{12}$$

The prime marks on $\left\{M'\right\}_i$ and $\left\{T'\right\}_i$ indicate that the moments carried across the wing break from the outer part of the wing are not included.

In these equations the station at the wing break may be considered to be the last one on the inner part of the wing or the first one on the outer part of the wing or both. In the following derivation the last-named alternative is implied, except where specified otherwise.

[redacted]

In order to find the bending and twisting deformations along the wing, the accumulated bending moment M_Λ about axes perpendicular to the elastic axis and the accumulated torque T_Λ about the elastic axis must be known. These new moments at any station may be obtained by means of the transformation

$$\begin{Bmatrix} M_\Lambda \\ T_\Lambda \end{Bmatrix} = \begin{bmatrix} \cos\Lambda & -\sin\Lambda \\ \sin\Lambda & \cos\Lambda \end{bmatrix} \begin{Bmatrix} M \\ T \end{Bmatrix} \tag{13}$$

which yields

$$\left\{M'_\Lambda\right\}_i = \frac{d_i^2\left(\frac{b}{2}\right)^2}{\cos\Lambda_i}\left[II\right]_i\{l\}_i - d_i\frac{b}{2}\sin\Lambda_i\left[I\right]_i\{t\}_i \tag{14}$$

$$\left\{M_\Lambda\right\}_o = \frac{d_o^2\left(\frac{b}{2}\right)^2}{\cos\Lambda_o}\left[II'\right]_o\{l\}_o - d_o\frac{b}{2}\sin\Lambda_o\left[I'\right]_o\{t\}_o \tag{15}$$

$$\left\{T'_\Lambda\right\}_i = d_i\frac{b}{2}\cos\Lambda_i\left[I\right]_i\{t\}_i \tag{16}$$

$$\left\{T_\Lambda\right\}_o = d_o\frac{b}{2}\cos\Lambda_o\left[I'\right]_o\{t\}_o \tag{17}$$

When the moments carried across the wing break from the outer part of the wing are added to the moments $\left[M'_\Lambda\right]_i$ and $\left[T'_\Lambda\right]_i$ the following expressions are obtained:

$$\left\{M_\Lambda\right\}_i = \left\{M'_\Lambda\right\}_i + \cos(\Lambda_i - \Lambda_o)\left\|l_B\right\|_i\left\{M_\Lambda\right\}_o - \sin(\Lambda_i - \Lambda_o)\left\|l_B\right\|_i\left\{T_\Lambda\right\}_o +$$

$$\frac{d_o\left(\frac{b}{2}\right)^2}{\cos\Lambda_i}\left[y^*_B - y^*\right]_i\left\|l_B\right\|_i\left[I'\right]_o\{l\}_o \tag{18}$$

[redacted]

$$\left\{T_\Lambda\right\}_i = \left\{T'_\Lambda\right\}_i + \sin(\Lambda_i - \Lambda_o)\left\|l_B\right\|_i \left\{M_\Lambda\right\}_o + \cos(\Lambda_i - \Lambda_o)\left\|l_B\right\|_i \left\{T_\Lambda\right\}_o \tag{19}$$

where the matrix $\left\|l_B\right\|_i$ is a rectangular matrix defined as

$$\left\|l_B\right\|_i = \begin{Vmatrix} 1 & 0 & \cdots & 0 \\ 1 & 0 & \cdots & 0 \\ \cdot & \cdot & \cdots & \cdot \\ \cdot & \cdot & \cdots & \cdot \\ 1 & 0 & \cdots & 0 \end{Vmatrix} \tag{20}$$

in which the number of rows is equal to the number of stations on the inner part of the wing and the number of columns is equal to the number of stations on the outer part of the wing. The diagonal matrix $\left|y^*_B - y^*\right|$ is composed of the dimensionless moment arms of the normal shear at the wing break about the stations on the inner part of the wing. The term of equation (18) in which it occurs represents the contribution of the vertical shear at the wing break to the bending moment at sections on the inner part of the wing.

The preceding equations may be combined as follows:

$$\left\{M_\Lambda\right\}_i = qc_r\left(\frac{b}{2}\right)^2 \left\{\left[\mu\right]_{ii}\left\{\frac{cc_l}{c_r}\right\}_i + \left\|\mu\right\|_{io}\left\{\frac{cc_l}{c_r}\right\}_o\right\} \tag{21}$$

$$\left\{M_\Lambda\right\}_o = qc_r\left(\frac{b}{2}\right)^2 \left[\mu\right]_{oo}\left\{\frac{cc_l}{c_r}\right\}_o \tag{22}$$

$$\left\{T_\Lambda\right\}_i = qc_r\left(\frac{b}{2}\right)^2 \left\{\left[\tau\right]_{ii}\left\{\frac{cc_l}{c_r}\right\}_i + \left\|\tau\right\|_{io}\left\{\frac{cc_l}{c_r}\right\}_o\right\} \tag{23}$$

$$\left\{T_\Lambda\right\}_o = qc_r\left(\frac{b}{2}\right)^2 \left[\tau\right]_{oo}\left\{\frac{cc_l}{c_r}\right\}_o \tag{24}$$

[redacted]

the matrices $[\mu]$ and $[\tau]$ (with subscripts) being defined as

$$[\mu]_{ii} = \frac{d_i^2}{\cos \Lambda_i}[II]_i - d_i \frac{c_r}{b/2} \sin \Lambda_i [I]_i \left[\frac{e_1 c}{c_r}\right]_i \tag{25}$$

$$\|\mu\|_{io} = d_o^2 \frac{\cos(\Lambda_i - \Lambda_o)}{\cos \Lambda_o} \|l_B\|_i [II']_o + \frac{d_o}{\cos \Lambda_i} \left[y^*_B - \bar{y^*}\right] \|l_B\|_i [I']_o - d_o \frac{c_r}{b/2} \sin \Lambda_i \|l_B\|_i [I']_o \left[\frac{e_1 c}{c_r}\right]_o \tag{26}$$

$$[\mu]_{oo} = \frac{d_o^2}{\cos \Lambda_o}[II']_o - d_o \frac{c_r}{b/2} \sin \Lambda_o [I']_o \left[\frac{e_1 c}{c_r}\right]_o \tag{27}$$

$$[\tau]_{ii} = d_i \frac{c_r}{b/2} \cos \Lambda_i [I]_i \left[\frac{e_1 c}{c_r}\right]_i \tag{28}$$

$$\|\tau\|_{io} = d_o^2 \frac{\sin(\Lambda_i - \Lambda_o)}{\cos \Lambda_o} \|l_B\|_i [II']_o + d_o \frac{c_r}{b/2} \cos \Lambda_i \|l_B\|_i [I']_o \left[\frac{e_1 c}{c_r}\right]_o \tag{29}$$

$$[\tau]_{oo} = d_o \frac{c_r}{b/2} \cos \Lambda_o [I']_o \left[\frac{e_1 c}{c_r}\right]_o \tag{30}$$

According to simple beam theory, the equations of equilibrium of the deformed wing are

$$GJ \frac{d\varphi}{d\left(\frac{y}{\cos \Lambda}\right)} = T_\Lambda \tag{31}$$

[redacted]

for twisting about the elastic axis and

$$EI \frac{d\Gamma}{d\left(\frac{y}{\cos \Lambda}\right)} = M_{\Lambda} \tag{32}$$

for bending along the elastic axis. These equations may be integrated to obtain φ and Γ with the matrix $[I]''$ given in table 3. This integrating matrix is (as explained in ref. 3) the double transpose of $[I]$ if the stations taken along the wing span are equally spaced.

The wing root is considered to be the wing section perpendicular to the elastic axis which passes through the intersection of the elastic axis and the side of the fuselage. Unlike the case of an unswept wing there are rotations of this section when the wing is subjected to bending moments and torques. These rotations have the nature of rigid-body rotations imparted to the rest of the wing and are caused by the flexibility of the root triangle and of the carry-through bay inside the fuselage. They can be calculated by analyzing these components in detail and can be expressed in terms of the four dimensionless flexibility constants defined in reference 3:

$$Q_{\varphi_T} = \frac{\varphi_{r_T}/T_{\Lambda_r}}{w_e/(GJ)_r} \tag{33}$$

$$Q_{\varphi_M} = \frac{\varphi_{r_M}/M_{\Lambda_r}}{w_e/(GJ)_r} \tag{34}$$

$$Q_{\Gamma_T} = \frac{\Gamma_{r_T}/T_{\Lambda_r}}{w_e/(EI)_r} \tag{35}$$

$$Q_{\Gamma_M} = \frac{\Gamma_{r_M}/M_{\Lambda_r}}{w_e/(EI)_r} \tag{36}$$

w_e being defined as in figure 1. They must then be added to the values of φ and Γ obtained from equations (31) and (32). As pointed out in reference 3, the values of $(GJ)_r$ and $(EI)_r$ serve only for reference purposes, so that their exact values are immaterial. The values obtained by extrapolating curves of GJ and EI plotted along the span to the root station are probably the most convenient ones to use.

[redacted]

The resulting expressions for the wing deformations are

$$\{\varphi\}_i = \frac{d_i \frac{b}{2}}{(GJ)_r \cos \Lambda_i} \left\{ \left[[I]_i '' \left| \frac{(GJ)_r}{GJ} \right|_i + \frac{w_e \cos \Lambda_i}{d_i \frac{b}{2}} Q_{\varphi_T} [l_o] \right] \{T_\Lambda\}_i + \frac{w_e \cos \Lambda_i}{d_i \frac{b}{2}} Q_{\varphi_M} [l_o] \{M_\Lambda\}_i \right\} \tag{37}$$

$$\{\varphi\}_o = \frac{d_o \frac{b}{2}}{(GJ)_r \cos \Lambda_o} [I]_o '' \left| \frac{(GJ)_r}{GJ} \right|_o \{T_\Lambda\}_o \tag{38}$$

$$\{\Gamma\}_i = \frac{d_i \frac{d}{2}}{(EI)_r \cos \Lambda_i} \left\{ \left[[I]_i '' \left| \frac{(EI)_r}{EI} \right|_i + \frac{w_e \cos \Lambda_i}{d_i \frac{b}{2}} Q_{\Gamma_M} [l_o] \right] \{M_\Lambda\}_i + \frac{w_e \cos \Lambda_i}{d_i \frac{b}{2}} Q_{\Gamma_T} [l_o] \{T_\Lambda\}_i \right\} \tag{39}$$

and

$$\{\Gamma\}_o = \frac{d_o \frac{b}{2}}{(EI)_r \cos \Lambda_o} [I]_o '' \left| \frac{(GJ)_r}{GJ} \right|_o \{M_\Lambda\}_o \tag{40}$$

where the values of φ and Γ on the outer panel are measured relative to the station at the wing break rather than to the station at the wing root. The matrix $[l_o]$ is a square matrix which has as many

[redacted]

columns as these stations on the inner part of the wing and is defined by

$$\left[l_o\right] = \begin{bmatrix} 0 & 0 & 0 & \cdots & 0 \\ 1 & 0 & 0 & \cdots & 0 \\ 1 & 0 & 0 & \cdots & 0 \\ \cdot & \cdot & \cdot & \cdots & \cdot \\ \cdot & \cdot & \cdot & \cdots & \cdot \\ 1 & 0 & 0 & \cdots & 0 \end{bmatrix}$$

Rigid-body-rotation constants could also be introduced to take into account the effect of local distortions in the vicinity of the wing break on the deformations of the outer part of the wing. No such constants have, however, been used in the calculations described in this paper because no simple method of calculating them was available, and if they had been calculated for a specific case, the results would not necessarily have applied to other cases. Also, inasmuch as they affect only the deformations of the outer part of the wing, whereas those considered in the preceding paragraphs affect the entire wing (and even those do not have a large effect on the wing deformations except for wings of low aspect ratio), there is good reason to believe that the rigid-body-deformation constants appropriate to the wing break can be neglected.

The angle of attack due to structural deformations α_s is related to φ and Γ (for small angles) by

$$\left\{\alpha_s\right\}_i = \cos \Lambda_i \left\{\varphi\right\}_i - \sin \Lambda_i \left\{\Gamma\right\}_i \tag{41}$$

$$\left\{\alpha_s\right\}_o = \left\|l_B\right\|_o \left\{\alpha_s\right\}_i + \cos \Lambda_o \left\{\varphi\right\}_o - \sin \Lambda_o \left\{\Gamma\right\}_o \tag{42}$$

where the rectangular matrix $\left\|l_B\right\|_o$ defined by

$$\left\|l_B\right\|_o = \begin{Vmatrix} 0 & \cdots & 0 & 1 \\ 0 & \cdots & 0 & 1 \\ \cdot & \cdots & \cdot & \cdot \\ \cdot & \cdots & \cdot & \cdot \\ 0 & \cdots & 0 & 1 \end{Vmatrix} \tag{43}$$

[redacted]

has as many rows as there are stations on the outer part of the wing and as many columns as there are stations on the inner part of the wing.

The substitution of equations (37) and (39) into equation (41), and of equations (38) and (40) into equation (42) yields

$$\left\{\alpha_s\right\}_i = \frac{b/2}{(GJ)_r}\left\{\left[K_T\right]_i\left\{T_\Lambda\right\}_i - \left[K_M\right]_i\left\{M_\Lambda\right\}_i\right\} \tag{44}$$

$$\left\{\alpha_s\right\}_o = \left\|l_B\right\|_o\left\{\alpha_s\right\}_i + \frac{b/2}{(GJ)_r}\left\{\left[K_T\right]_o\left\{T_\Lambda\right\}_o - \left[K_M\right]_o\left\{T_\Lambda\right\}_o\right\} \tag{45}$$

where the matrices $\left[K\right]$ are defined by

$$\left[K_T\right]_i = d_i\left[I\right]_i''\left|\frac{(GJ)_r}{GJ}\right|_i + \frac{w_e \cos\Lambda_i}{b/2}\left(Q_{\varphi_T} - \frac{(GJ)_r}{(EI)_r}\tan\Lambda_i Q_{\Gamma_T}\right)\left[l_o\right] \tag{46}$$

$$\left[K_M\right]_i = d_i\frac{(GJ)_r}{(EI)_r}\tan\Lambda_i\left[I\right]_i''\left|\frac{(EI)_r}{EI}\right|_i - \frac{w_e \cos\Lambda_i}{b/2}\left(Q_{\varphi_M} - \frac{(GJ)_r}{(EI)_r}\tan\Lambda_i Q_{\Gamma_M}\right)\left[l_o\right] \tag{47}$$

$$\left[K_T\right]_o = d_o\left[I\right]_o''\left|\frac{(GJ)_r}{GJ}\right|_o \tag{48}$$

$$\left[K_M\right]_o = d_o\frac{(GJ)_r}{(EI)_r}\tan\Lambda_o\left[I\right]_o''\left|\frac{(EI)_r}{EI}\right|_o \tag{49}$$

[redacted]

The combination of equations (21), (22), (23), (24), (44), and (45) then gives

$$\begin{Bmatrix} \{\alpha_s\}_i \\ \{\alpha_s\}_o \end{Bmatrix} = \frac{qc_r\left(\frac{b}{2}\right)^3}{(GJ)_r} \begin{bmatrix} [B]_{ii} \| B \|_{io} \\ \| B \|_{oi} [B]_{oo} \end{bmatrix} \begin{Bmatrix} \left\{\frac{cc_l}{c_r}\right\}_i \\ \left\{\frac{cc_l}{c_r}\right\}_o \end{Bmatrix} \tag{50}$$

where the matrices $[B]$ and $\|B\|$ (with subscripts) are defined as

$$[B]_{ii} = [K_T]_i [\tau]_{ii} - [K_M]_i [\mu]_{ii} \tag{51}$$

$$\|B\|_{io} = [K_T]_i [\tau]_{io} - [K_M]_i [\mu]_{io} \tag{52}$$

$$\|B\|_{oi} = \|l_B\|_o [B]_{ii} \tag{53}$$

$$[B]_{oo} = \|l_B\|_o \|B\|_{io} + [K_T]_o [\tau]_{oo} - [K_M]_o [\mu]_{oo} \tag{54}$$

Equation (50) may be written as

$$\{\alpha_s\}_w = \frac{qc_r\left(\frac{b}{2}\right)^3}{(GJ)_r} [B] \left\{\frac{cc_l}{c_r}\right\}_w \tag{55}$$

The matrix $[B]$ is defined as

$$[B] = \begin{bmatrix} [B]_{ii} \| B \|_{io} \\ \| B \|_{oi} [B]_{oo} \end{bmatrix} \tag{56}$$

[redacted]

In combining the four submatrices the order of the resulting matrix may be reduced by one because the station at the break is represented twice - by two rows and two columns. The combination is effected by omitting the first rows of the submatrices $\|B\|_{oi}$ and $[B]_{oo}$ and by adding the first column of the submatrices $\|B\|_{io}$ and $[B]_{oo}$ to the last columns of submatrices $[B]_{ii}$ and $\|B\|_{oi}$, respectively.

Substitution of equation (2) into equation (55) yields the desired aeroelastic equation for symmetric flight

$$\{\alpha_s\}_w = \tilde{q}[A]\{\alpha\}_w \tag{57}$$

where the dimensionless parameter $\tilde{q}$ is defined by

$$\tilde{q} = \frac{qC_{L_{\alpha_0}} c_r \left(\frac{b}{2}\right)^3}{(GJ)_r} \tag{58}$$

and the aeroelastic matrix $[A]$ is defined by

$$[A] = [B][Q] \tag{59}$$

Solution of aeroelastic equation for dynamic pressure at divergence.- The condition for divergence is that the elements of $\{\alpha\}_s$ be finite when the geometric angle-of-attack $\{\alpha_g\}$ is zero along the entire span; therefore, the value of the parameter $\tilde{q}$ at divergence is the lowest real positive value of $\tilde{q}_D$ which satisfies the equation

$$\{\alpha_s\}_w = \tilde{q}_D[A]\{\alpha_s\}_w \tag{60}$$

If the lowest root is real and distinct, it can be computed by simple iteration. Often, however, the dominant roots of the matrix $[A]$ for M- and W-wings are not very well distinct and the simple iteration

procedure does not converge. If the matrix $[A]$ does have two dominant roots distinct from the others, the iteration procedure converges rapidly to the following relation between successive iteration columns:

$$\frac{1}{\tilde{q}_D^{(1)}\tilde{q}_D^{(2)}}\left\{[A]^{n-2}\{\alpha_t\}\right\} - \left(\frac{1}{\tilde{q}_D^{(1)}} + \frac{1}{\tilde{q}_D^{(2)}}\right)\left\{[A]^{n-1}\{\alpha_t\}\right\} + \left\{[A]^{n}\{\alpha_t\}\right\} = 0$$

where $\tilde{q}_D^{(1)}$ and $\tilde{q}_D^{(2)}$ are the dominant characteristic values and $\{\alpha_t\}$ is the trial column for $\{\alpha_s\}$. This equation represents as many linear algebraic equations as there are rows or columns in the matrix $[A]$. Each equation involves the two unknowns $\frac{1}{\tilde{q}_D^{(1)}\tilde{q}_D^{(2)}}$ and $\left(\frac{1}{\tilde{q}_D^{(1)}} + \frac{1}{\tilde{q}_D^{(2)}}\right)$, and any two of the equations can be solved for these unknowns, and, hence, for $\tilde{q}_D^{(1)}$ and $\tilde{q}_D^{(2)}$. (See also ref. 18.)

If the simple iteration of equation (60) yields a small negative value of $\tilde{q}_D$, there is the possibility that for these compounded configurations the next larger values (in the absolute sense) may be positive and still low enough to be of concern. The next higher value of $\tilde{q}_D$ may be found in the following manner. The modal column $\{\alpha_s\}_w^{(1)}$ obtained by the simple iteration of equation (60) is orthogonal to a modal row $\lfloor\beta\rfloor^{(2)}$ which corresponds to the second mode of divergence and satisfies the relation

$$\lfloor\beta\rfloor^{(2)} = \tilde{q}_D\lfloor\beta\rfloor^{(2)}[A]$$

The orthogonal relationship between $\{\alpha_s\}_w^{(1)}$ and $\lfloor\beta\rfloor^{(2)}$ may be expressed by

$$\lfloor\beta\rfloor^{(2)}\{\alpha_s\}_w^{(1)} = 0$$

or

$$\lfloor\beta\rfloor^{(2)} = \lfloor\beta\rfloor^{(2)}[S]$$

[redacted]

where the matrix $[S]$ is defined by

$$[S] = [1] - \begin{bmatrix} 0 & 0 & \cdots & 0 & \alpha_{s_1}^{(1)}/\alpha_{s_n}^{(1)} \\ 0 & 0 & \cdots & 0 & \alpha_{s_2}^{(1)}/\alpha_{s_n}^{(1)} \\ \cdot & \cdot & \cdots & \cdot & \cdot \\ \cdot & \cdot & \cdots & \cdot & \cdot \\ 0 & 0 & \cdots & 0 & \alpha_{s_{n-1}}^{(1)}/\alpha_{s_n}^{(1)} \\ 0 & 0 & \cdots & 0 & 1 \end{bmatrix}$$

The substitution of $[\beta]^{(2)}[S]$ for $[\beta]^{(2)}$ yields

$$[\beta]^{(2)} = \tilde{q}_D[\beta]^{(2)}[S][A]$$

The first mode of divergence has been eliminated in this equation; hence, the value of $\tilde{q}_D^{(2)}$ may be obtained by simple iteration. The correct value of $\tilde{q}_D^{(2)}$ may also be obtained by the iteration of $[S][A]$ with a column matrix, although the modal column obtained is spurious in the sense that it will not satisfy equation (60). (See also ref. 18.)

Solution of the aeroelastic equation at subcritical conditions.- Equation (57) may be rearranged to read

$$\left[[1] - \tilde{q}[A]\right]\{\alpha\}_w = \{\alpha_g\}_w \tag{61}$$

because

$$\{\alpha\} = \{\alpha_s\} + \{\alpha_g\} \tag{62}$$

The total angle of attack can then be found for any type of geometrical angle of attack by solving the simultaneous equations represented by matrix equation (61), using the given geometrical angle-of-attack distributions as the "knowns" on the right side of equation (61). Then the

[redacted]

corresponding lift distribution is obtained by premultiplying the angle-of-attack distribution by the matrix $[Q]$. For instance, the additional lift distribution for the flexible wing is obtained by setting α_g equal to unity along the entire semispan in equation (61) and then premultiplying the resulting column $\{\alpha\}$ by $[Q]$, namely

$$\left\{\frac{cc_l}{c_r C_{L_{\alpha_0}}}\right\}_w = [Q]\{\alpha\}_w \tag{63}$$

Within the limitations of the assumptions in the derivation of the matrix $[Q]$ (see ref. 5), the lift distribution on that part of the wing covered by the fuselage is proportional to the rigid-wing lift distribution in that region and is determined in magnitude by the angle of attack at the wing root; specifically,

$$\left\{\frac{cc_l}{c_r C_{L_{\alpha_0}}}\right\}_f = \frac{l_r}{l_{r_0}}\left\{\frac{cc_l}{c_r C_{L_{\alpha_0}}}\right\}_{f_0} \tag{64}$$

Integration of the lift distribution represented by equations (63) and (64) yields the lift coefficient,

$$C_L = \frac{L}{qS}$$

$$= \frac{c_r}{\bar{c}} C_{L_{\alpha_0}}\left(\frac{w}{b}\frac{l_r}{l_{r_0}}\left[I_1\right]_f\left\{\frac{cc_l}{c_r C_{L_{\alpha_0}}}\right\}_{f_0} + d_i\left[I_1\right]_i\left\{\frac{cc_l}{c_r C_{L_{\alpha_0}}}\right\}_i + d_o\left[I_1'\right]_o\left\{\frac{cc_l}{c_r C_{L_{\alpha_0}}}\right\}_o\right) \tag{65}$$

[redacted]

and the bending-moment coefficient

$$C_B = \frac{4M_{\frac{r}{2}}}{qSb}$$

$$= \frac{c_r}{\bar{c}} C_{L_{\alpha_0}} \left(\left(\frac{w}{b}\right)^2 \frac{l_r}{l_{r_0}} \left[II_1\right]_f \left\{ \frac{cc_l}{c_r C_{L_{\alpha_0}}} \right\}_{f_0} + d_i \left[d_i \left[II_1\right]_i + \right.\right.$$

$$\left.\left. \frac{w}{b} \left[I_1\right]_i \left\{ \frac{cc_l}{c_r C_{L_{\alpha_0}}} \right\}_i + d_o \left[d_o \left[II_1'\right]_o + \left(d_i + \frac{w}{b}\right) \left[I_1'\right]_o \right] \left\{ \frac{cc_l}{c_r C_{L_{\alpha_0}}} \right\}_o \right) \tag{66}$$

where the row matrices $\left[I_1\right]$ and $\left[II_1\right]$ are the first rows of the integrating matrices $\left[I\right]$ and $\left[II\right]$, respectively.

Similarly the pitching-moment coefficient is

$$C_m = \frac{M_p}{qS\bar{\bar{c}}}$$

$$= -\frac{c_r}{\bar{c}} C_{L_{\alpha_0}} \left(\frac{w}{b} \frac{l_r}{l_{r_0}} \left[I_1\right]_f \left[\frac{x}{\bar{\bar{c}}}\right]_f \left\{ \frac{cc_l}{c_r C_{L_{\alpha_0}}} \right\}_{f_0} + d_i \left[I_1\right]_i \left[\frac{x}{\bar{\bar{c}}}\right]_i \left\{ \frac{cc_l}{c_r C_{L_{\alpha_0}}} \right\}_i + \right.$$

$$\left. d_o \left[I_1'\right]_o \left[\frac{x}{\bar{\bar{c}}}\right]_o \left\{ \frac{cc_l}{c_r C_{L_{\alpha_0}}} \right\}_o \right) \tag{67}$$

the parameter x being the streamwise distance of the local aerodynamic center rearward of an unswept reference line through the quarter-chord point of the mean aerodynamic chord.

The lateral center of pressure $\bar{y}^*$ and the position of the wing aerodynamic center $\bar{a}$ may be calculated from the lift and moment coefficients given by equating (65), (66), and (67) as follows:

[redacted]

$$\bar{y}^* = \frac{C_B}{C_L} \tag{68}$$

$$\bar{a} = \frac{1}{4} - \frac{C_m}{C_L} \tag{69}$$

Antisymmetrical Flight Condition - Damping in Roll

The aerodynamic influence coefficients.- Equation (1) holds for antisymmetric lift distributions provided the aerodynamic influence-coefficient matrix $[Q]$ is replaced by a matrix $[Q_a]$. A method for calculating this matrix is given in reference 5 but, as is true for the symmetric lift distributions, certain modifications have to be made in the case of M-, W-, and Λ-wings. The modified matrix is

$$[Q_a] = \frac{C_{l_{d_0}}}{C_{L_{\alpha_0}}} \frac{\bar{c}}{c_r} \left[\frac{cc_l}{\bar{c}C_{l_{d_0}}}\right]_{w_0} \left[k_3 K' \left[\frac{1}{y^*}\right]_w + \right.$$

$$\frac{b}{w}\left(1 - K' + \left(\frac{w}{b}\right)^2 \left[II_1\right]_f \left[\frac{cc_l}{\bar{c}C_{l_{d_0}}}\right]_{f_0}\right)[l_r] +$$

$$\left. \frac{1 - k_3}{2} K' \left(\frac{b'}{b}\right)^2 \{1\} \left[II_1'\right]_w \left[\frac{cc_l}{y^*\bar{c}C_{l_{d_0}}}\right]_{w_0} \right] \tag{70}$$

where the parameter k_3 is

$$k_3 = \frac{F\sqrt{1 + \frac{16}{F^2}} + 4}{F\sqrt{1 + \frac{64}{F^2}} + 8} \tag{71}$$

and where the constant K' obtained from the rigid-wing lift distributions due to aileron deflection and due to antisymmetrical linear twist is

$$K' = \frac{C_{l_{\delta_0}}}{\frac{C_{l_{\alpha_0}}}{2}\int_0^1 \left(\frac{\alpha_\delta \delta}{y^*}\right)\left(\frac{cc_l}{\bar{c}C_{l_{\alpha_0}}}\right)_0 y^*\, dy^*} \tag{72}$$

Again, if strip theory is assumed for supersonic flow, $\left[Q_a\right]$ becomes

$$\left[Q_a\right] = \left[\frac{c}{c_r}\right] \tag{73}$$

The aeroelastic equation.- Equations (57) and (61) apply to antisymmetrical loadings provided the aeroelastic matrix $[A]$ is replaced by a matrix $\left[A_a\right]$ defined by

$$\left[A_a\right] = [B]\left[Q_a\right] \tag{74}$$

Solution of the aeroelastic equation.- The unit antisymmetrical linear lift distribution for the flexible wing is obtained by setting α_g equal to y^* in the antisymmetrical equivalent of equation (61) and premultiplying the resulting column $\{\alpha\}_w$ by $\left[Q_a\right]$, as follows

$$\left\{\frac{cc_l}{c_r C_{l_{\alpha_0}}}\right\}_w = \left[Q_a\right]\{\alpha\}_w \tag{75}$$

Equation (64), which gives the symmetrical lift on that part of the wing span covered by the fuselage, also applies to antisymmetrical lift and is

$$\left\{\frac{cc_l}{c_r C_{L_{\alpha_0}}}\right\}_f = \frac{l_r}{l_{r_0}}\left\{\frac{cc_l}{c_r C_{L_{\alpha_0}}}\right\}_{f_0}$$

[redacted]

the parameters l_r, l_{r_0}, and $\frac{cc_l}{c_r C_{L_{\alpha_0}}}$ now pertaining to the antisymmetrical case.

The damping-in-roll coefficient can be obtained by integrating this spanwise lift distribution, so that

$$C_{l_p} = -\frac{2M_{\xi}}{qSb}$$

$$= -\frac{1}{2}\frac{c_r}{\bar{c}} C_{L_{\alpha_0}}\left(\left(\frac{w}{b}\right)^2 \frac{l_r}{l_{r_0}}\left[II_1\right]_f \left\{\frac{cc_l}{c_r C_{L_{\alpha_0}}}\right\}_{f_0} + d_i\left[d_i\left[II_1\right]_i + \right.\right.$$

$$\left.\left.\frac{w}{b}\left[I_1\right]_i\right]\left\{\frac{cc_l}{c_r C_{L_{\alpha_0}}}\right\}_i + d_o\left[d_o\left[II_1'\right] + \left(d_i + \frac{w}{b}\right)\left[I_1'\right]_o\right]\left\{\frac{cc_l}{c_r C_{L_{\alpha_0}}}\right\}_o\right) \tag{76}$$

Antisymmetrical Flight Condition - Wing Loading Due to Aileron Deflection

The aeroelastic equation.- The running load on a flexible wing with aileron deflected is

$$\{l\} = qc_r\left\{\left\{\frac{cc_l}{c_r}\right\}^{(\alpha_s)} + \left\{\frac{cc_l}{c_r}\right\}^{(\delta)}\right\} \tag{77}$$

where the superscripts (α_s) and (δ) refer to the lift distributions due to wing deformation and unit aileron deflection, respectively. The corresponding running torque is

$$\{t\} = qc_r^2\left\{\left[\frac{e_1 c}{c_r}\right]\left\{\frac{cc_l}{c_r}\right\}^{(\alpha_s)} - \left[\frac{e_2 c}{c_r}\right]\left\{\frac{cc_l}{c_r}\right\}^{(\delta)}\right\} \tag{78}$$

[redacted]

The subscripts i and o used in the following analysis on the matrices of equations (76) and (77) refer, again, to the inner and outer part of the wing, respectively.

The use of the two preceding expressions in equations (14) to (24) yields

$$\left\{M_\Lambda\right\}_i = qc_r\left(\frac{b}{2}\right)^2\left\{\left[\mu\right]_{ii}\left\{\frac{cc_l}{c_r}\right\}_i^{(\alpha_s)} + \left[\bar{\mu}\right]_{ii}\left\{\frac{cc_l}{c_r}\right\}_i^{(\delta)} + \left\|\mu\right\|_{io}\left\{\frac{cc_l}{c_r}\right\}_o^{(\alpha_s)} + \left\|\bar{\mu}\right\|_{io}\left\{\frac{cc_l}{c_r}\right\}_o^{(\delta)}\right\} \tag{79}$$

$$\left\{M_\Lambda\right\}_o = qc_r\left(\frac{b}{2}\right)^2\left\{\left[\mu\right]_{oo}\left\{\frac{cc_l}{c_r}\right\}_o^{(\alpha_s)} + \left[\bar{\mu}\right]_{oo}\left\{\frac{cc_l}{c_r}\right\}_o^{(\delta)}\right\} \tag{80}$$

$$\left\{T_\Lambda\right\}_i = qc_r\left(\frac{b}{2}\right)^2\left\{\left[\tau\right]_{ii}\left\{\frac{cc_l}{c_r}\right\}_i^{(\alpha_s)} + \left[\bar{\tau}\right]_{ii}\left\{\frac{cc_l}{c_r}\right\}_i^{(\delta)} + \left\|\tau\right\|_{io}\left\{\frac{cc_l}{c_r}\right\}_o^{(\alpha_s)} + \left\|\bar{\tau}\right\|_{io}\left\{\frac{cc_l}{c_r}\right\}_o^{(\delta)}\right\} \tag{81}$$

$$\left\{T_\Lambda\right\}_o = qc_r\left(\frac{b}{2}\right)^2\left\{\left[\tau\right]_{oo}\left\{\frac{cc_l}{c_r}\right\}_o^{(\alpha_s)} + \left[\bar{\tau}\right]_{oo}\left\{\frac{cc_l}{c_r}\right\}_o^{(\delta)}\right\} \tag{82}$$

[redacted]

where the matrices $\left[\bar{\mu}\right]$ and $\left[\bar{\tau}\right]$ (with subscripts) are the same as the corresponding matrixes $\left[\mu\right]$ and $\left[\tau\right]$, except that $\left|\frac{e_1 c}{c_r}\right|$ must be replaced everywhere by the diagonal matrix - $\left|\frac{e_2 c}{c_r}\right|$; thus,

$$\left[\bar{\mu}\right]_{ii} = \frac{d_i^2}{\cos \Lambda_i}\left[II\right]_i + d_i \frac{c_r}{b/2} \sin \Lambda_i \left[I\right]_i \left|\frac{e_2 c}{c_r}\right|_i \tag{83}$$

$$\left\|\bar{\mu}\right\|_{io} = d_o^2 \frac{\cos(\Lambda_i - \Lambda_o)}{\cos \Lambda_o}\left\|l_B\right\|_i \left[II'\right]_o + \frac{d_o}{\cos \Lambda_i}\left|y^*_B - y^*\right| \left\|l_B\right\|_i \left[I'\right]_o +$$

$$d_o \frac{c_r}{b/2} \sin \Lambda_i \left\|l_B\right\|_i \left[I'\right]_o \left|\frac{e_2 c}{c_r}\right|_o \tag{84}$$

$$\left[\bar{\mu}\right]_{oo} = \frac{d_o^2}{\cos \Lambda_o}\left[II'\right]_o + d_o \frac{c_r}{b/2} \sin \Lambda_o \left[I'\right]_o \left|\frac{e_2 c}{c_r}\right|_o \tag{85}$$

$$\left[\bar{\tau}\right]_{ii} = -d_i \frac{c_r}{b/2} \cos \Lambda_i \left[I\right]_i \left|\frac{e_2 c}{c_r}\right|_i \tag{86}$$

$$\left\|\bar{\tau}\right\|_{io} = d_o^2 \frac{\sin(\Lambda_i - \Lambda_o)}{\cos \Lambda_o}\left\|l_B\right\|_i \left[II'\right]_o -$$

$$d_o \frac{c_r}{b/2} \cos \Lambda_i \left\|l_B\right\|_i \left[I'\right]_o \left|\frac{e_2 c}{c_r}\right|_o \tag{87}$$

[redacted]

$$\left[\bar{\tau}\right]_{oo} = -d_o \frac{c_r}{b/2} \cos \Lambda_o \left[I'\right]_o \left[\frac{e_2 c}{c_r}\right]_o \tag{88}$$

Substitution of equations (79) to (82) into equations (44) and (45) yields

$$\begin{Bmatrix} \{\alpha_s\}_i \\ \{\alpha_s\}_o \end{Bmatrix} = \frac{qc_r\left(\frac{b}{2}\right)^3}{(GJ)_r} \begin{bmatrix} \left[\bar{B}\right]_{ii} \left\|B\right\|_{io} \\ \left\|B\right\|_{oi} \left[\bar{B}\right]_{oo} \end{bmatrix} \begin{Bmatrix} \left\{\frac{cc_l}{c_r}\right\}_i^{(\alpha_s)} \\ \left\{\frac{cc_l}{c_r}\right\}_o^{\{\alpha_s\}} \end{Bmatrix} + \frac{qc_r\left(\frac{b}{2}\right)^3}{(GJ)_r} \begin{bmatrix} \left[\bar{B}\right]_{ii} \left\|\bar{B}\right\|_{io} \\ \left\|\bar{B}\right\|_{oi} \left[\bar{B}\right]_{oo} \end{bmatrix} \begin{Bmatrix} \left\{\frac{cc_l}{c_r}\right\}_i^{(\delta)} \\ \left\{\frac{cc_l}{c_r}\right\}_o^{(\delta)} \end{Bmatrix} \tag{89}$$

the various matrices $\left[\bar{B}\right]$ (with subscripts) being defined as

$$\left[\bar{B}\right]_{ii} = \left[K_T\right]_i \left[\bar{\tau}\right]_{ii} - \left[K_M\right]_i \left[\bar{\mu}\right]_{ii} \tag{90}$$

$$\left\|\bar{B}\right\|_{io} = \left[K_T\right]_i \left\|\bar{\tau}\right\|_{io} - \left[K_M\right]_i \left\|\bar{\mu}\right\|_{io} \tag{91}$$

$$\left\|\bar{B}\right\|_{oi} = \left\|l_B\right\|_o \left[\bar{B}\right]_{ii} \tag{92}$$

$$\left[\bar{B}\right]_{oo} = \left\|l_B\right\|_o \left[\bar{B}\right]_{io} + \left[K_T\right]_o \left[\bar{\tau}\right]_{oo} - \left[K_M\right]_o \left[\bar{\mu}\right]_{oo} \tag{93}$$

[redacted]

Equation (89) may then be rewritten as

$$\left\{\alpha_s\right\}_w = \frac{qc_r\left(\frac{b}{2}\right)^3}{(GJ)_r}\left\{\left[B\right]\left\{\frac{cc_l}{c_r}\right\}_w^{(\alpha_s)} + \left[\bar{B}\right]\left\{\frac{cc_l}{c_r}\right\}_w^{(\delta)}\right\} \tag{94}$$

where

$$\left[\bar{B}\right] = \begin{bmatrix} \left[\bar{B}\right]_{ii} & \left\|\bar{B}\right\|_{io} \\ \left\|\bar{B}\right\|_{oi} & \left[\bar{B}\right]_{oo} \end{bmatrix} \tag{95}$$

except that, again, in the processes of constructing the matrix $\left[\bar{B}\right]$ from its submatrices, it is reduced in order in the same manner as the matrix $\left[B\right]$.

The aeroelastic equation for aileron deflection is then obtained by substituting equations (74) and (75) in equation (94), so that

$$\left[\left[1\right] - \tilde{q}\left[A_a\right]\right]\left\{\alpha_s\right\}_w^{(\delta)} = \tilde{q}\left[\bar{B}\right]\left\{\frac{cc_l}{c_r C_{L_{\alpha_0}}}\right\}_w^{(\delta)} \tag{96}$$

Solution of the aeroelastic equation.- Equation (96) can be solved in the same manner as equation (61). Once it has been solved for a given set of knowns defined by the right side of equation (96), the rolling-moment coefficient due to a unit aileron deflection can be obtained from

$$c_{l_\delta} = \frac{2M_{x'}^{(\delta)}}{qSb}$$

$$= c_{l_{\delta_0}} + \frac{1}{2}\frac{c_r}{\bar{c}} C_{L_{\alpha_0}}\left(\left(\frac{w}{b}\right)^2 \frac{l_r}{l_{r_0}}\left[II\right]_f\left\{\frac{cc_l}{c_r C_{L_{\alpha_0}}}\right\}_{f_0} + \right.$$

$$d_i\left[d_i\left[II_1\right]_i + \frac{w}{b}\left[I_1\right]_i\right]\left\{\frac{cc_l}{c_r C_{L_{\alpha_0}}}\right\}_i^{(\alpha_s)} +$$

$$\left. d_o\left[d_o\left[II_1'\right]_o + \left(d_i + \frac{w}{b}\right)\left[I_1'\right]_o\right]\left\{\frac{cc_l}{c_r C_{L_{\alpha_0}}}\right\}_o^{(\alpha_s)}\right) \tag{97}$$

[redacted]

where

$$\left\{\frac{cc_l}{c_r C_{L_{\alpha_0}}}\right\}_w^{(\alpha_s)} = \left[\hat{a}_a\right]\left\{\alpha_s\right\}_w^{(\delta)} \tag{98}$$

The rate of roll per unit aileron deflection is then given by

$$\left(\frac{pb}{2V}\right)_{\delta=1} = -\frac{C_{l_\delta}}{C_{l_p}} \tag{99}$$

If C_{l_δ} is for unit effective aileron deflection $\left(\text{unit } \alpha_\delta\delta\right)$ instead of unit actual aileron deflection then

$$\left(\frac{pb}{2V}\right)_{\delta=1} = -\alpha_\delta\delta\,\frac{C_{l_\delta}}{C_{l_p}} \tag{100}$$

The condition for aileron reversal is that the rolling-moment coefficient C_{l_δ} be zero. Combining the row integrating matrices of equation (97) into one row matrix, and setting the resulting expression equal to zero yields

$$C_{l_{\delta_0}} + \frac{1}{2} C_{l_{\alpha_0}}\left[II_0\right]\left[\hat{a}_a\right]\left\{\alpha_s\right\}_w^{(\delta)} = 0 \tag{101}$$

the row matrix $\left[II_0\right]$ being defined by

$$\left[II_0\right] = \left[\left[II_0\right]_i, \left[II_0\right]_o\right] = \left[II_0\right]_r \tag{102}$$

where, as in the case of the matrices $\left[B\right]$ and $\left[\bar{B}\right]$, the order of the first row matrix on the right side of equation (102) is of order one lower than the sum of the orders of the constituent row matrices, because

[redacted]

in combining these constituent row matrices the first element of submatrix $\left\lfloor II_0 \right\rfloor_o$ is added to the last element of $\left\lfloor II_0 \right\rfloor_i$. These submatrices are, in turn, defined by

$$\left\lfloor II_0 \right\rfloor_i = \frac{c_r}{\bar{c}} \left\lfloor d_i^2 \left\lfloor II \right\rfloor_i + d_i \frac{w}{b} \left\lfloor I \right\rfloor_i \right\rfloor \tag{103}$$

$$\left\lfloor II_0 \right\rfloor_o = \frac{c_r}{\bar{c}} \left\lfloor d_o^2 \left\lfloor II' \right\rfloor_o + d_o \left(d_i + \frac{w}{b} \right) \left\lfloor I' \right\rfloor_o \right\rfloor \tag{104}$$

and the row matrix $\left\lfloor II_0 \right\rfloor_r$ is defined by

$$\left\lfloor II_0 \right\rfloor_r = \frac{c_r}{\bar{c}} \frac{\left(\frac{w}{b} \right)^2}{\left(\frac{cc_l}{\bar{c} C_{l_{d_0}}} \right)_{r_0}} \left\lfloor II \right\rfloor_f \left\{ \frac{cc_l}{\bar{c} C_{l_{d_0}}} \right\}_{f_0} \left\lfloor 1 \; 0 \; 0 \; \ldots \; 0 \right\rfloor \tag{105}$$

The quantities $\left(\frac{cc_l}{\bar{c} C_{l_d}} \right)_{f_0}$ are the same as those used in the derivation of the matrix $\left[Q_a \right]$ in equation (70).

Division of equation (101) by $C_{l_{\delta_0}}$ yields

$$1 = -\frac{C_{L_{\alpha_0}}}{2 C_{L_{\delta_0}}} \left| II_0 \right| \left[Q_a \right] \left\{ \alpha_s \right\}_w^{(\delta)} \tag{106}$$

and subsequent premultiplication of this equation by the column matrix $\left\{ \frac{cc_l}{c_r C_{L_{\alpha_0}}} \right\}_w^{(\delta)}$ yields

[redacted]

$$\left\{\frac{cc_l}{c_r C_{L\alpha_0}}\right\}_w^{(\delta)} = -\frac{C_{L\alpha_0}}{2C_{l\delta_0}}\left\{\frac{cc_l}{c_r C_{L\alpha_0}}\right\}_w^{(\delta)} \left[II_0\right]\left[Q_a\right]\left\{\alpha_s\right\}_w^{(\delta)} \tag{107}$$

This expression may now be used to eliminate $\left\{\frac{cc_l}{c_r C_{L\alpha_0}}\right\}_w^{(\delta)}$ from equation (96) with the result that

$$\left\{\alpha_s\right\}_w^{(\delta)} = \tilde{q}_R\left[A_R\right]\left\{\alpha_s\right\}_w^{(\delta)} \tag{108}$$

where the aileron reversal matrix $\left[A_R\right]$ is defined as

$$\left[A_R\right] = \left[A_a\right] - \frac{C_{L\alpha}}{2C_{l\delta_0}}\left[\bar{B}\right]\left\{\frac{cc_l}{c_r C_{L\alpha_0}}\right\}_w^{(\delta)} \left[II_0\right]\left[Q_a\right]\left\{\alpha_s\right\}_w^{(\delta)} \tag{109}$$

The value of $\tilde{q}$ at aileron reversal is the lowest real positive value of $\tilde{q}_R$ which satisfies equation (108).

[redacted]

REFERENCES

1. Diederich, Franklin W., and Foss, Kenneth A.: Charts and Approximate Formulas for the Estimation of Aeroelastic Effects on the Loading of Swept and Unswept Wings. NACA TN 2608, 1952.

2. Diederich, Franklin W., and Foss, Kenneth A.: The Calculation of Certain Static Aeroelastic Phenomena of Wings With Tip Tanks or Boom-Mounted Lifting Surfaces. NACA RM L52A22, 1952.

3. Diederich, Franklin W.: Calculation of the Aerodynamic Loading of Swept and Unswept Flexible Wings of Arbitrary Stiffness. NACA Rep. 1000, 1950. (Supersedes NACA TN 1876.)

4. Diederich, Franklin W.: Calculation of the Lateral Control of Swept and Unswept Flexible Wings of Arbitrary Stiffness. NACA Rep. 1024, 1951.

5. Diederich, Franklin W.: A Simple Approximate Method for Calculating Spanwise Lift Distributions and Aerodynamic Influence Coefficients at Subsonic Speeds. NACA TN 2751, 1952.

6. Diederich, Franklin W., and Latham, W. Owen: Calculated Aerodynamic Loadings of M, W, and Λ Wings in Incompressible Flow. NACA RM L51E29, 1951.

7. Evvard, John C.: Use of Source Distributions for Evaluating Theoretical Aerodynamics of Thin Finite Wings at Supersonic Speeds. NACA Rep. 951, 1950.

8. Cohen, Doris: The Theoretical Lift of Flat Swept-Back Wings at Supersonic Speeds. NACA TN 1555, 1948.

9. Foss, Kenneth A., and Diederich, Franklin W.: Charts and Approximate Formulas for the Estimation of Aeroelastic Effects on the Lateral Control of Swept and Unswept Wings. NACA TN 2747, 1952.

10. Malvestuto, Frank S., Jr., Margolis, Kenneth, and Ribner, Herbert S.: Theoretical Lift and Damping in Roll at Supersonic Speeds of Thin Sweptback Tapered Wings With Streamwise Tips, Subsonic Leading Edges, and Supersonic Trailing Edges. NACA Rep. 970, 1950. (Supersedes NACA TN 1860.)

11. Harmon, Sidney M., and Jeffreys, Isabella: Theoretical Lift and Damping in Roll of Thin Wings With Arbitrary Sweep and Taper at Supersonic Speeds. Supersonic Leading and Trailing Edges. NACA TN 2114, 1950.

[redacted]

12. Margolis, Kenneth: Theoretical Lift and Damping in Roll of Thin Sweptback Tapered Wings With Raked-In and Cross-Stream Wing Tips at Supersonic Speeds. Subsonic Leading Edges. NACA TN 2048, 1950.

13. Jones, Arthur L., and Alksne, Alberta: The Damping Due to Roll of Triangular, Trapezoidal, and Related Plan Forms in Supersonic Flow. NACA TN 1548, 1948.

14. Diederich, Franklin W., and Budiansky, Bernard: Divergence of Swept Wings. NACA TN 1680, 1948.

15. Katz, Ellis R., Marlay, Edward T., and Pepper, William B.: Flight Investigation at Mach Numbers From 0.8 to 1.4 to Determine the Zero-Lift Drag of Wings With "M" and "W" Plan Forms. NACA RM L50G31, 1950.

16. Margolis, Kenneth: Supersonic Wave Drag of Sweptback Tapered Wings at Zero Lift. NACA TN 1448, 1947.

17. Margolis, Kenneth: Supersonic Wave Drag of Nonlifting Sweptback Tapered Wings With Mach Lines Behind the Line of Maximum Thickness. NACA TN 1672, 1948.

18. Frazer, R. A., Duncan, W. J., and Collar, A. R.: Elementary Matrices and Some Applications to Dynamic and Differential Equations. The Macmillan Co., 1946.

TABLE 1

GEOMETRIC, STRUCTURAL, AND AERODYNAMIC PARAMETERS

Wing number	Geometric and structural parameters										Aerodynamic parameters					
											Subsonic			Supersonic		
	Plan form	Type	A	λ	$\Lambda_{\frac{c}{4}}$	$\Lambda_{\frac{c}{2}}$	y^*_B	w/b	e	$(GJ)_r/(EI)_r$	Mach number	$C_{L_{\alpha_0}}$	$C_{l_{\delta_a}}$	Mach number	$C_{L_{\alpha_0}}$	$C_{l_{\delta_a}}$
1		M	6	0.5	-45°	45°	0.3	0.1	0.45	0.794	0	3.63	0.370	2	2.83	0.393
2		M	6	.5	-45°	45°	.5	.1	.45	.794	0	3.54	.379	2	2.83	.393
3		M	6	.5	-45°	45°	.7	.1	.45	.794	0	3.46	.378	2	2.83	.393
4		W	6	.5	45°	-45°	.3	.1	.45	.794	0	3.55	.359	2	2.83	.393
5		W	6	.5	45°	-45°	.5	.1	.45	.794	0	3.57	.368	2	2.83	.393
6		W	6	.5	45°	-45°	.7	.1	.45	.794	0	3.57	.376	2	2.83	.393
7		A	6	.5	45°	0°	.3	.1	.45	.794	0	4.16	.440	2	2.50	.347
8		A	6	.5	45°	0°	.7	.1	.45	.794	0	3.69	.408	2	2.71	.376
9		Inv. A	6	.5	-45°	0°	.7	.1	.45	.794	0	3.55	.400	2	2.71	.376
10		Swept-forward	6	.5	-45°	----	---	.1	.45	.794	0	3.33	.342	2	2.83	.393
11		Unswept	6	.5	0°	----	---	.1	.45	.794	0	4.32	.413	2	2.30	.320
12	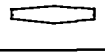	Swept-back	6	.5	45°	----	---	.1	.45	.794	0	3.44	.355	2	2.83	.393

Root rotation constants					
Λ_1	Q_{α_T}	Q_{α_M}	Q_{Γ_T}	Q_{Γ_M}	w_e
-45°	0	-0.40	-1.60	-0.25	0.0896
0°	0	0	0	0	0
45°	0	0.40	1.60	-0.25	0.0896

Aileron parameters				
		b_a/b	c_a/c	c_δ
Subsonic	All wings	0.5	0.2	0.5
	Movable tips	0.3	1.0	1.0
Supersonic	All wings	0.3	0.2	0.2
	Ordinary wings	0.5	0.2	0.2

TABLE 2

SUMMARY OF RESULTS

(a) Subsonic flow

Wing number	Aileron configuration[1]	$\tilde{q}_D$		$\tilde{q}_R$	$\tilde{q}$	$\frac{C_L}{C_{L_0}}$	$\bar{y}^*$	$\bar{a}$	$\frac{C_{l_p}}{C_{l_{p_0}}}$	$\frac{C_{l_\delta}}{C_{l_{\delta_0}}}$	$\left(\frac{pb}{2V}\right)_{\delta=1}$
1	(1)	-9.43	-183.5	18.5	0	1.000	0.441	0.263	1.000	1.000	0.542
					3.0	.864	.417	.226	.773	.609	.427
					6.0	.781	.397	.196	.633	.379	.324
2	(1)	-15.49	65.9	20.3	0	1.000	.430	.257	1.000	1.000	.557
					3.0	.966	.428	.253	.875	.696	.443
					6.0	.949	.408	.248	.788	.483	.341
3	(1)	11.86		17.1	0	1.000	.416	.288	1.000	1.000	.573
					3.0	1.240	.435	.247	1.293	1.047	.464
					6.0	1.726	.458	.199	1.878	1.176	.359
4	(1)	6.70		18.2	0	1.000	.406	.325	1.000	1.000	.558
					3.0	1.460	.453	.266	1.818	1.586	.487
5	(1)	8.07		16.8	0	1.000	.429	.294	1.000	1.000	.546
					3.0	1.244	.370	.301	1.490	1.288	.472
6	(1)	16.63		14.1	0	1.000	.450	.270	1.000	1.000	.541
					3.0	.983	.461	.281	1.053	.850	.437
					6.0	.987	.479	.301	1.150	.698	.328
6	(2)	16.63		Complex	0	1.000	.450	.270	1.000	1.000	.655
					3.0	.983	.461	.281	1.053	1.124	.699
					6.0	.987	.479	.301	1.150	1.319	.750
7	(1)	24.73		16.0	0	1.000	.448	.244	1.000	1.000	.554
					3.0	1.076	.461	.252	1.119	.920	.455
					6.0	1.176	.476	.262	1.273	.809	.352
8	(1)	-20.68	70.7	11.9	0	1.000	.466	.319	1.000	1.000	.547
					3.0	.899	.458	.296	.884	.656	.406
					6.0	.820	.451	.275	.791	.387	.268
8	(2)	-20.68	70.7	Complex	0	1.000	.466	.319	1.000	1.000	.699
					3.0	.899	.458	.296	.884	.874	.691
					6.0	.820	.451	.275	.791	.774	.683
9	(1)	6.32		11.7	0	1.000	.418	.276	1.000	1.000	.570
					3.0	1.582	.468	.165	1.934	1.451	.428
10	(1)	7.76		14.3	0	1.000	.378	.374	1.000	1.000	.586
					3.0	1.406	.407	.311	2.171	1.830	.494
11	(1)	28.30		17.3	0	1.000	.425	.239	1.000	1.000	.572
					3.0	1.086	.433	.240	1.115	.927	.475
					6.0	1.194	.442	.241	1.262	.834	.378
12	(1)	-8.82	-78.4	14.4	0	1.000	.455	.310	1.000	1.000	.565
					3.0	.816	.438	.262	.751	.570	.428
					6.0	.705	.423	.221	.602	.322	.302

[1]Aileron configurations:
(1) 50-percent-semispan outboard aileron, 20 percent chord.
(2) 30-percent-semispan outboard aileron, 100 percent chord.
(3) 30-percent-semispan outboard aileron, 20 percent chord.

NACA

[redacted]

TABLE 2 - Concluded

SUMMARY OF RESULTS

(b) Supersonic flow

Wing number	Aileron configuration[1]	$\tilde{q}_D$		$\tilde{q}_R$	$\tilde{q}$	$\frac{C_L}{C_{L_0}}$	$\bar{y}^*$	$\bar{a}$	$\frac{C_{l_p}}{C_{l_{p_0}}}$	$\frac{C_{l_\delta}}{C_{l_{\delta_0}}}$	$\left(\frac{pb}{2V}\right)_{\delta=1}$
1	(3)	-4.56	-47.5	5.55	0	1.000	0.444	0.450	1.000	1.000	0.1397
					3.0	.823	.394	.371	.648	.250	.0538
					6.0	.747	.363	.326	.494	-.029	-.0081
2	(3)	-5.75	Complex	5.65	0	1.000	.444	.450	1.000	1.000	.1397
					3.0	.902	.412	.436	.751	.293	.0545
					6.0	.870	.392	.430	.634	-.027	-.0060
3	(3)	-12.70	15.8	5.74	0	1.000	.444	.450	1.000	1.000	.1397
					3.0	1.102	.458	.402	1.105	.542	.0686
					6.0	1.303	.472	.357	1.326	-.049	-.0052
4	(3)	6.03		10.85	0	1.000	.444	.450	1.000	1.000	.1397
					3.0	1.427	.523	.337	1.902	1.584	.1163
5	(3)	7.61		11.07	0	1.000	.444	.450	1.000	1.000	.1397
					3.0	1.193	.493	.442	1.494	1.288	.1204
6	(3)	-15.44	18.9	8.74	0	1.000	.444	.450	1.000	1.000	.1397
					3.0	.924	.432	.409	.926	.650	.0981
					6.0	.964	.432	.391	.905	.328	.0506
7	(3)	-134.05		8.40	0	1.000	.444	.450	1.000	1.000	.1397
					3.0	.997	.437	.440	.981	.633	.0901
					6.0	.980	.435	.437	.962	.277	.0402
8	(3)	-8.29	-190.1	7.10	0	1.000	.444	.450	1.000	1.000	.1397
					3.0	.861	.402	.343	.739	.410	.0775
					6.0	.768	.376	.277	.588	.084	.0200
9	(3)	8.04		7.41	0	1.000	.444	.450	1.000	1.000	.1397
					3.0	1.323	.501	.310	1.584	.983	.0867
10	(3)	4.70		8.41	0	1.000	.444	.450	1.000	1.000	.1397
					3.0	1.765	.564	.125	2.615	2.001	.1069
10	(1)	4.70		6.60	0	1.000	.444	.450	1.000	1.000	.2200
					3.0	1.765	.564	.125	2.615	1.633	.1374
11	(3)	∞		8.50	0	1.000	.444	.450	1.000	1.000	.1397
					3.0	1.000	.444	.450	1.000	.647	.0612
					6.0	1.000	.444	.450	1.000	.294	.0278
11	(1)	∞		9.60	0	1.000	.444	.450	1.000	1.000	.2200
					3.0	1.000	.444	.450	1.000	.688	.1025
12	(3)	-4.22	-39.3	5.11	0	1.000	.444	.450	1.000	1.000	.1397
					3.0	.820	.382	.275	.623	.215	.0482
					6.0	.732	.350	.185	.465	-.057	-.0172
12	(1)	-4.22	-39.3	8.57	0	1.000	.444	.450	1.000	1.000	.2200
					3.0	.820	.382	.275	.623	.355	.1255

[1]Aileron configurations:
(1) 50-percent-semispan outboard aileron, 20 percent chord.
(2) 30-percent-semispan outboard aileron, 100 percent chord.
(3) 30-percent-semispan outboard aileron, 20 percent chord.

NACA

[redacted]

TABLE 3

THE INTEGRATING MATRICES

(a) $y^*_B = 0.3$

$[I]_i$

y*	.1	.2	.3
.1	0.16667	0.66667	0.16667
.2	-.04167	.33333	.20833
.3	0	0	0

$[I']_o$

y*	.30	.44	.58	.72	.86
.30	0.06667	0.25000	0.18333	0.17895	0.27000
.44	-.01667	.11667	.20000	.17895	.27000
.58	0	-.01667	.11667	.17895	.27000
.72	0	0	-.01667	.09562	.27000
.86	0	0	0	-.03771	.18667

$[II]_i$

y*	.1	.2	.3
.1	0	0.33333	0.16667
.2	-.01042	.06250	.07292
.3	0	0	0

$[II']_o$

y*	.30	.44	.58	.72	.86
.30	0	0.04500	0.07833	0.10052	0.22776
.44	-.00167	.00500	.04000	.06473	.17376
.58	0	-.00167	.00500	.02894	.11976
.72	0	0	-.00167	-.00185	.06576
.86	0	0	0	-.00431	.01676

$[I]''_i$

y*	.1	.2	.3
.1	0	0	0
.2	.20833	.33333	-.04167
.3	.16667	.66667	.16667

$[I]''_o$

y*	.30	.44	.58	.72	.86
.30	0	0	0	0	0
.44	.08333	.13333	-.01667	0	0
.58	.08333	.21667	.11667	-.01667	0
.72	.08333	.21667	.20000	.11667	-.01667
.86	.08333	.21667	.20000	.20000	.11667

TABLE 3 - Continued

THE INTEGRATING MATRICES

(b) $y^*_3 = 0.5$

$[I]_i$

y*	.1	.2333	.3667	.5
.1	0.11111	0.41667	0.33333	0.13889
.2333	-.02778	.19444	.36111	.13889
.3667	0	-.02778	.22222	.13889
.5	0	0	0	0

$[I']_o$

y*	.5	.625	.75	.875
.5	0.08333	0.31250	0.20286	0.33750
.625	-.02083	.14583	.22369	.33750
.75	0	-.02083	.11953	.33750
.875	0	0	-.04714	.23333

$[II]_i$

y*	.1	.2333	.3667	.5
.1	0	0.12500	0.25000	0.12500
.2333	-.00463	.01389	.13426	.07870
.3667	0	-.00463	.02778	.03241
.5	0	0	0	0

$[II']_o$

y*	.5	.625	.75	.875
.5	0	0.07031	0.09854	0.27150
.625	-.00260	.00781	.04522	.18713
.75	0	-.00260	-.00289	.10275
.875	0	0	-.00673	.02619

$[I]''_i$

y*	.1	.2333	.3667	.5
.1	0	0	0	0
.2333	.13889	.22222	-.02778	0
.3667	.13889	.36111	.19444	-.02778
.5	.13889	.33333	.41667	.11111

$[I]''_o$

y*	.5	.625	.75	.875
.5	0	0	0	0
.625	.10417	.16667	-.02083	0
.75	.10417	.27083	.14583	-.02083
.875	.10417	.27083	.25000	.14583

NACA

[redacted]

TABLE 3 - Continued

THE INTEGRATING MATRICES

(c) $y^*_B = 0.7$

$[I]_i$

y*	.10	.25	.40	.55	.70
.10	0.08333	0.31250	0.22917	0.27083	0.10417
.25	-.02083	.14583	.25000	.27083	.10417
.40	0	-.02083	.14583	.27083	.10417
.55	0	0	-.02083	.16667	.10417
.70	0	0	0	0	0

$[I']_o$

y*	.7	.8	.9
.7	0.11111	0.38159	0.42222
.8	-.02778	.15937	.45000
.9	0	-.06285	.31111

$[II]_i$

y*	.10	.25	.40	.55	.70
.10	0	0.07031	0.12240	0.21094	0.09635
.25	-.00260	.00781	.06250	.14323	.07031
.40	0	-.00260	.00781	.07552	.04427
.55	0	0	-.00260	.01563	.01823
.70	0	0	0	0	0

$[II']_o$

y*	.7	.8	.9
.7	0	0.09427	0.32804
.8	-.00463	-.00514	.18267
.9	0	-.01197	.04656

$[I]''_i$

y*	.10	.25	.40	.55	.70
.10	0	0	0	0	0
.25	.10417	.16667	-.02083	0	0
.40	.10417	.27083	.14583	-.02083	0
.55	.10417	.27083	.25000	.14583	-.02083
.70	.10417	.27083	.22917	.31250	.08333

$[I]''_o$

y*	.7	.8	.9
.7	0	0	0
.8	.13889	.22222	-.02778
.9	.13889	.36111	.19444

NACA

TABLE 3 - Concluded

THE INTEGRATING MATRICES

(d) y^*_B = 1 or 0 (ordinary wings)

$[I']_w$

y*	.10	.25	.40	.55	.70	.85
.10	0.05556	0.20833	0.15278	0.16667	0.14913	0.22500
.25	-.01389	.09722	.16667	.16667	.14913	.22500
.40	0	-.01389	.09722	.16667	.14913	.22500
.55	0	0	-.01389	.09722	.14913	.22500
.70	0	0	0	-.01389	.07968	.22500
.85	0	0	0	0	-.03143	.15556

$[II']_w$

y*	.10	.25	.40	.55	.70	.85
.10	0	0.03125	0.05440	0.08333	0.09466	0.19567
.25	-.00116	.00347	.02778	.05556	.06980	.15817
.40	0	-.00116	.00347	.02778	.04495	.12067
.55	0	0	-.00116	.00347	.02010	.08317
.70	0	0	0	-.00116	-.00129	.04567
.85	0	0	0	0	-.00299	.01164

$[I]''_w$

y*	.10	.25	.40	.55	.70	.85
.10	0	0	0	0	0	0
.25	.06944	.11111	-.01389	0	0	0
.40	.06944	.18056	.09722	-.01389	0	0
.55	.06944	.18056	.16667	.09722	-.01389	0
.70	.06944	.18056	.16667	.16667	.09722	-.01389
.85	.06944	.18056	.16667	.16667	.16667	.09722

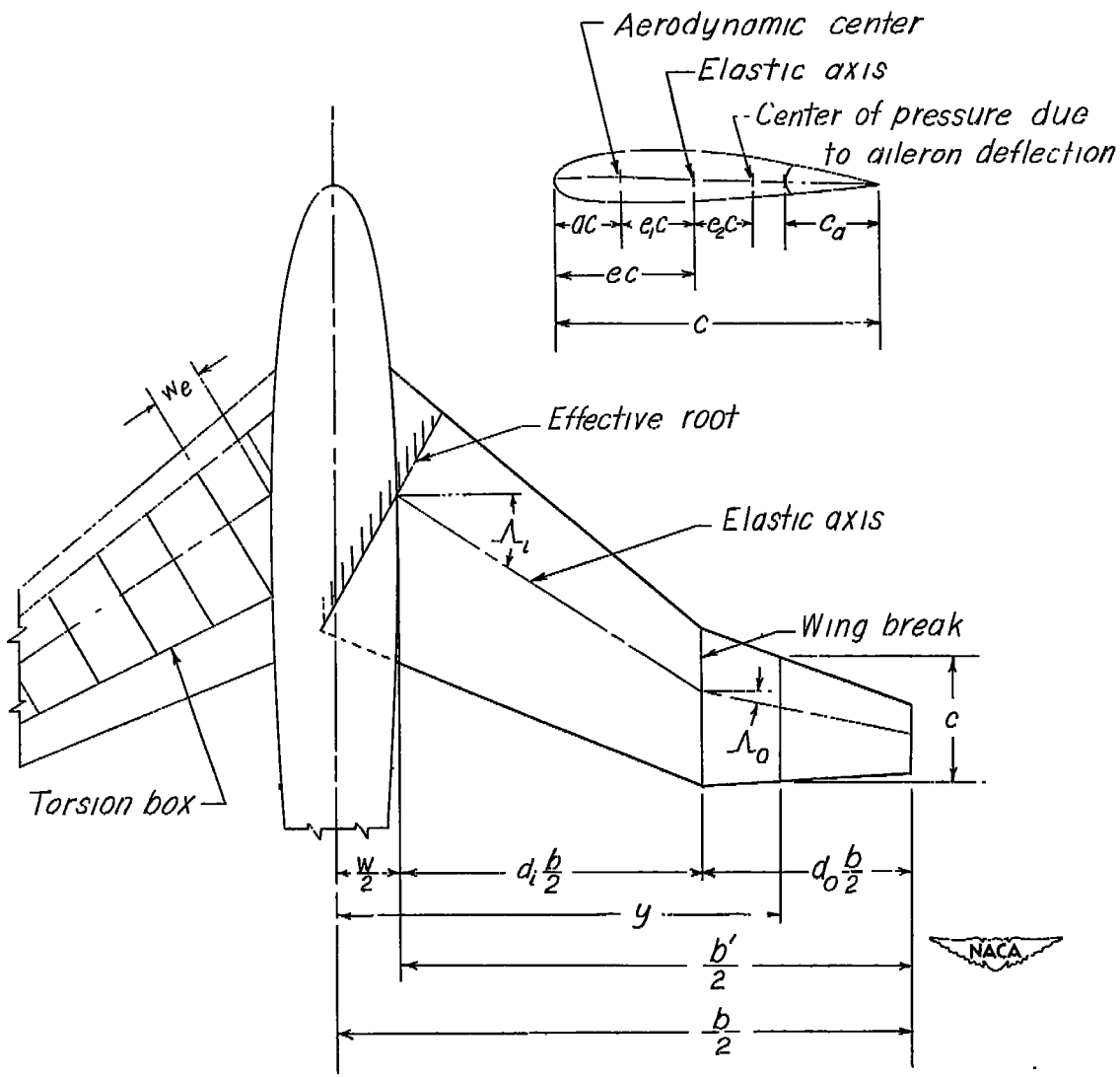

Figure 1.- Definitions of geometric parameters.

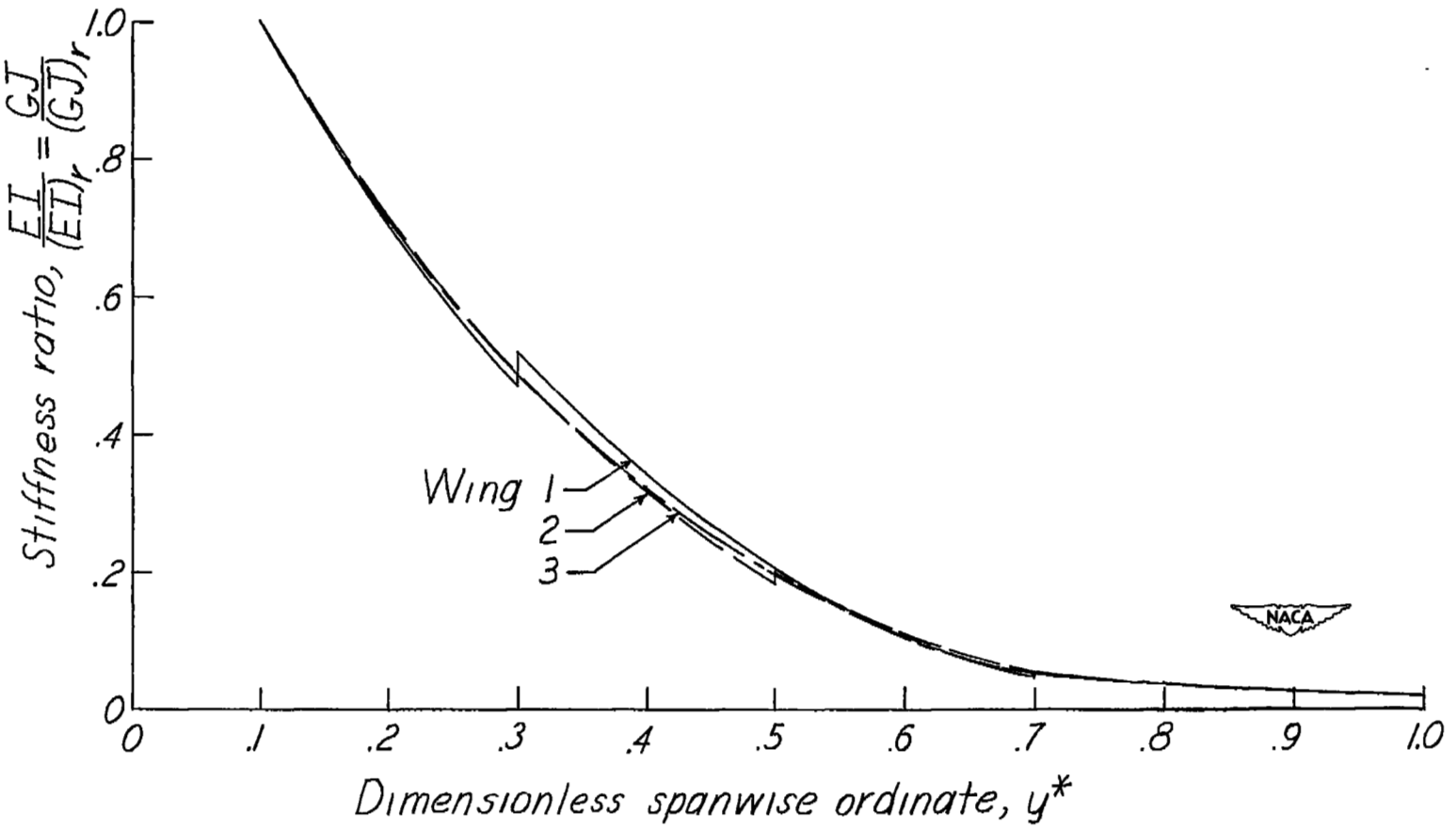

(a) M-wings.

Figure 2.- The spanwise variations of stiffness.

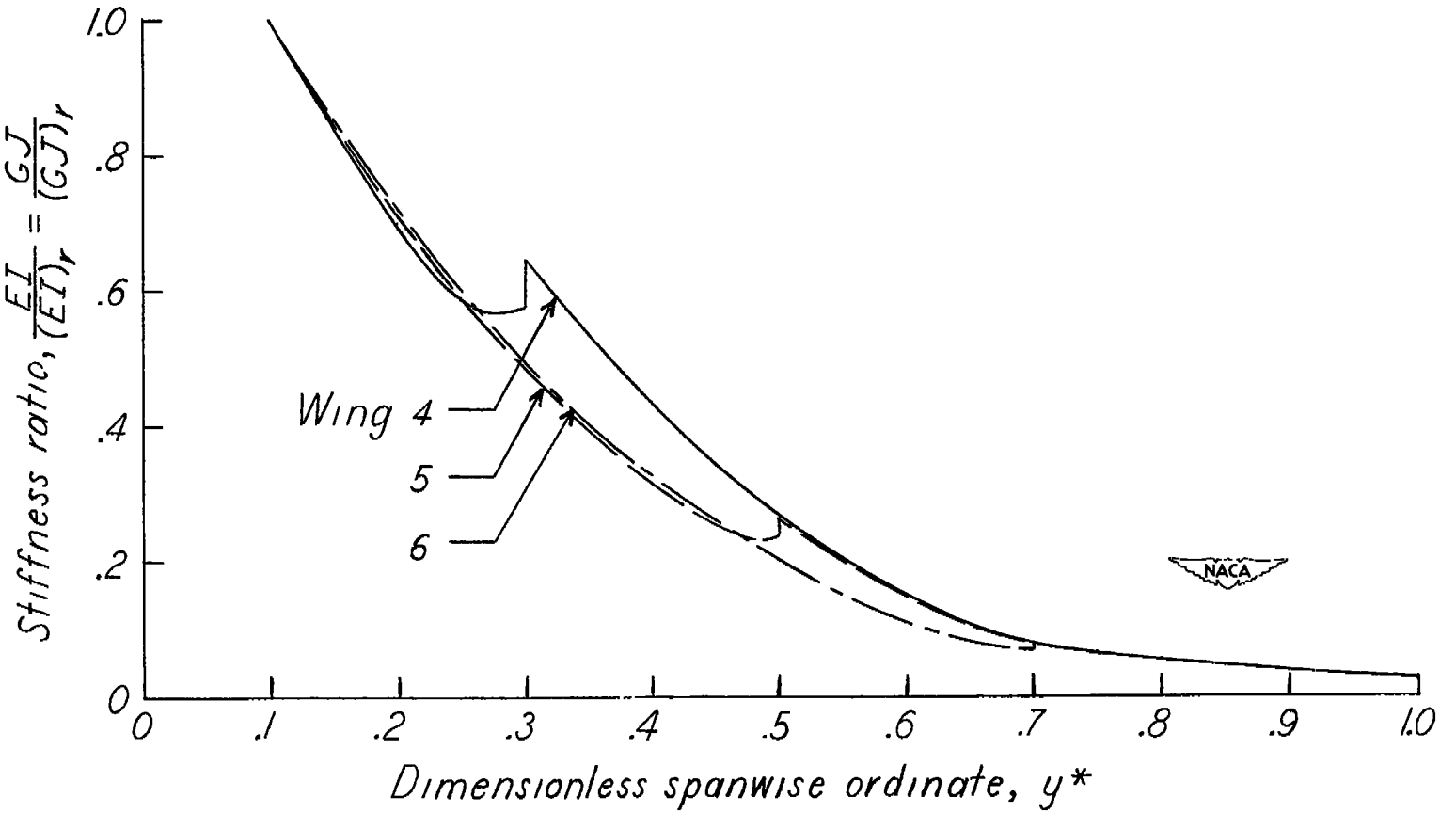

(b) W-wings.

Figure 2.- Continued.

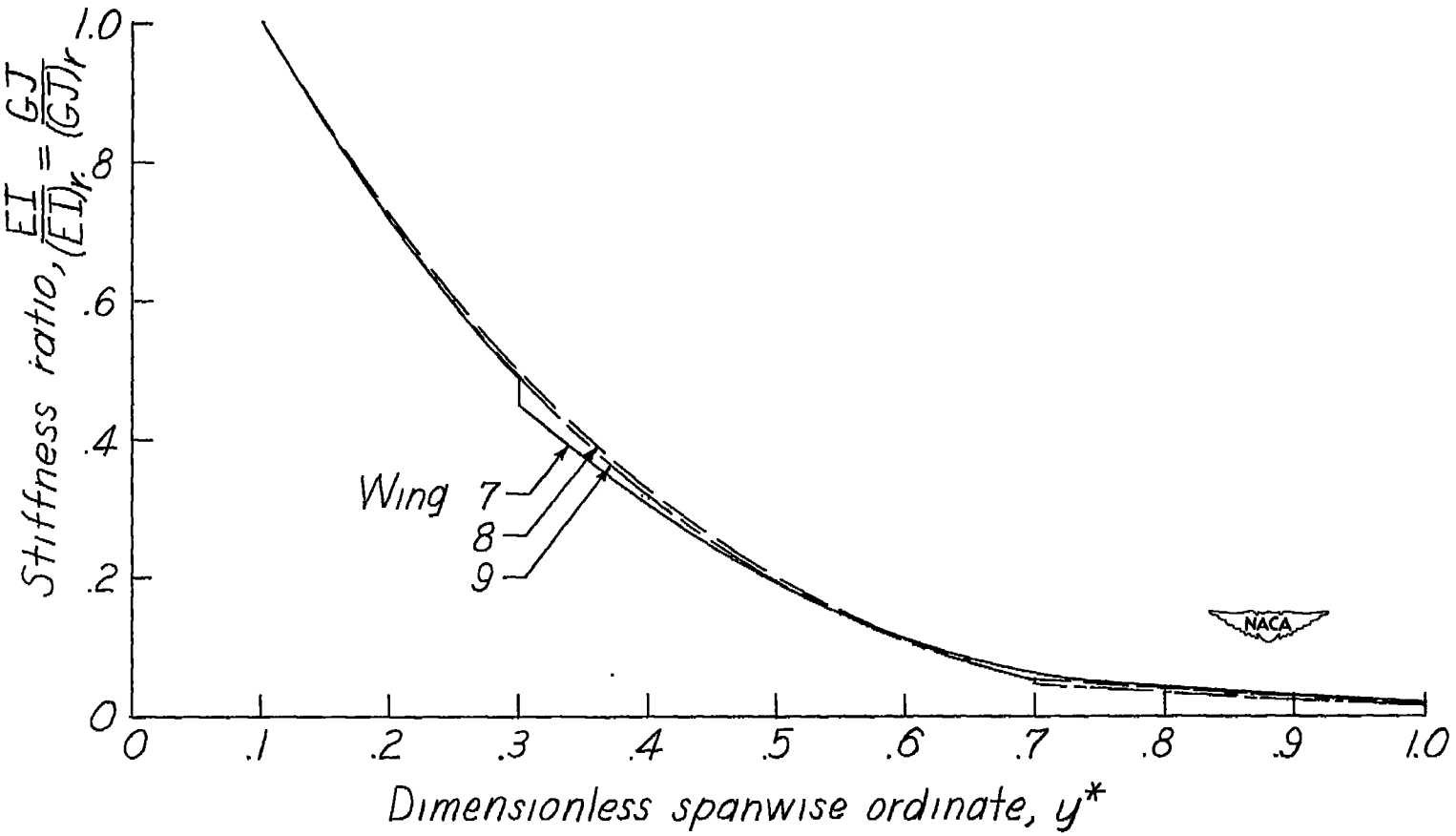

(c) Λ-wings and inverted Λ-wings.

Figure 2.- Continued.

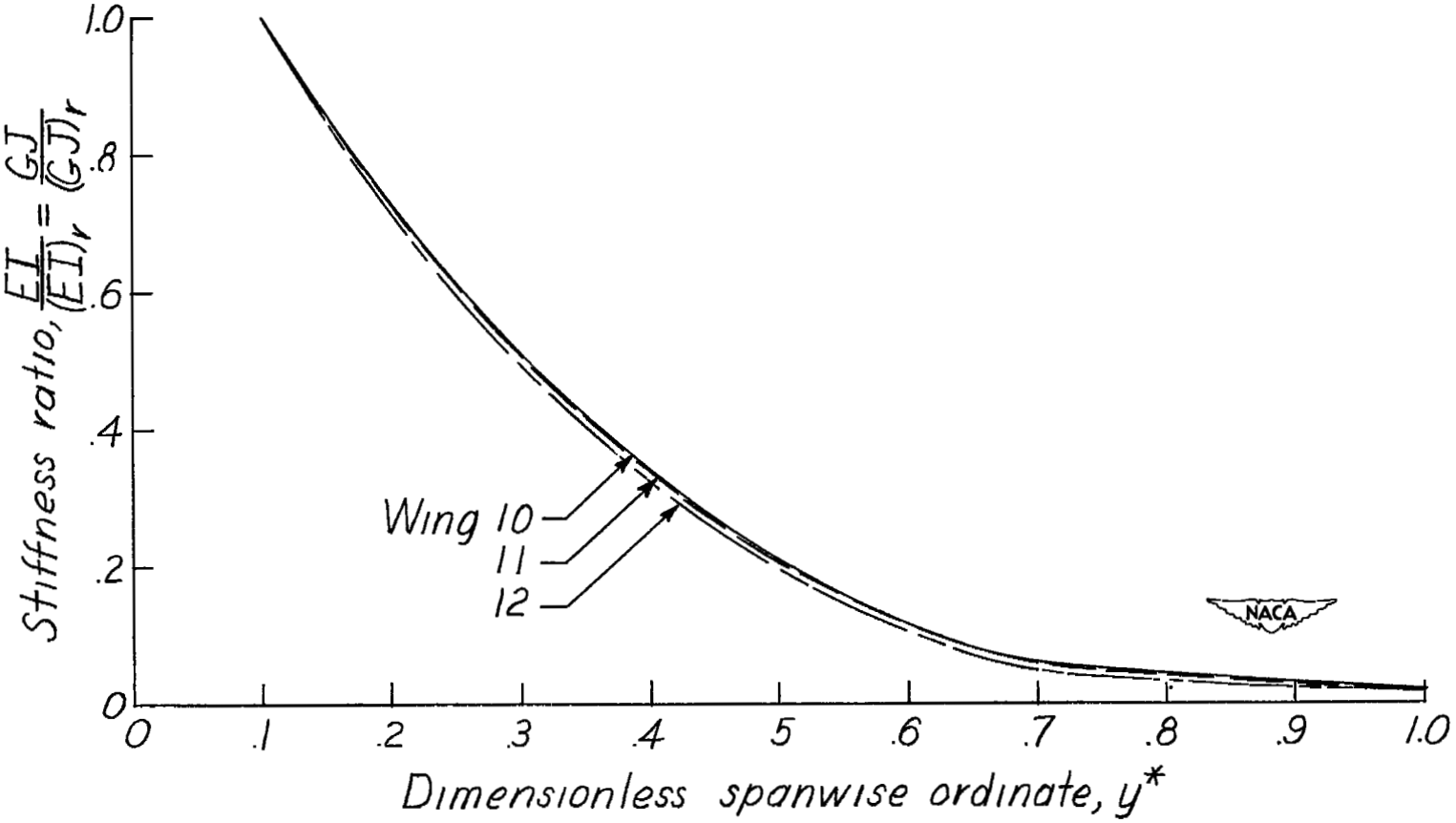

(d) Swept wings and unswept wing.

Figure 2.- Concluded.

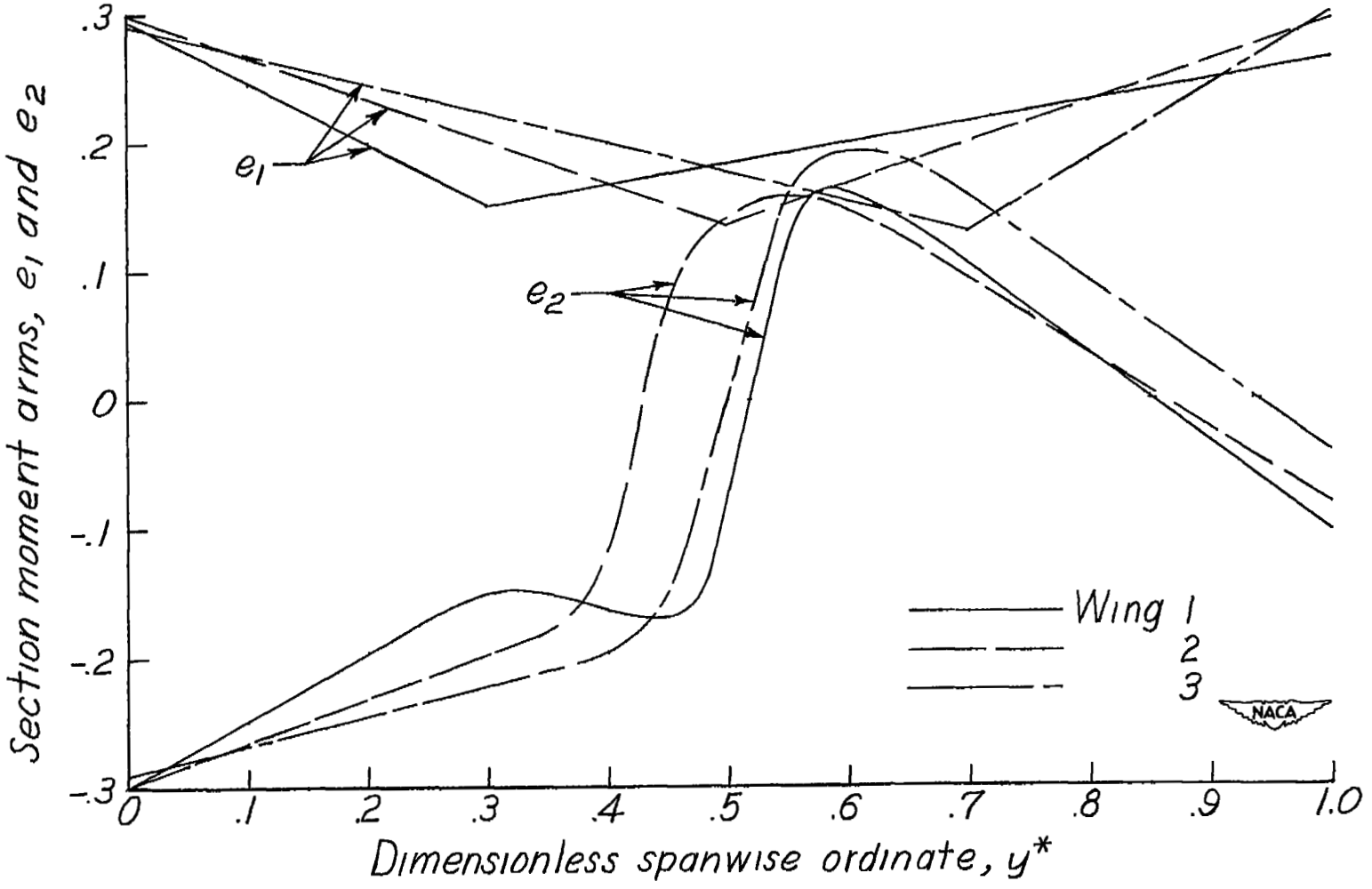

(a) M-wings.

Figure 3.- Spanwise variation of section moment arms.

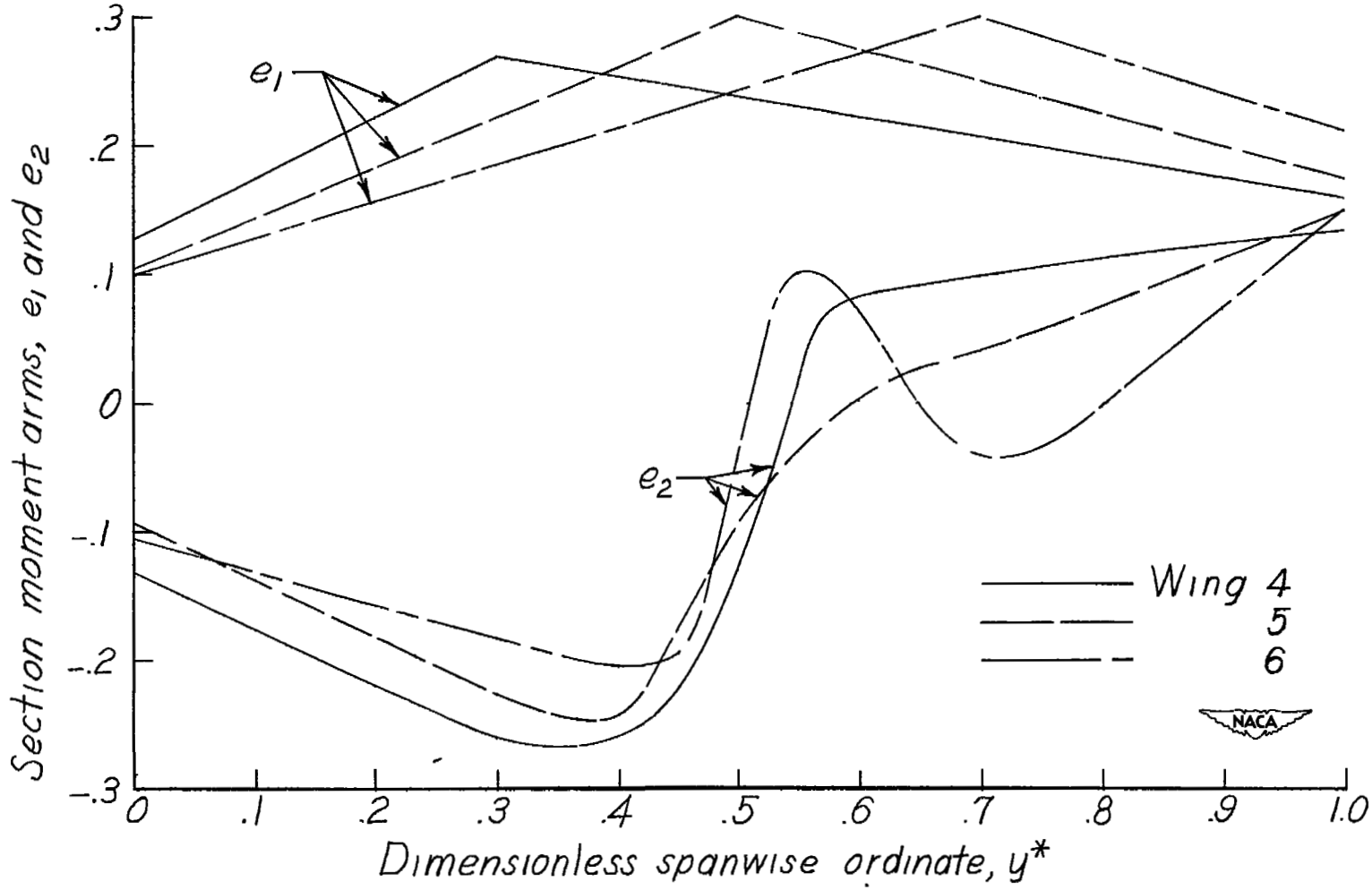

(b) W-wings.

Figure 3.- Continued.

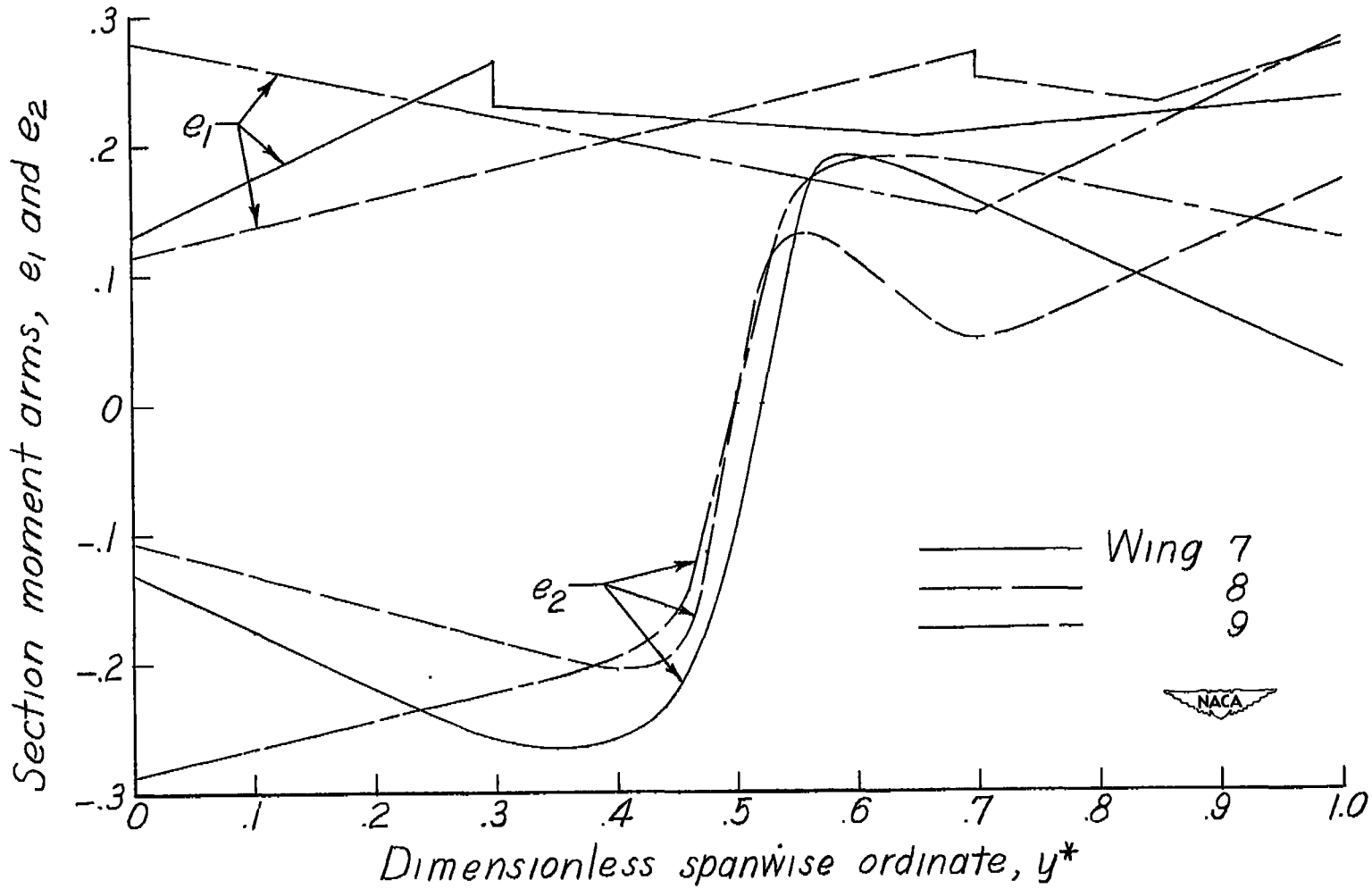

(c) Λ-wings and inverted Λ-wings.

Figure 3.- Continued.

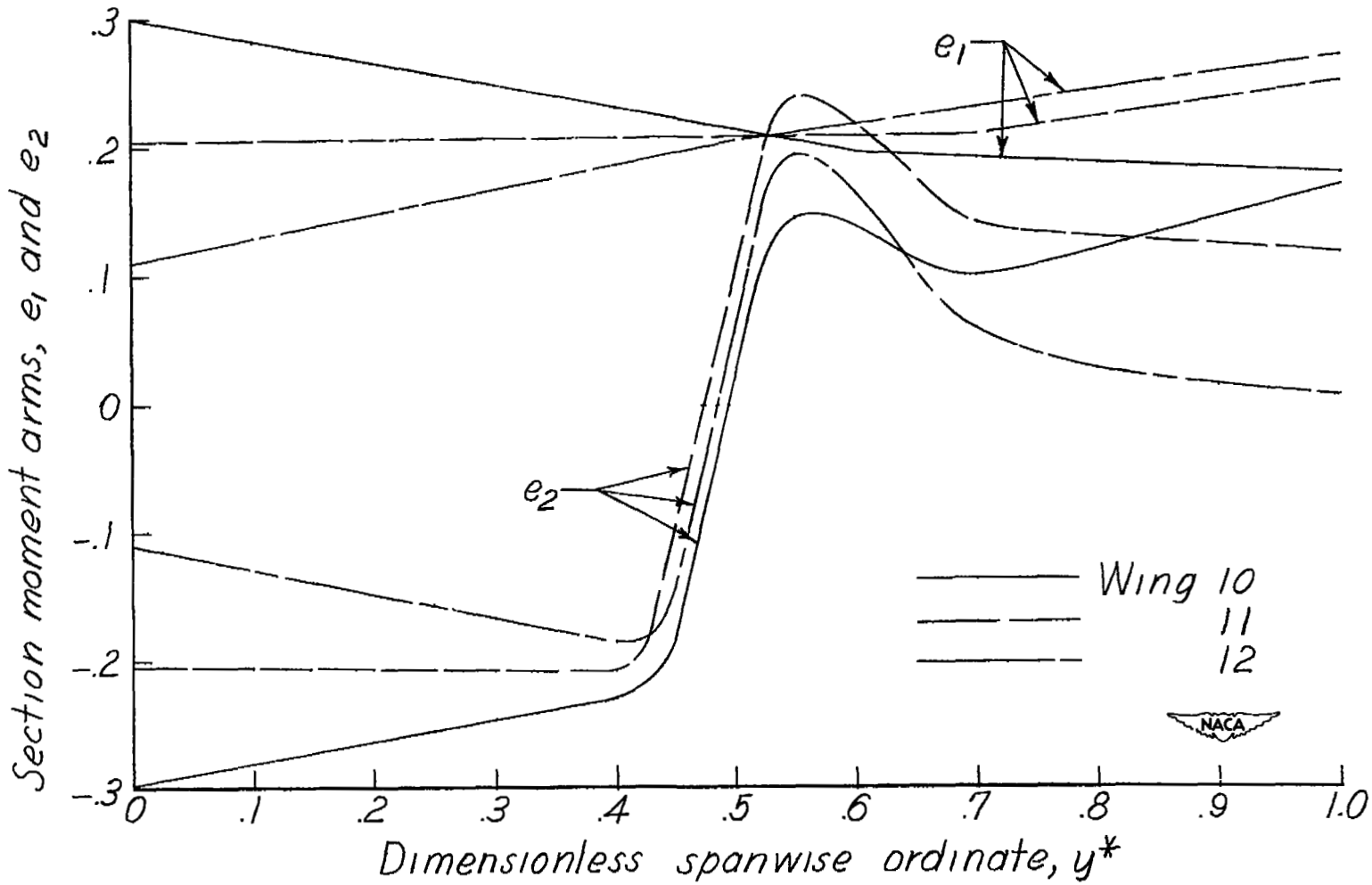

(d) Swept wings and unswept wing.

Figure 3.- Concluded.

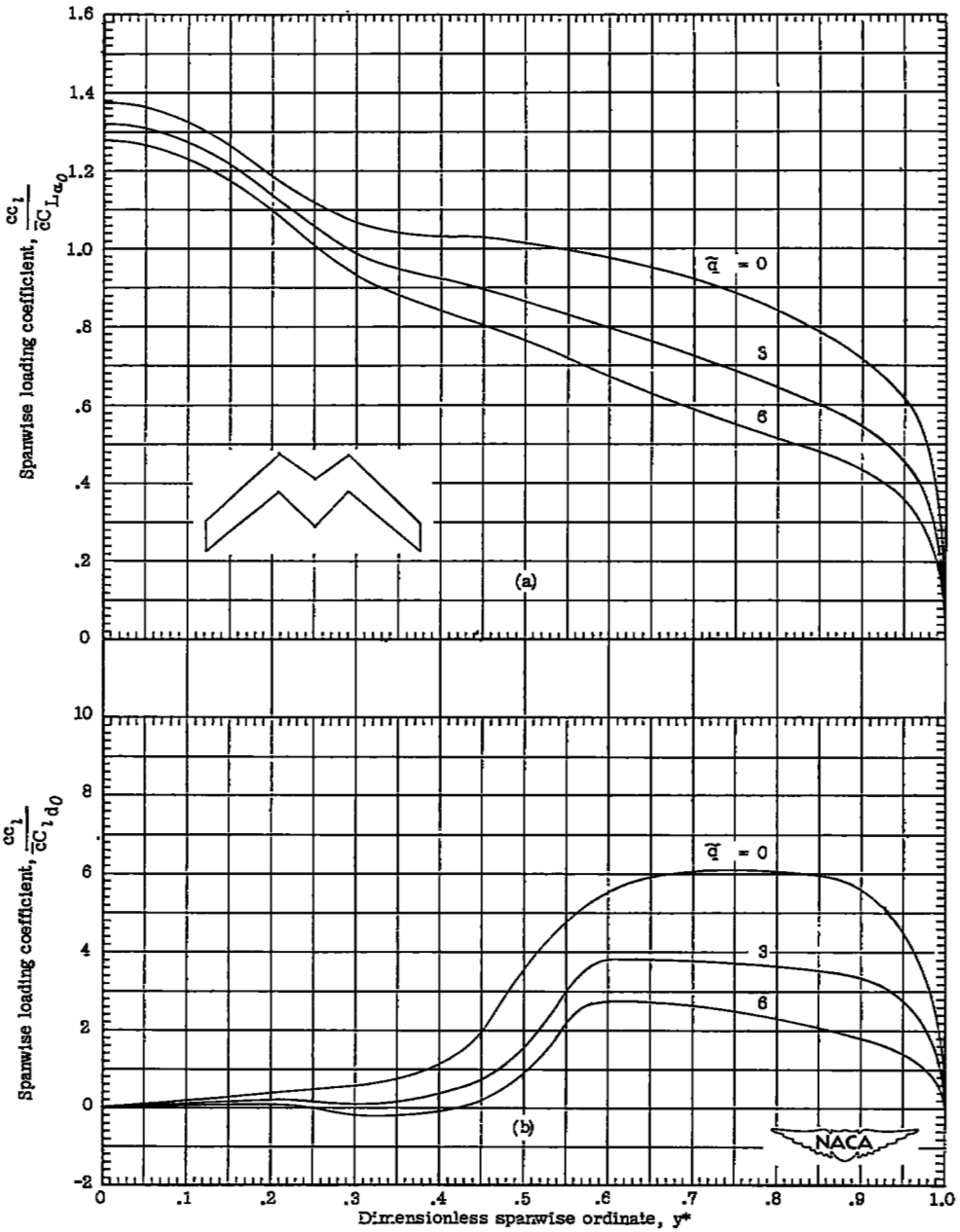

(a) Lift distributions due to unit airplane angle of attack (subsonic).

(b) Lift distributions due to unit effective aileron deflection (subsonic).

Figure 4.- Spanwise lift distributions for wing 1. (M-wing; $y^*_B = 0.3$.)

[redacted]

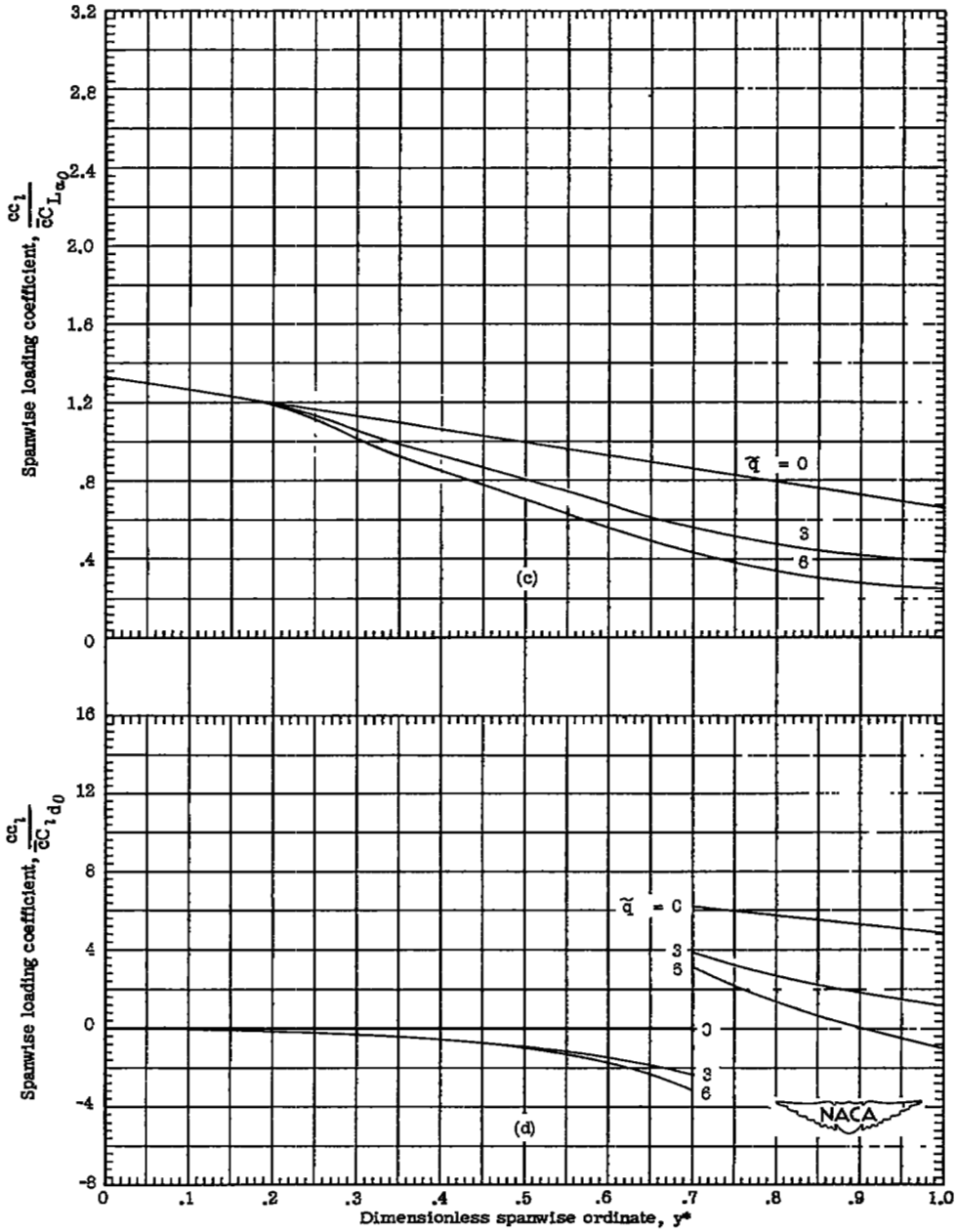

(c) Lift distributions due to unit airplane angle of attack (supersonic).

(d) Lift distributions due to unit effective aileron deflection (supersonic).

Figure 4.- Concluded.

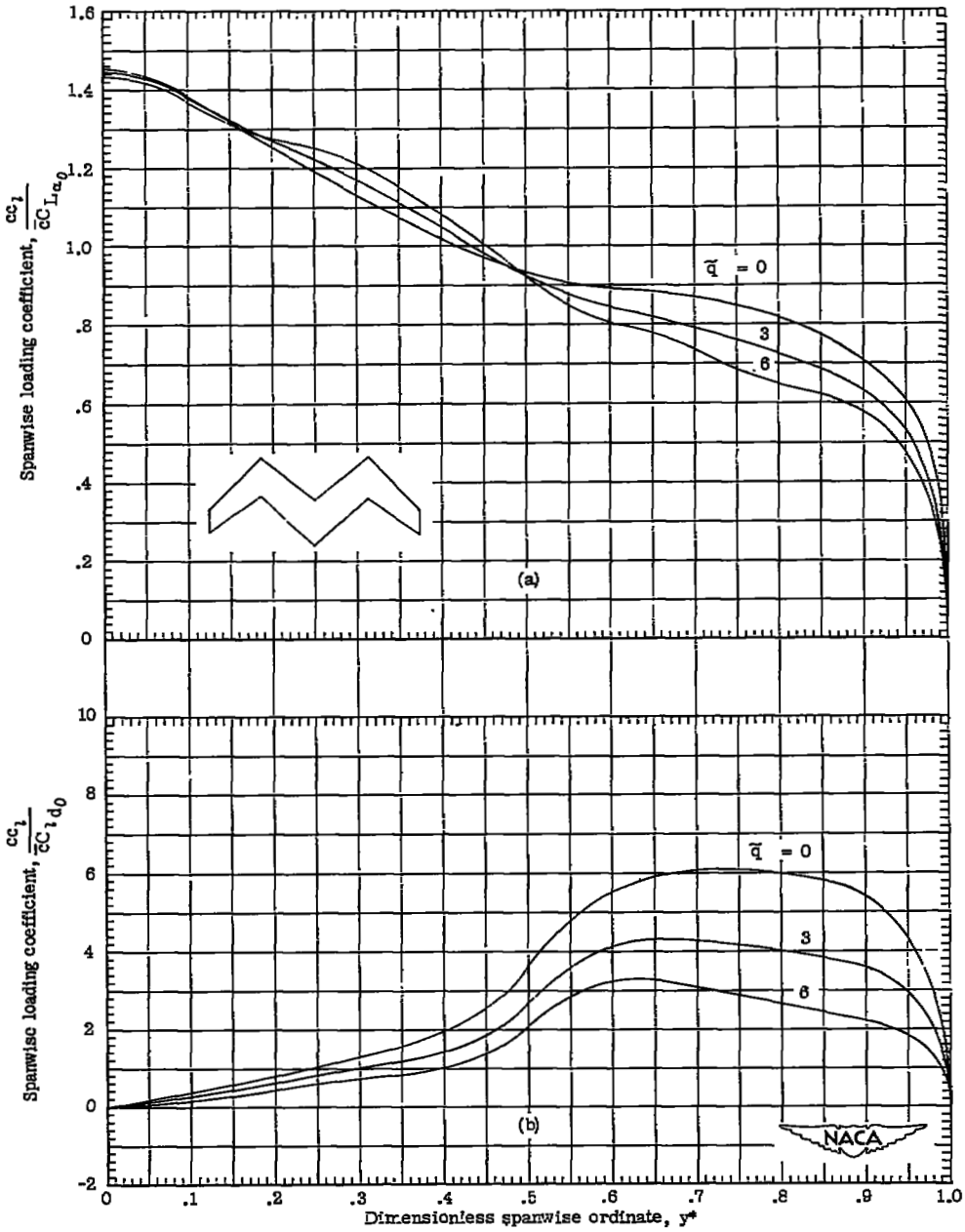

(a) Lift distributions due to unit airplane angle of attack (subsonic).

(b) Lift distributions due to unit effective aileron deflection (subsonic).

Figure 5.- Spanwise lift distributions for wing 2. (M-wing; $y^*_B = 0.5$.)

[redacted]

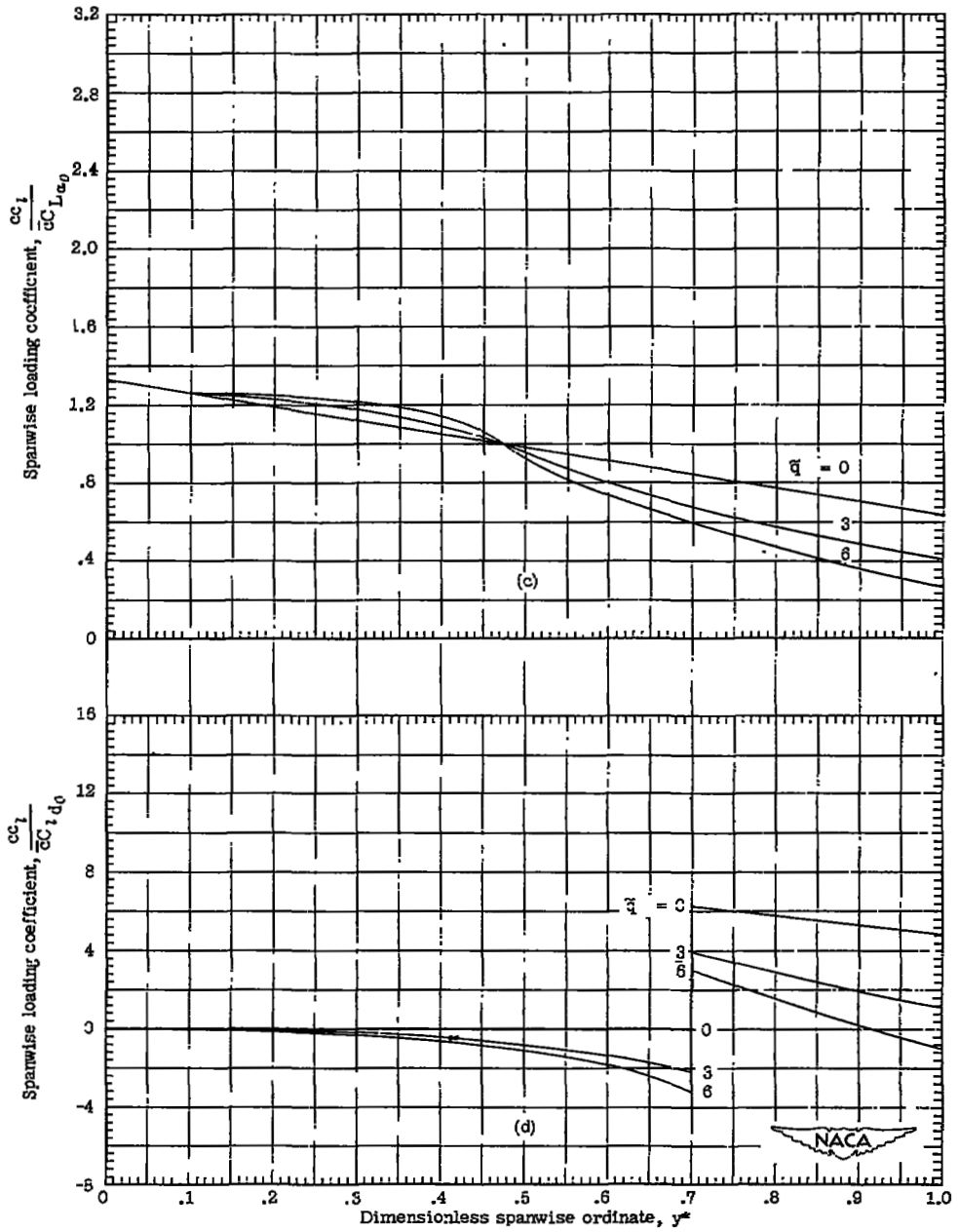

(c) Lift distributions due to unit airplane angle of attack (supersonic).

(d) Lift distributions due to unit effective aileron deflection (supersonic).

Figure 5.- Concluded.

[redacted]

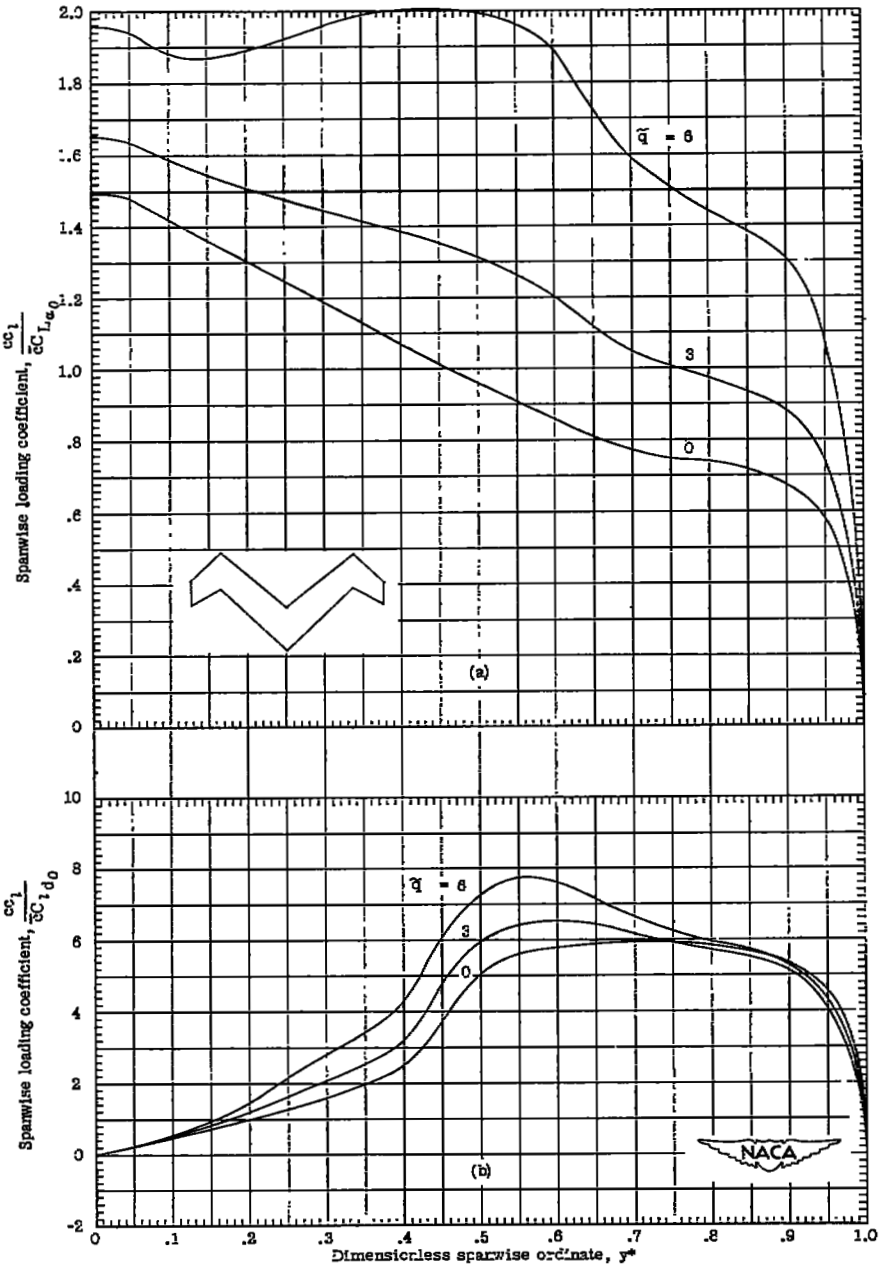

(a) Lift distributions due to unit airplane angle of attack (subsonic).

(b) Lift distributions due to unit effective aileron deflection (subsonic).

Figure 6.- Spanwise lift distributions for wing 3. (M-wing; $y^*_B = 0.7$.)

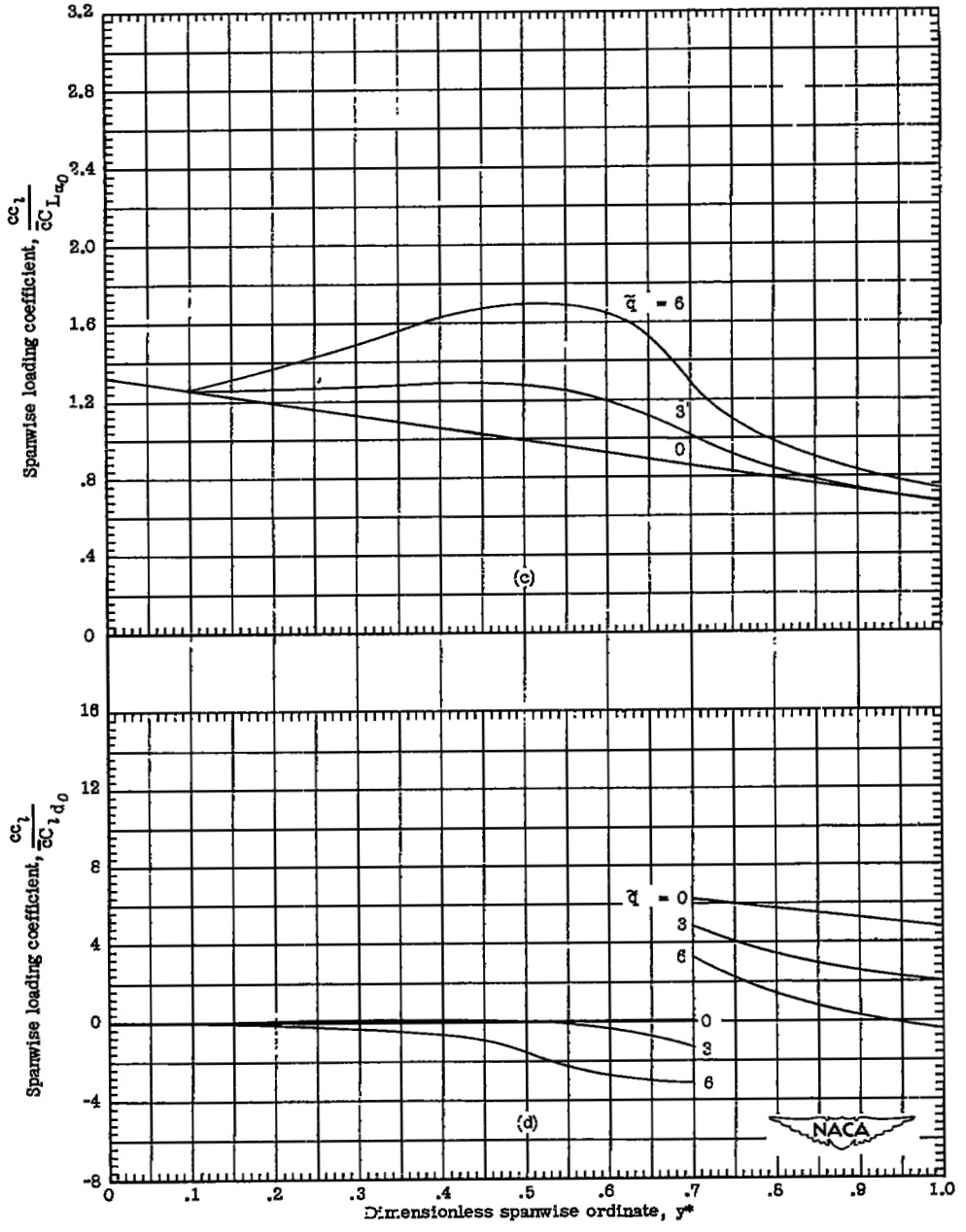

(c) Lift distributions due to unit airplane angle of attack (supersonic).

(d) Lift distributions due to unit effective aileron deflection (supersonic).

Figure 6.- Concluded.

[redacted]

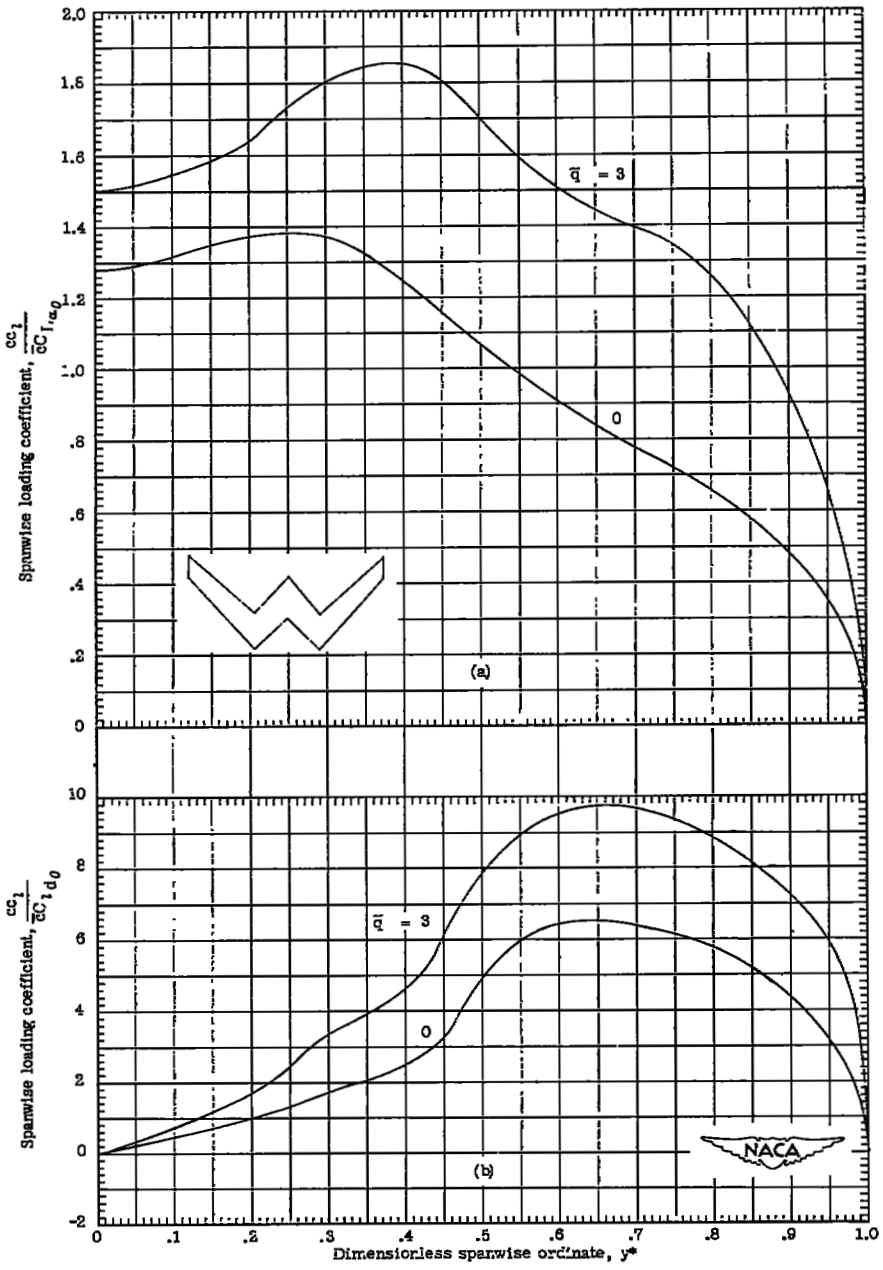

(a) Lift distributions due to unit airplane angle of attack (subsonic).

(b) Lift distributions due to unit effective aileron deflection (subsonic).

Figure 7.- Spanwise lift distributions for wing 4. (W-wing; $y^*_B = 0.3$.)

[redacted]

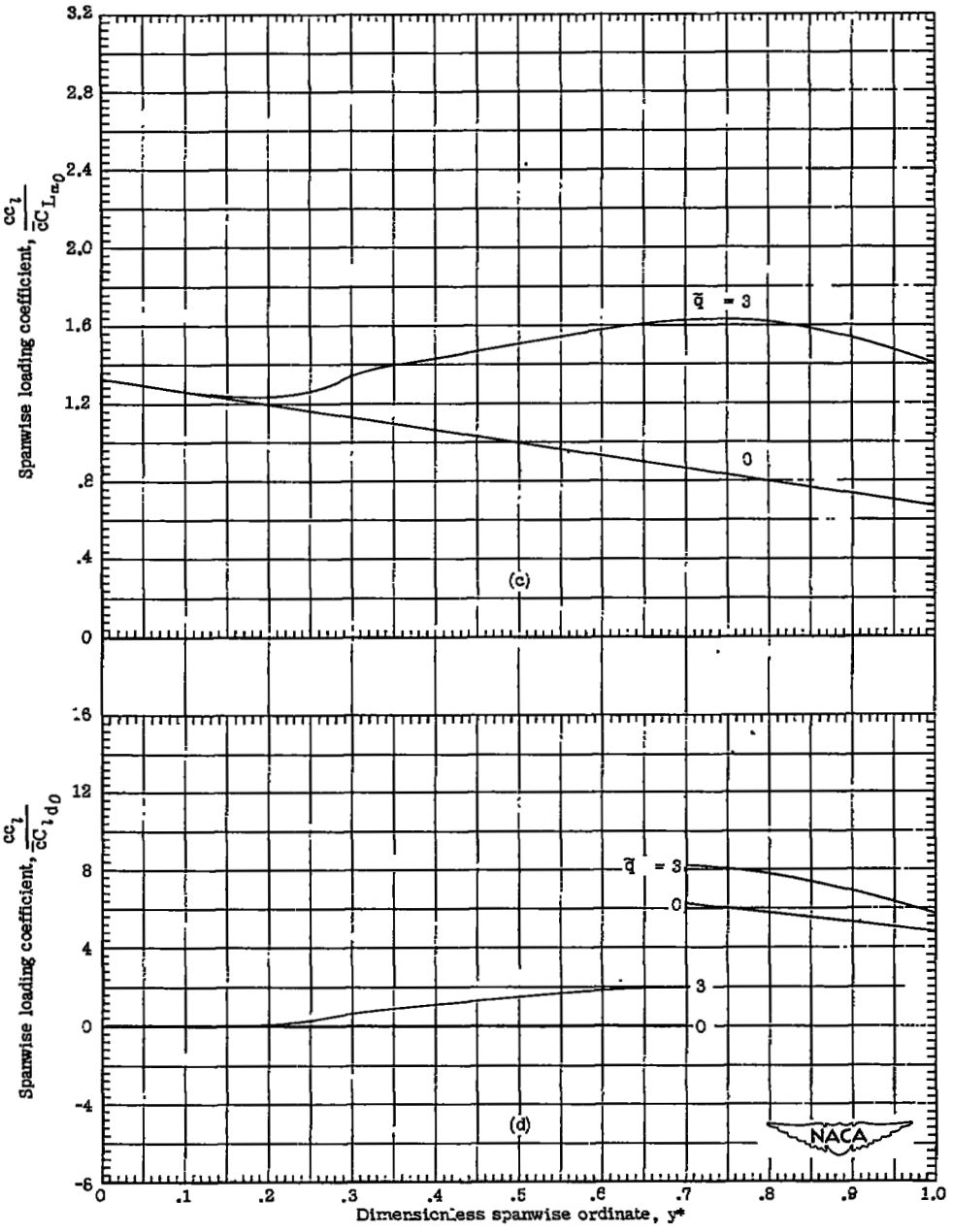

(c) Lift distributions due to unit airplane angle of attack (supersonic).

(d) Lift distributions due to unit effective aileron deflection (supersonic).

Figure 7.- Concluded.

[redacted]

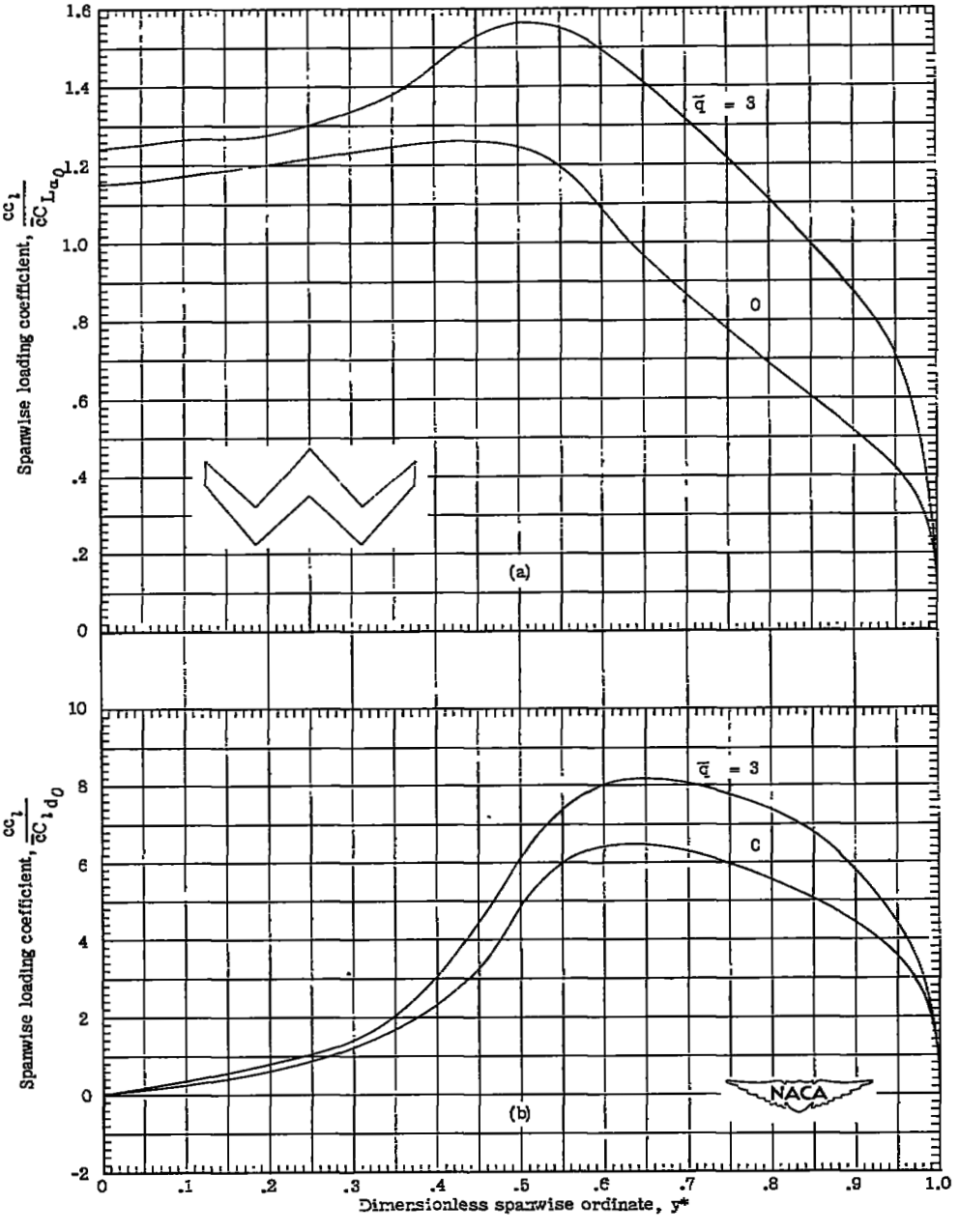

(a) Lift distributions due to unit airplane angle of attack (subsonic).

(b) Lift distributions due to unit effective aileron deflection (subsonic).

Figure 8.- Spanwise lift distributions for wing 5. (W-wing; $y^*_B = 0.5$.)

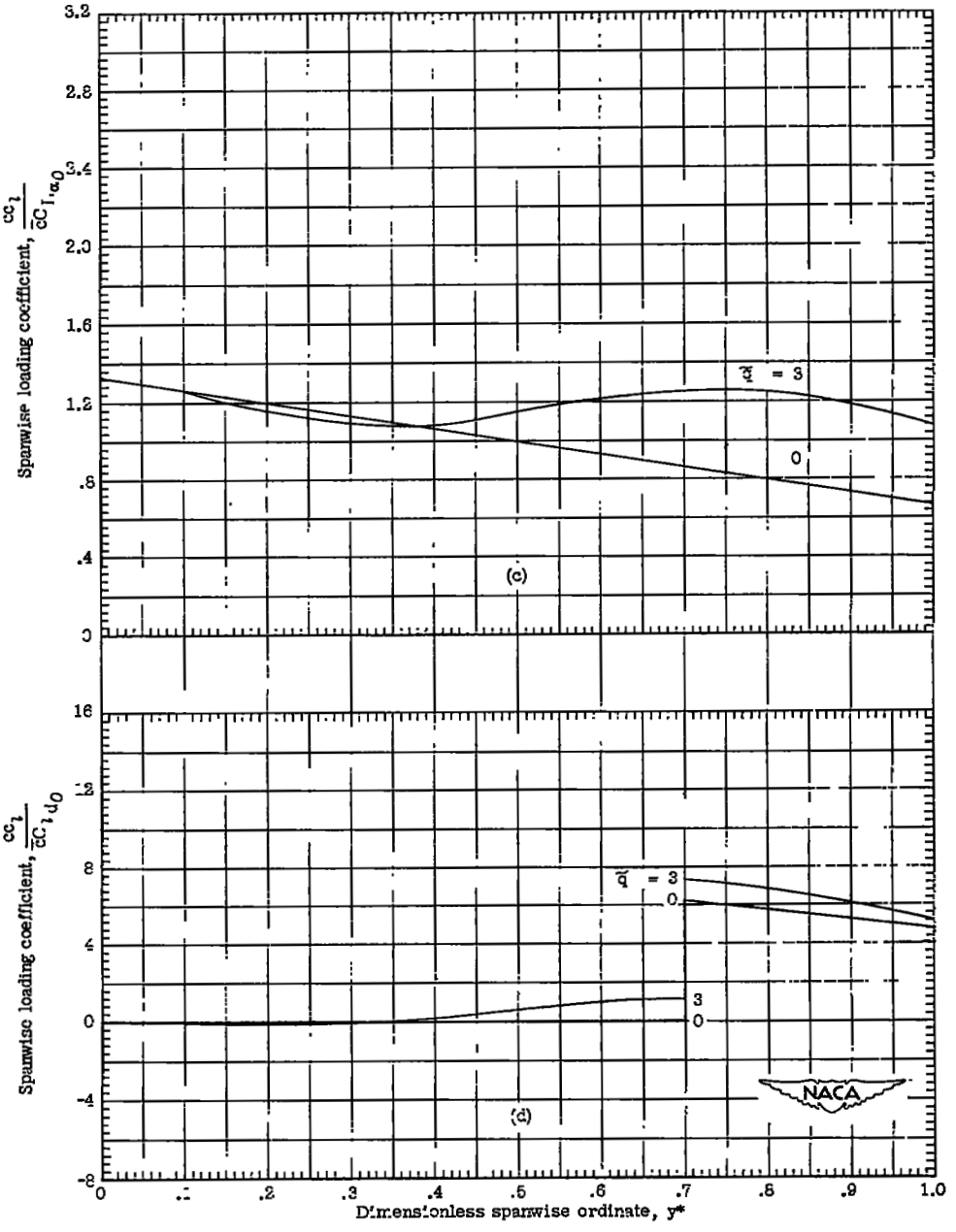

(c) Lift distributions due to unit airplane angle of attack (supersonic).

(d) Lift distributions due to unit effective aileron deflection (supersonic).

Figure 8.- Concluded.

[redacted]

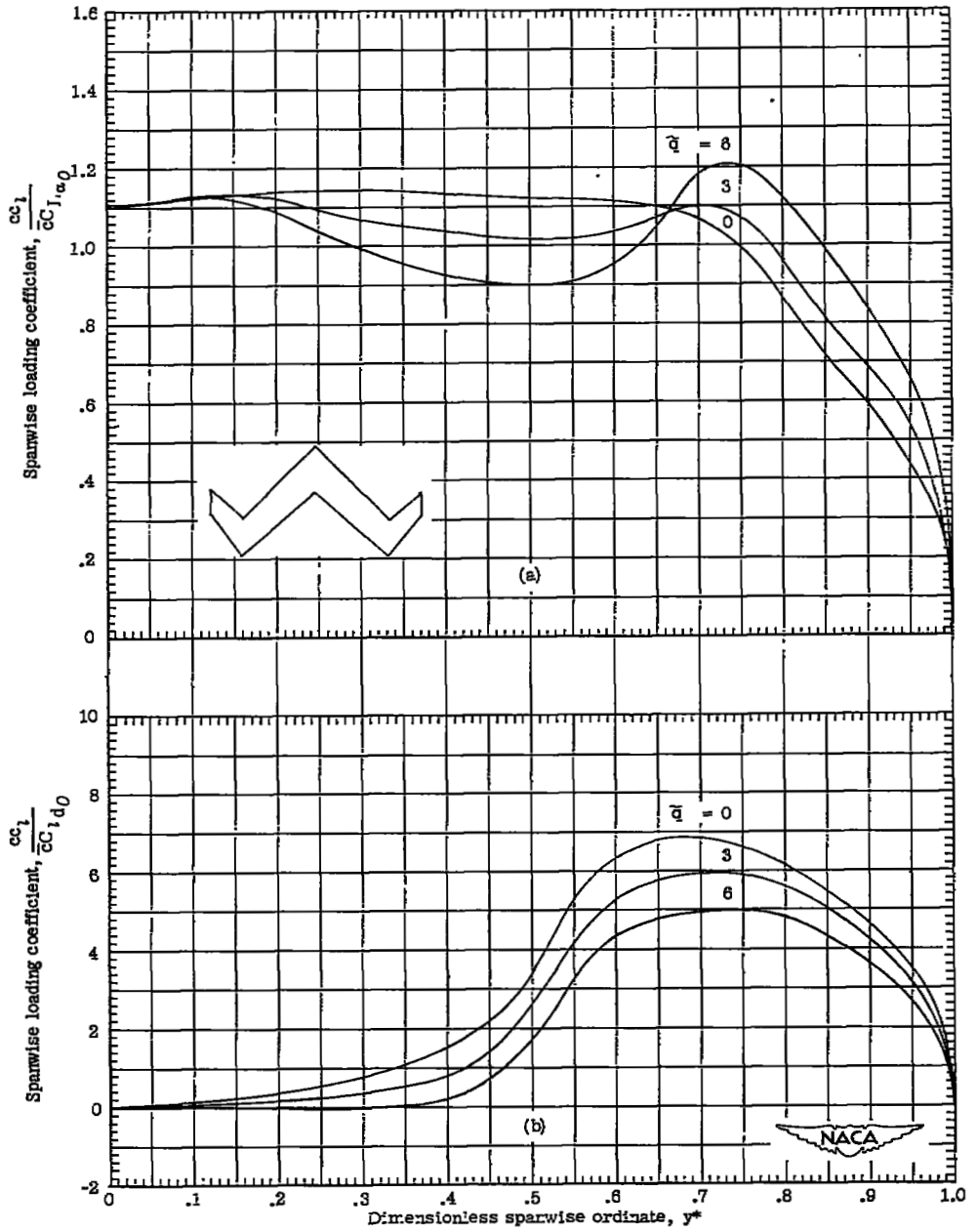

(a) Lift distributions due to unit airplane angle of attack (subsonic).

(b) Lift distributions due to unit effective aileron deflection (subsonic).

Figure 9.- Spanwise lift distributions for wing 6. (W-wing; $y^*_B = 0.7$.)

[redacted]

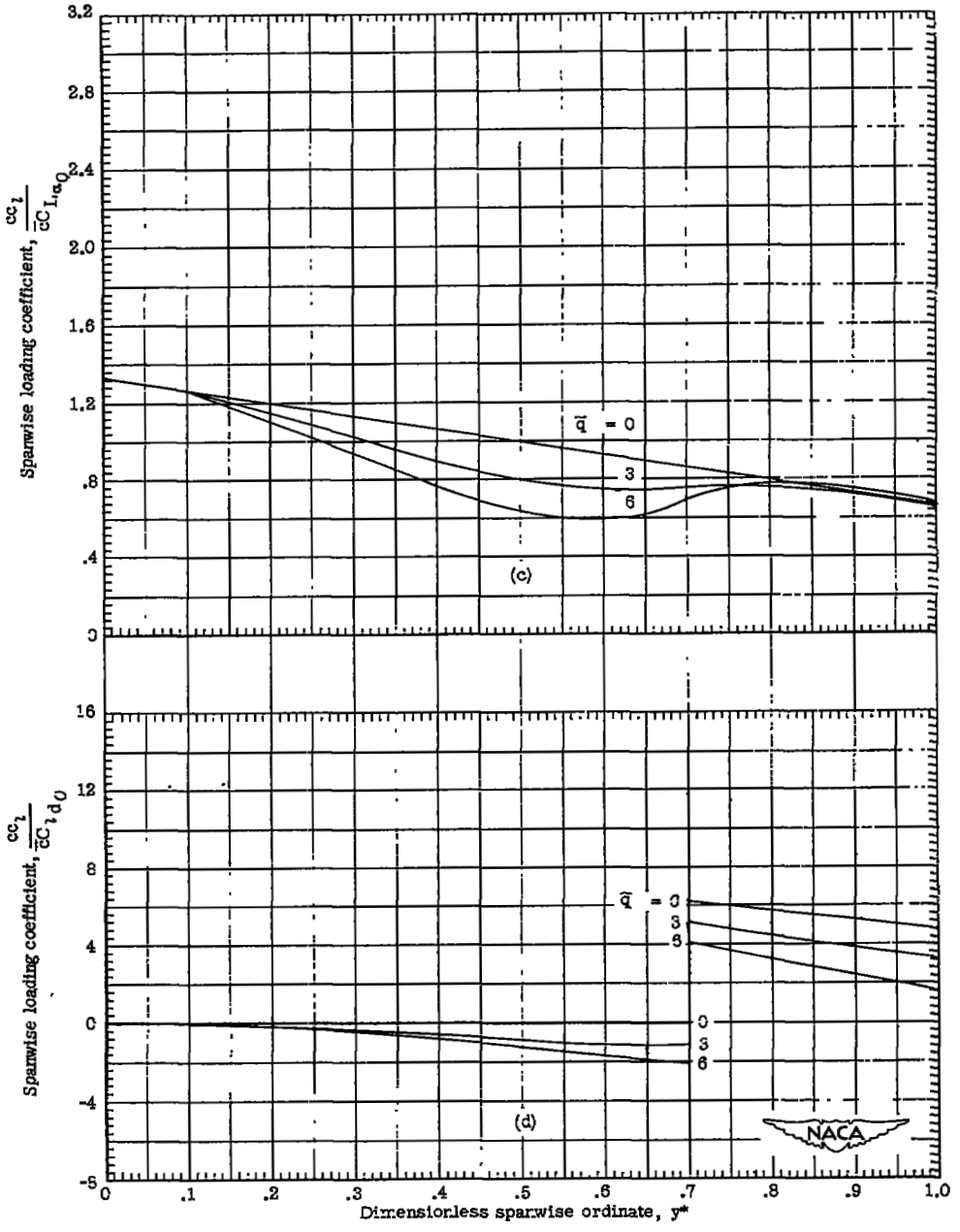

(c) Lift distributions due to unit airplane angle of attack (supersonic).

(d) Lift distributions due to unit effective aileron deflection (supersonic).

Figure 9.- Concluded.

[redacted]

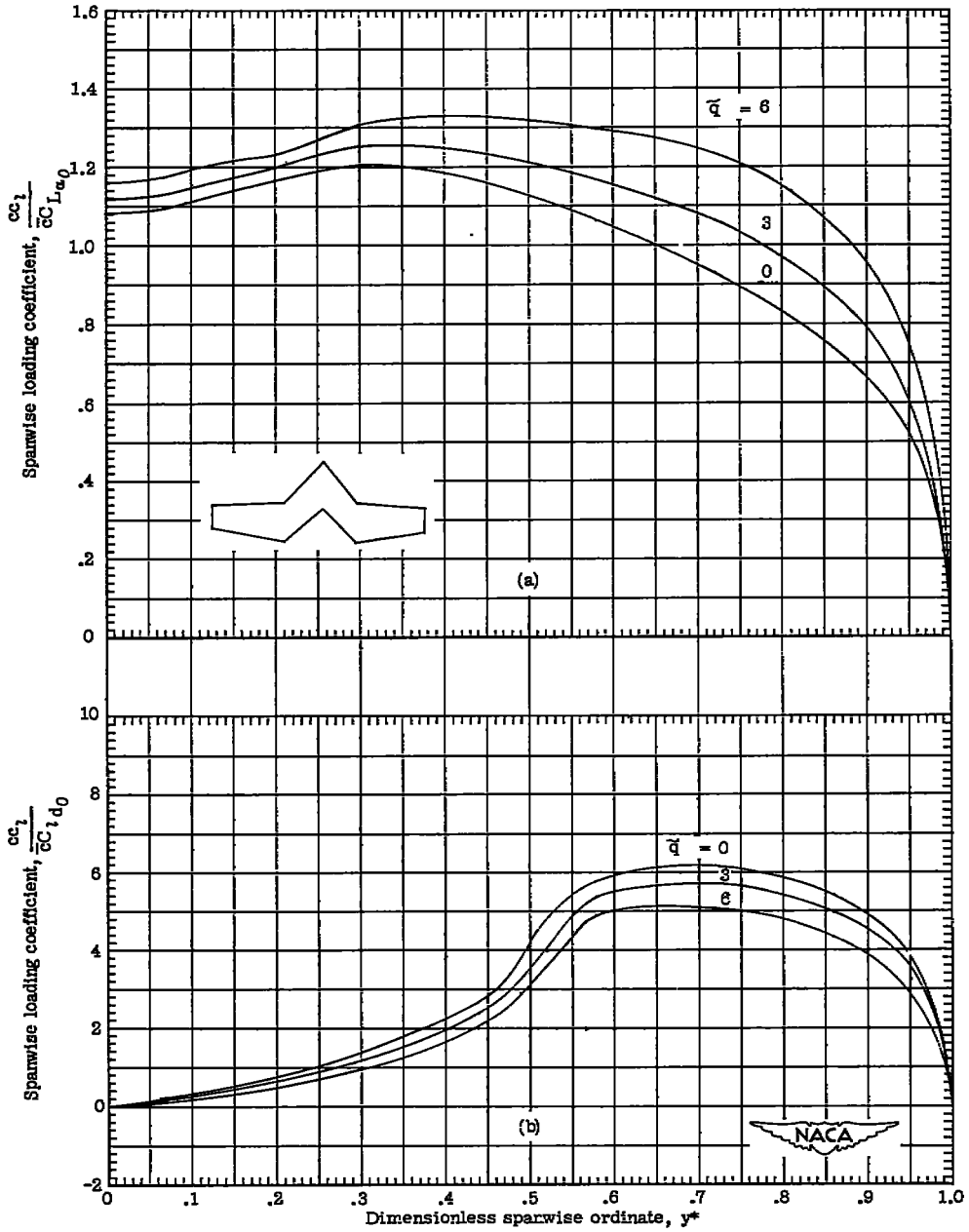

(a) Lift distributions due to unit airplane angle of attack (subsonic).

(b) Lift distributions due to unit effective aileron deflection (subsonic).

Figure 10.- Spanwise lift distributions for wing 7. (Λ-wing; $y^*_B = 0.3$.)

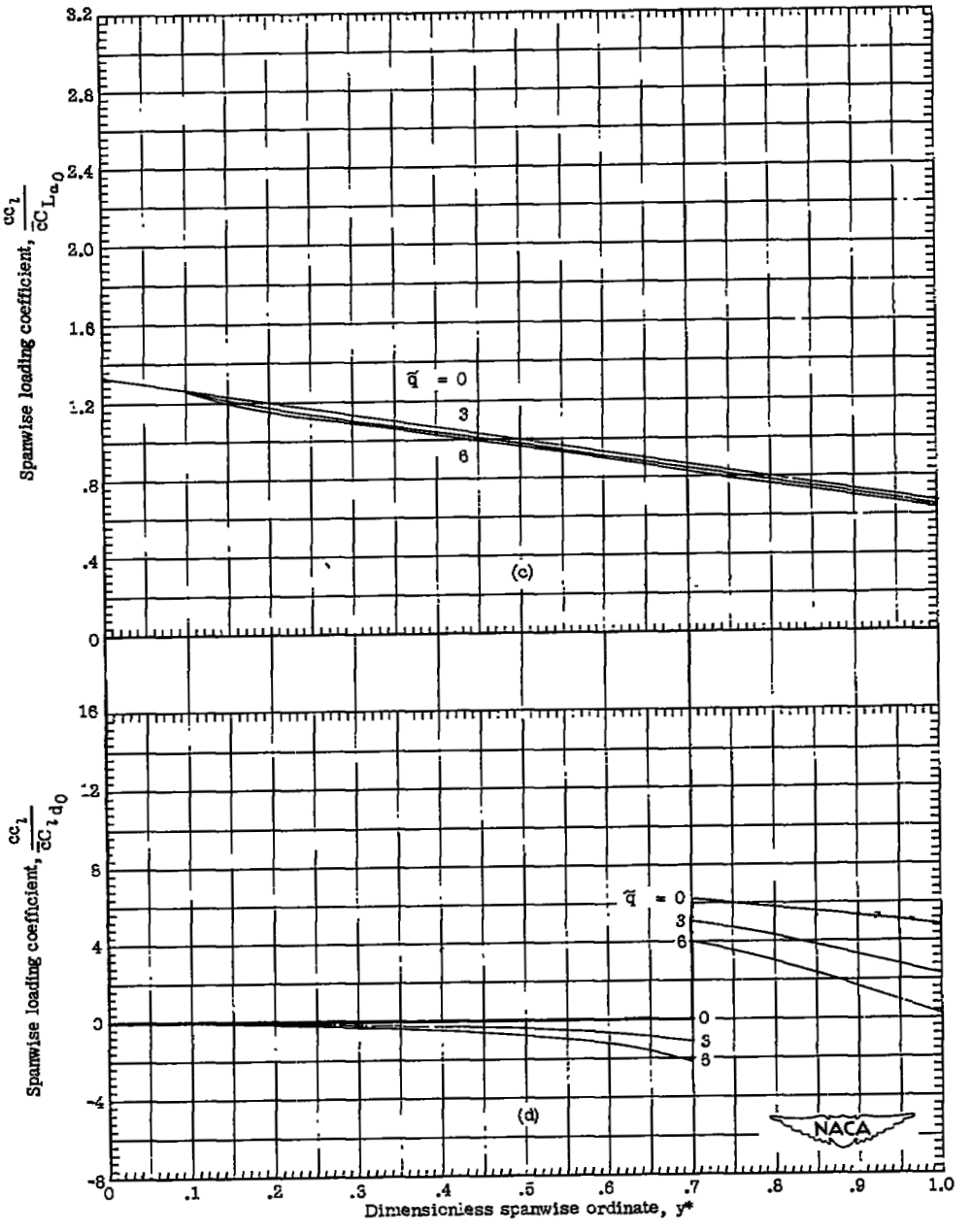

(c) Lift distributions due to unit airplane angle of attack (supersonic).

(d) Lift distributions due to unit effective aileron deflection (supersonic).

Figure 10.- Concluded.

[redacted]

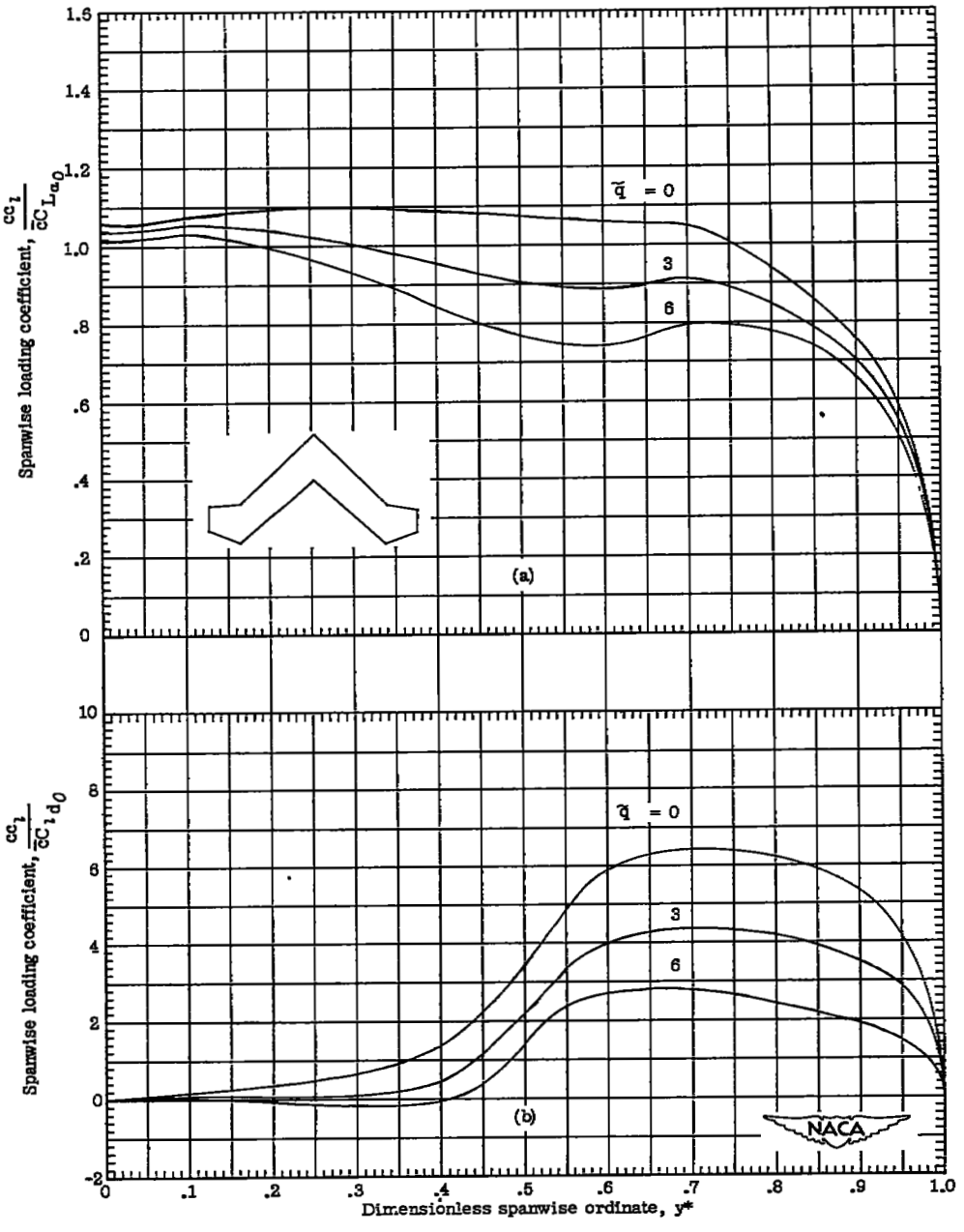

(a) Lift distributions due to unit airplane angle of attack (subsonic).

(b) Lift distributions due to unit effective aileron deflection (subsonic).

Figure 11.- Spanwise lift distributions for wing 8. (Λ-wing; $y^*_B = 0.7$.)

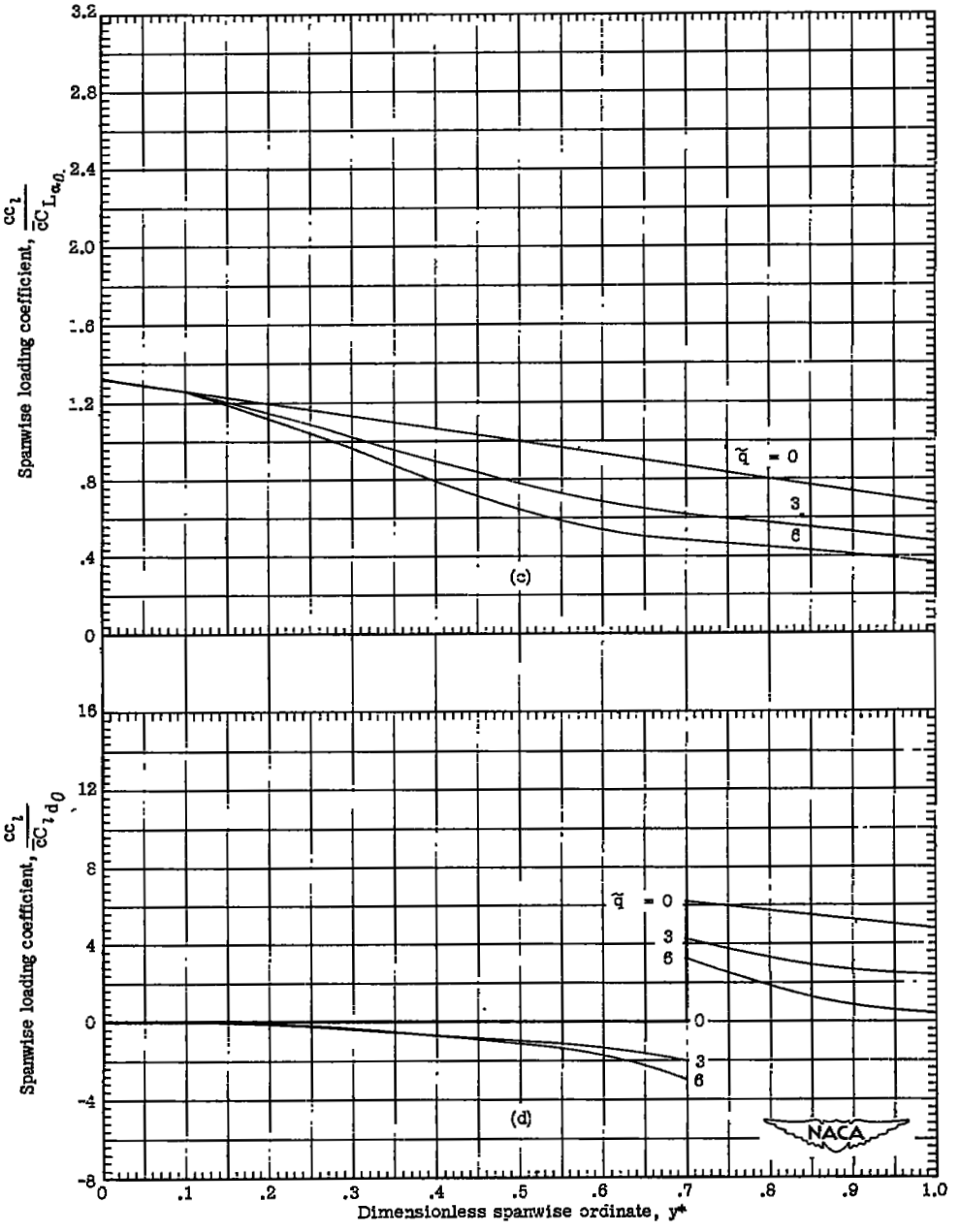

(c) Lift distributions due to unit airplane angle of attack (supersonic).

(d) Lift distributions due to unit effective aileron deflection (supersonic).

Figure 11.- Concluded.

[redacted]

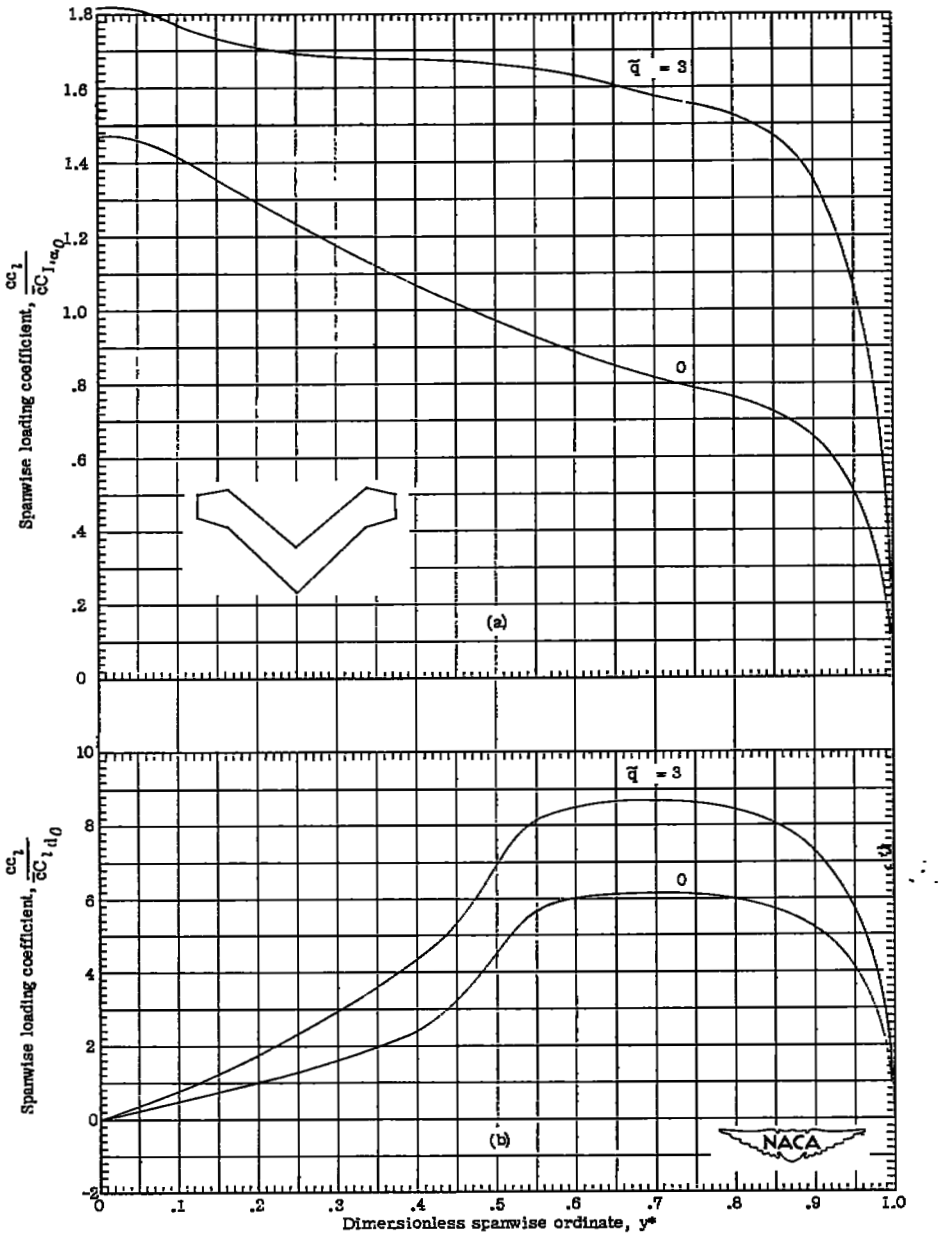

(a) Lift distributions due to unit airplane angle of attack (subsonic).

(b) Lift distributions due to unit effective aileron deflection (subsonic).

Figure 12.- Spanwise lift distributions for wing 9. (Inverted Λ-wing; $y^*_B = 0.7$.)

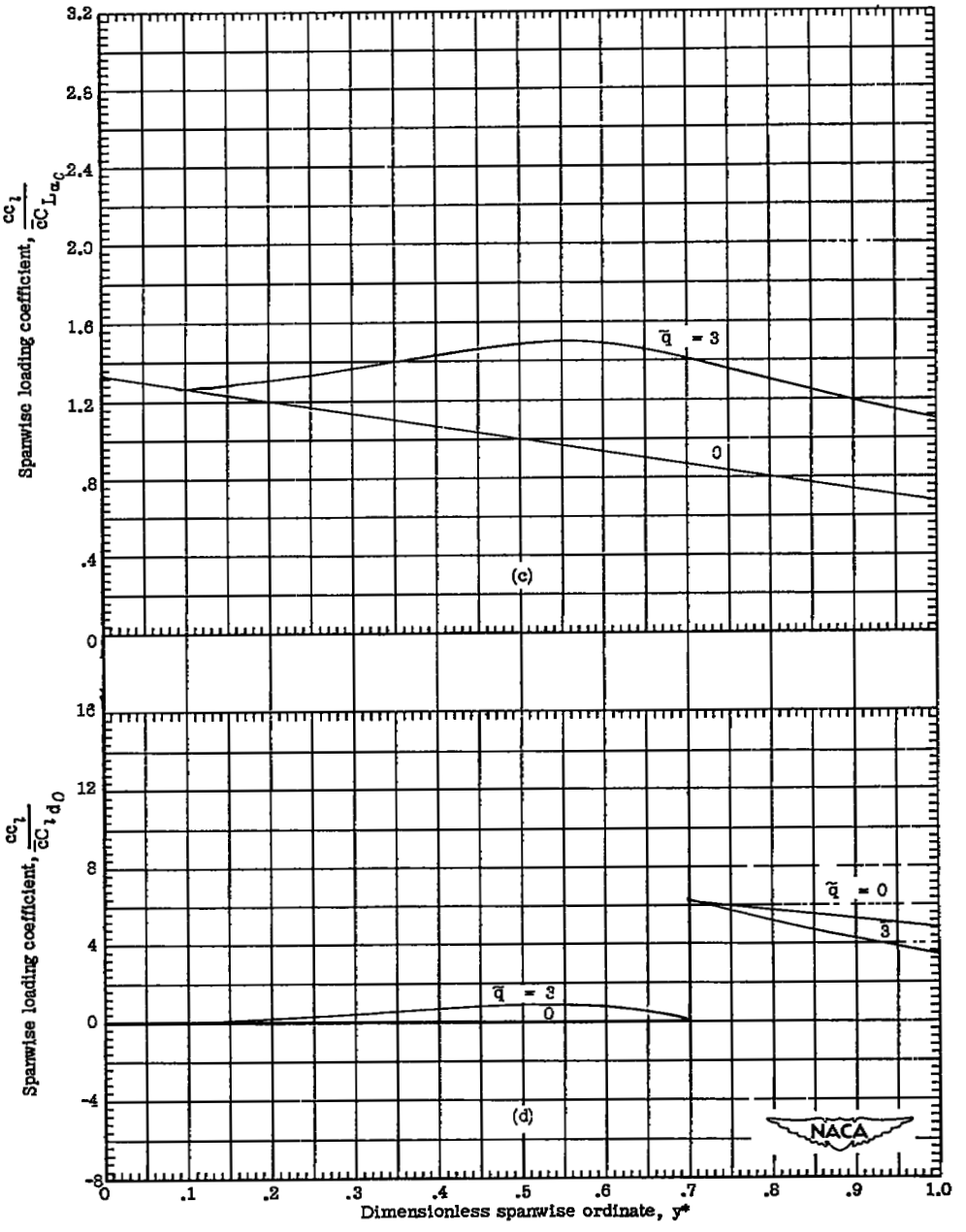

(c) Lift distributions due to unit airplane angle of attack (supersonic).

(d) Lift distributions due to unit effective aileron deflection (supersonic).

Figure 12.- Concluded.

[redacted]

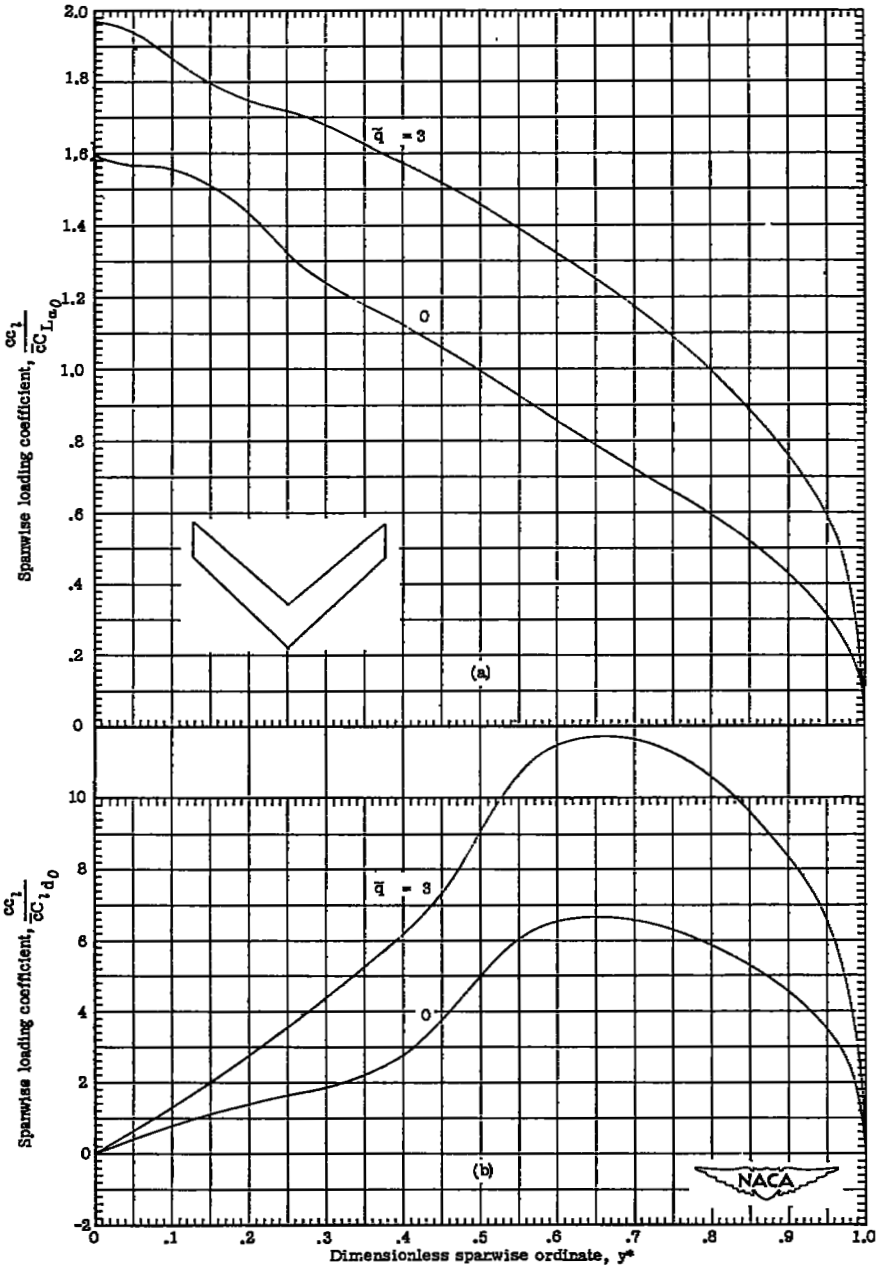

(a) Lift distributions due to unit airplane angle of attack (subsonic).

(b) Lift distributions due to unit effective aileron deflection (subsonic).

Figure 13.- Spanwise lift distributions for wing 10. (Sweptforward wing.)

[redacted]

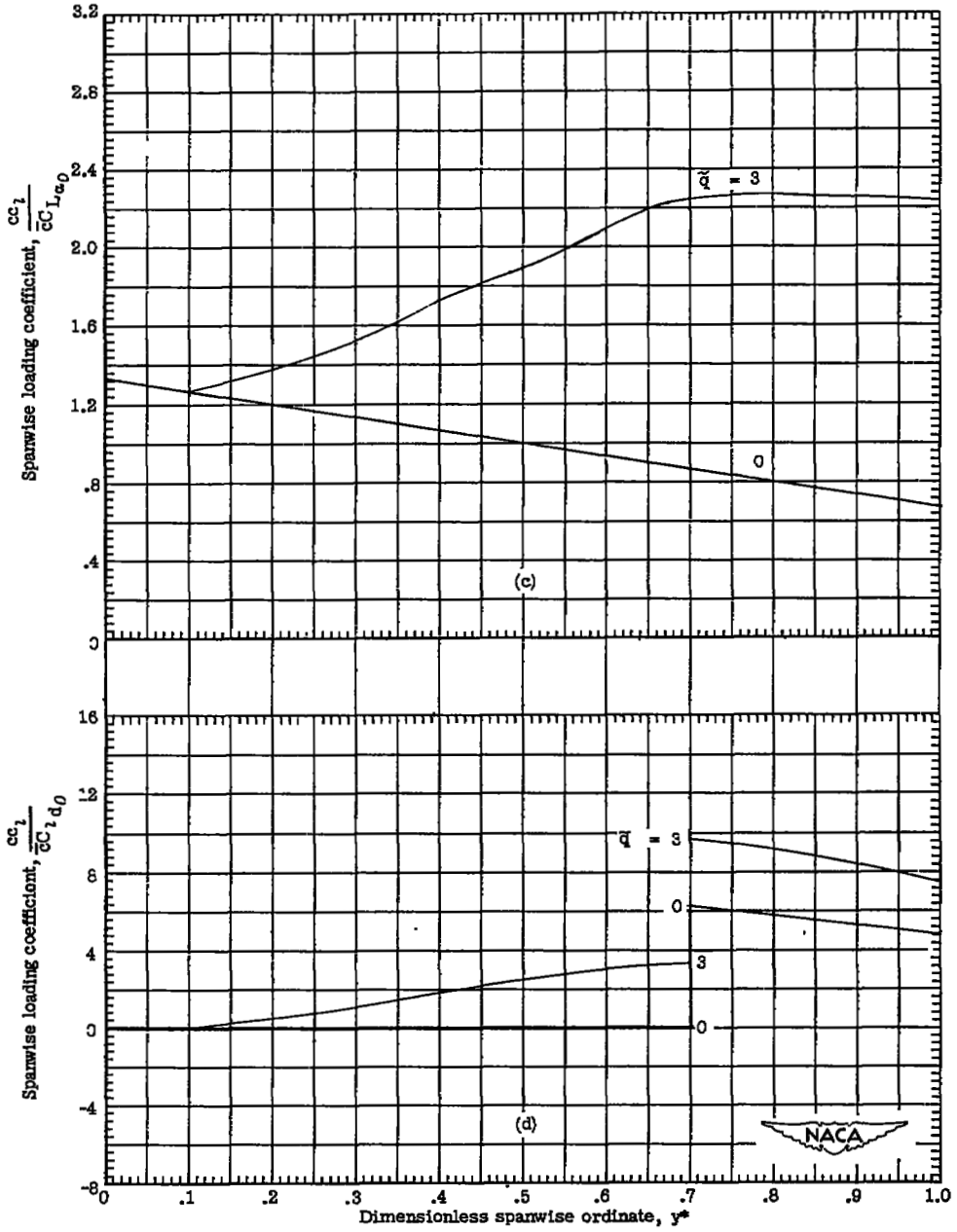

(c) Lift distributions due to unit airplane angle of attack (supersonic).

(d) Lift distributions due to unit effective aileron deflection (supersonic).

Figure 13.- Concluded.

[redacted]

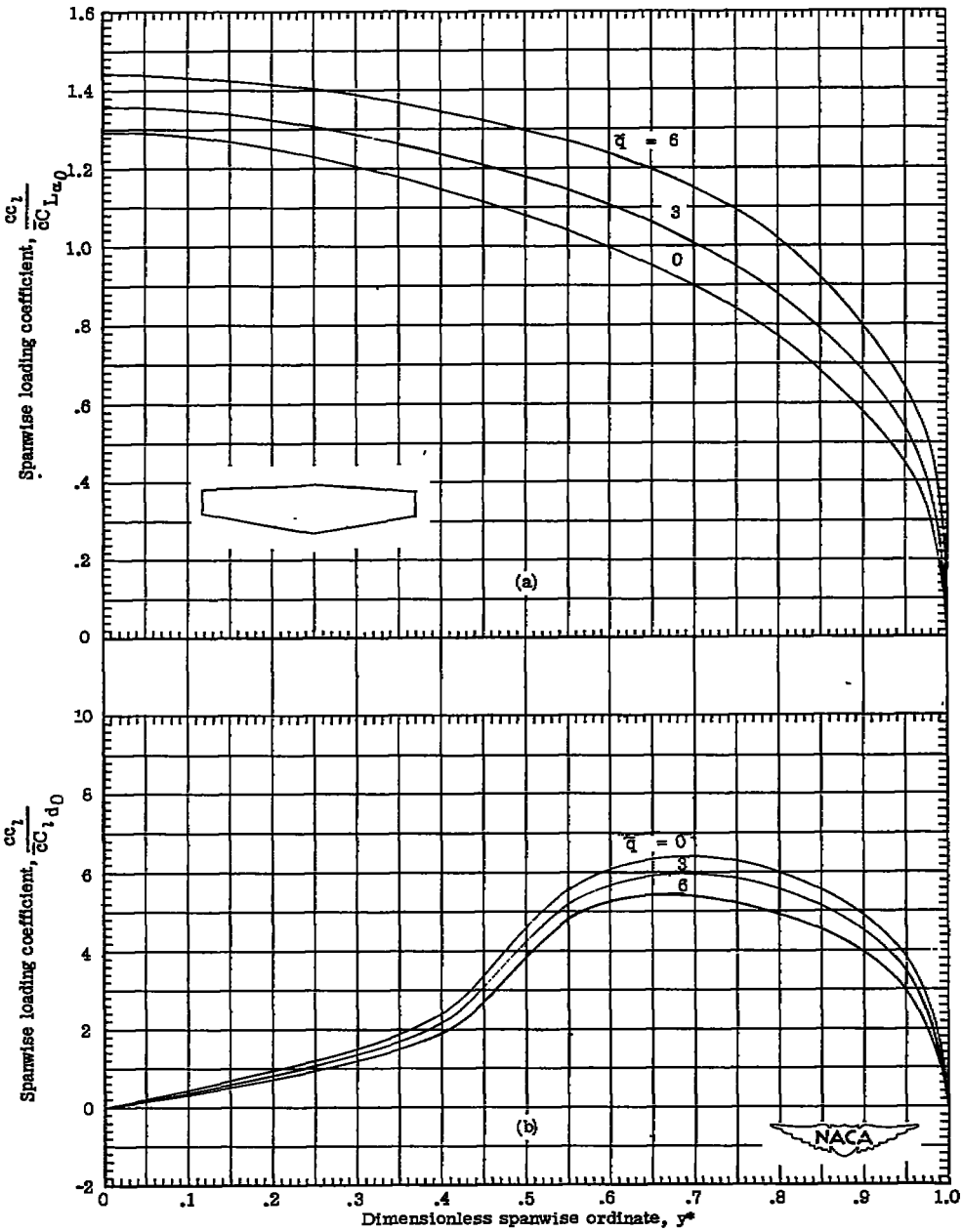

(a) Lift distributions due to unit airplane angle of attack (subsonic).

(b) Lift distributions due to unit effective aileron deflection (subsonic).

Figure 14.- Spanwise lift distributions for wing 11. (Unswept wing.)

[redacted]

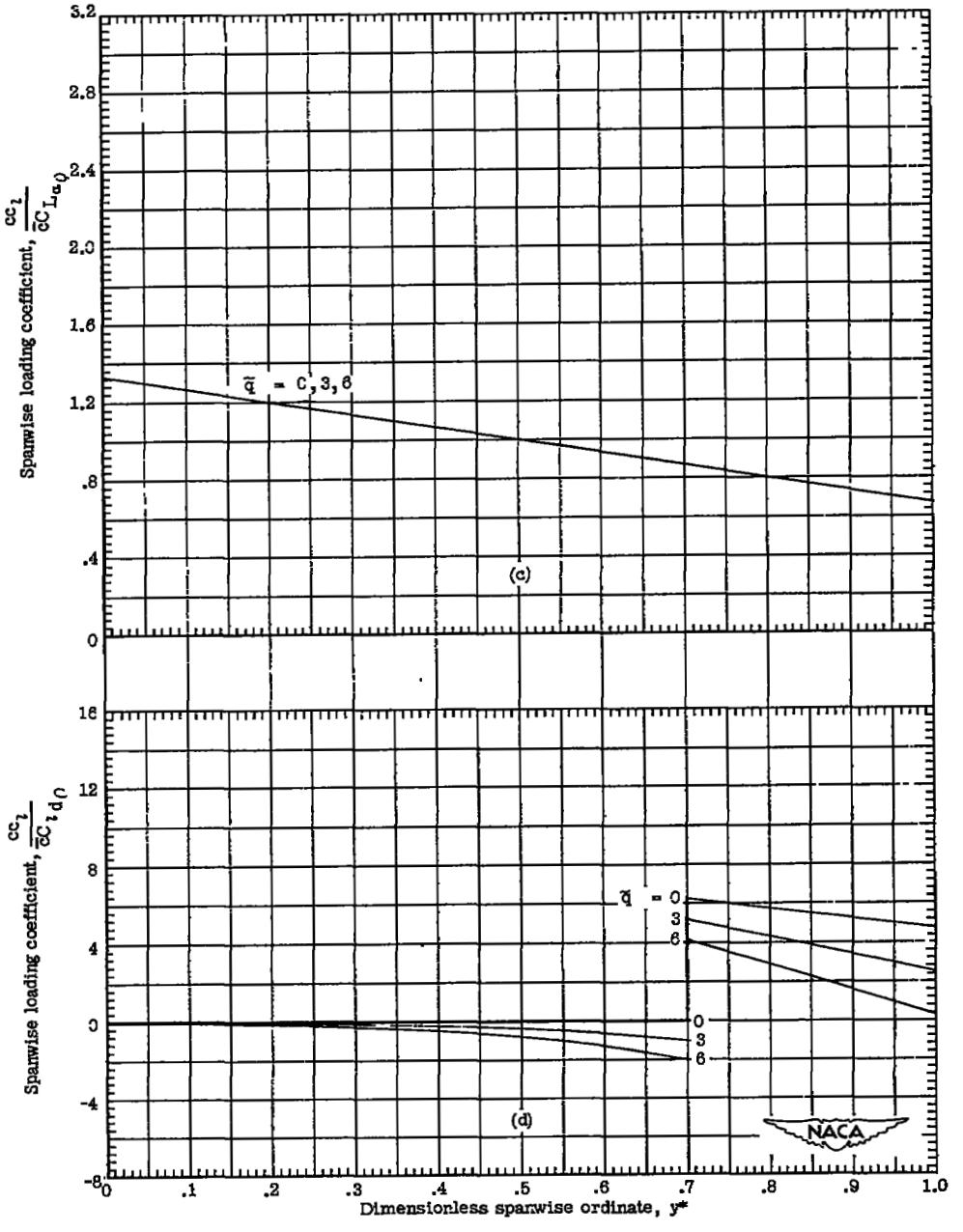

(c) Lift distributions due to unit airplane angle of attack (supersonic).

(d) Lift distributions due to unit effective aileron deflection (supersonic).

Figure 14.- Concluded.

[redacted]

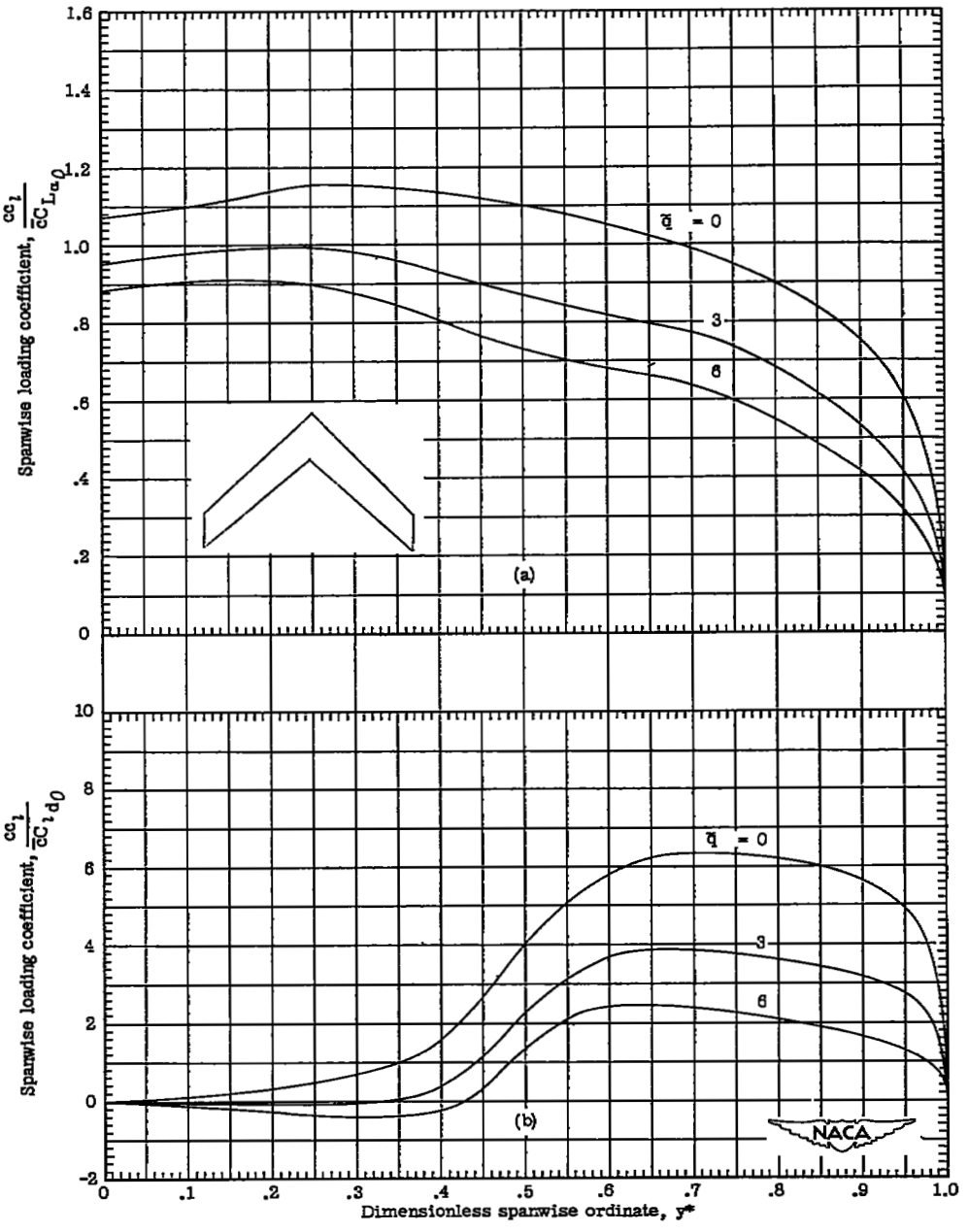

(a) Lift distributions due to unit airplane angle of attack (subsonic).

(b) Lift distributions due to unit effective aileron deflection (subsonic).

Figure 15.- Spanwise lift distributions for wing 12. (Sweptback wing.)

[redacted]

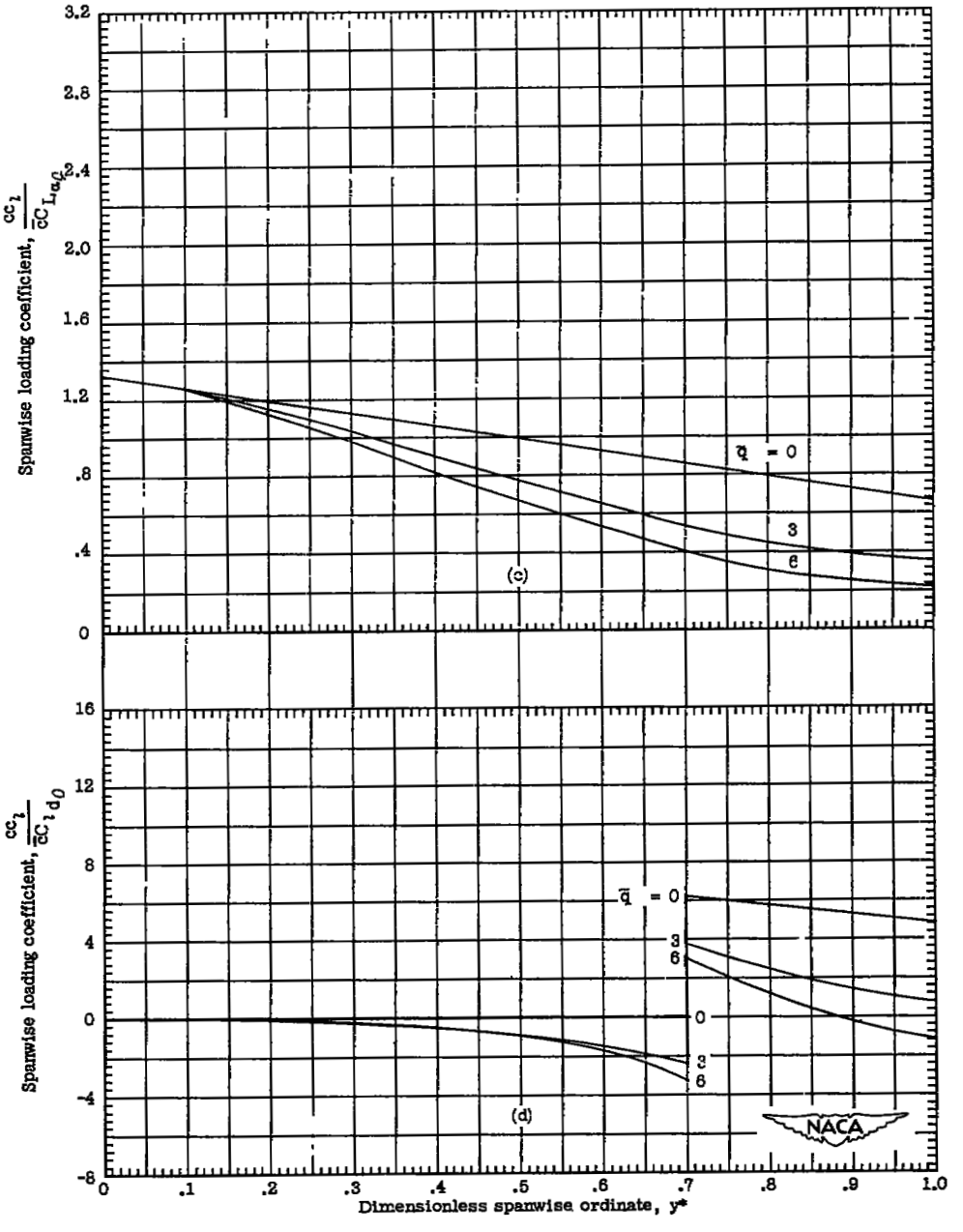

(c) Lift distributions due to unit airplane angle of attack (supersonic).

(d) Lift distributions due to unit effective aileron deflection (supersonic).

Figure 15.- Concluded.

[redacted]

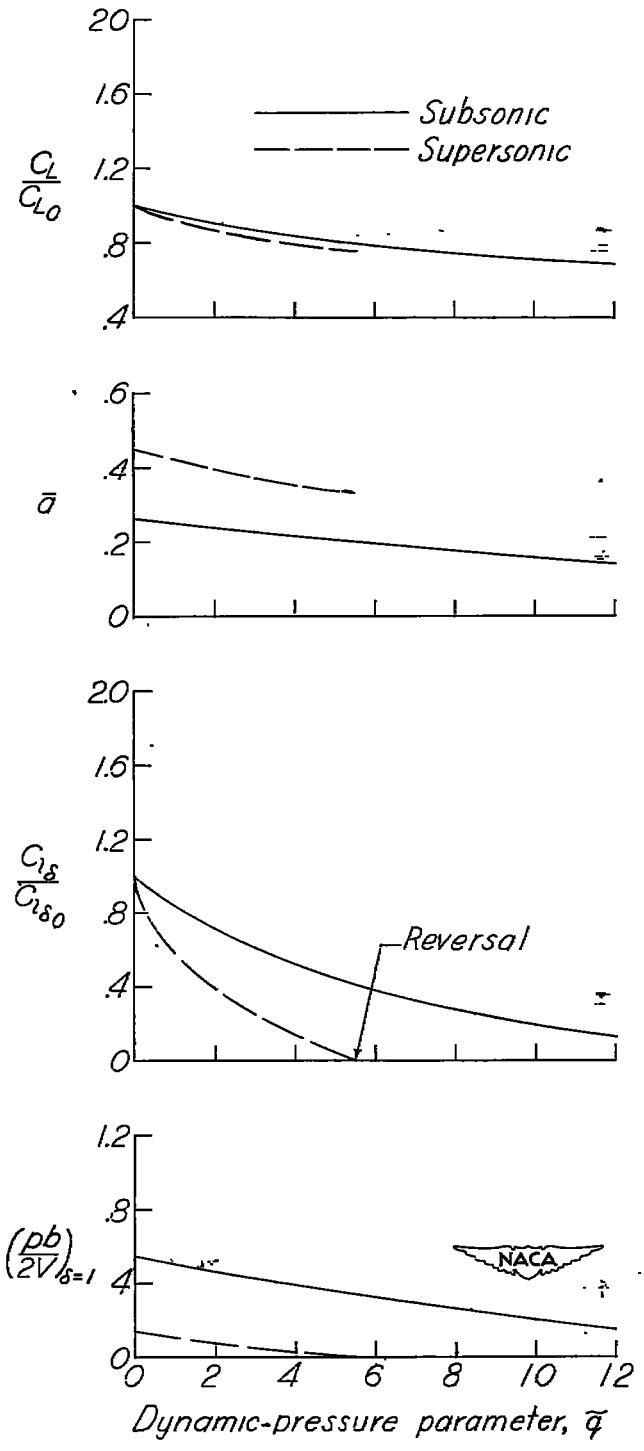

Figure 16.- Aeroelastic characteristics of wing 1. (M-wing; $y^*_B = 0.3$.)

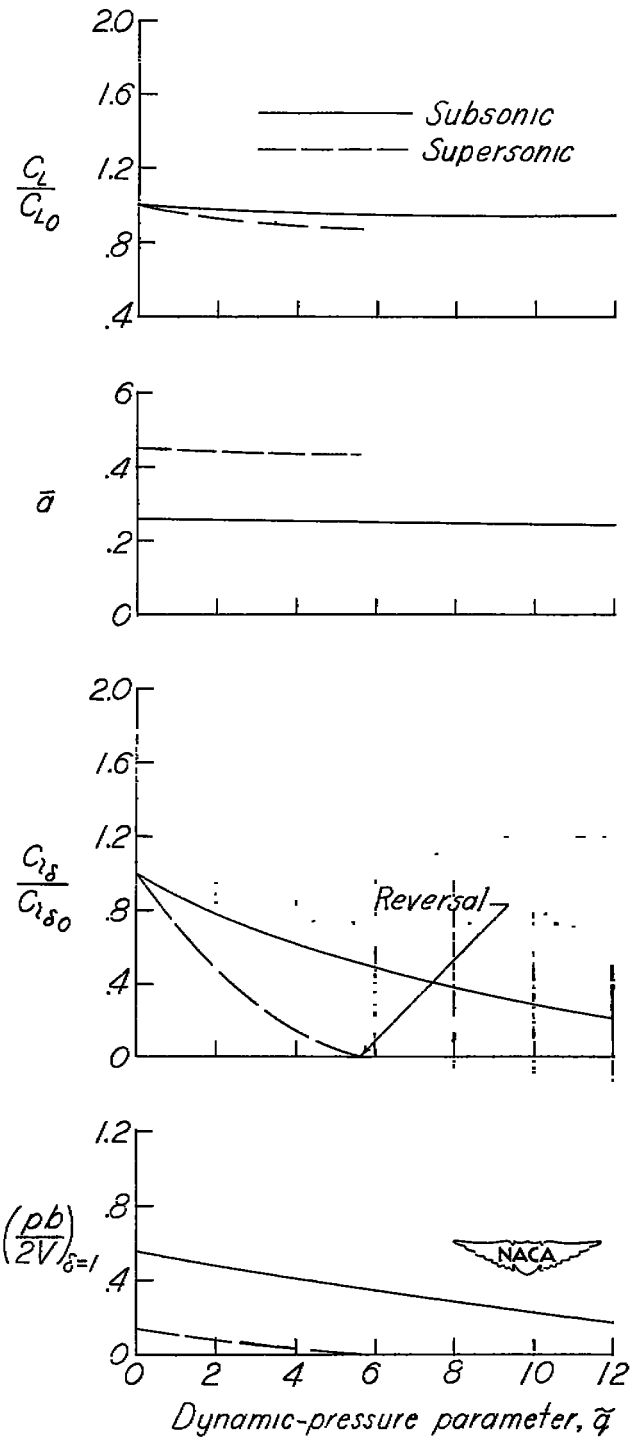

Figure 17.- Aeroelastic characteristics of wing 2. (M-wing; $y^*_B = 0.5$.)

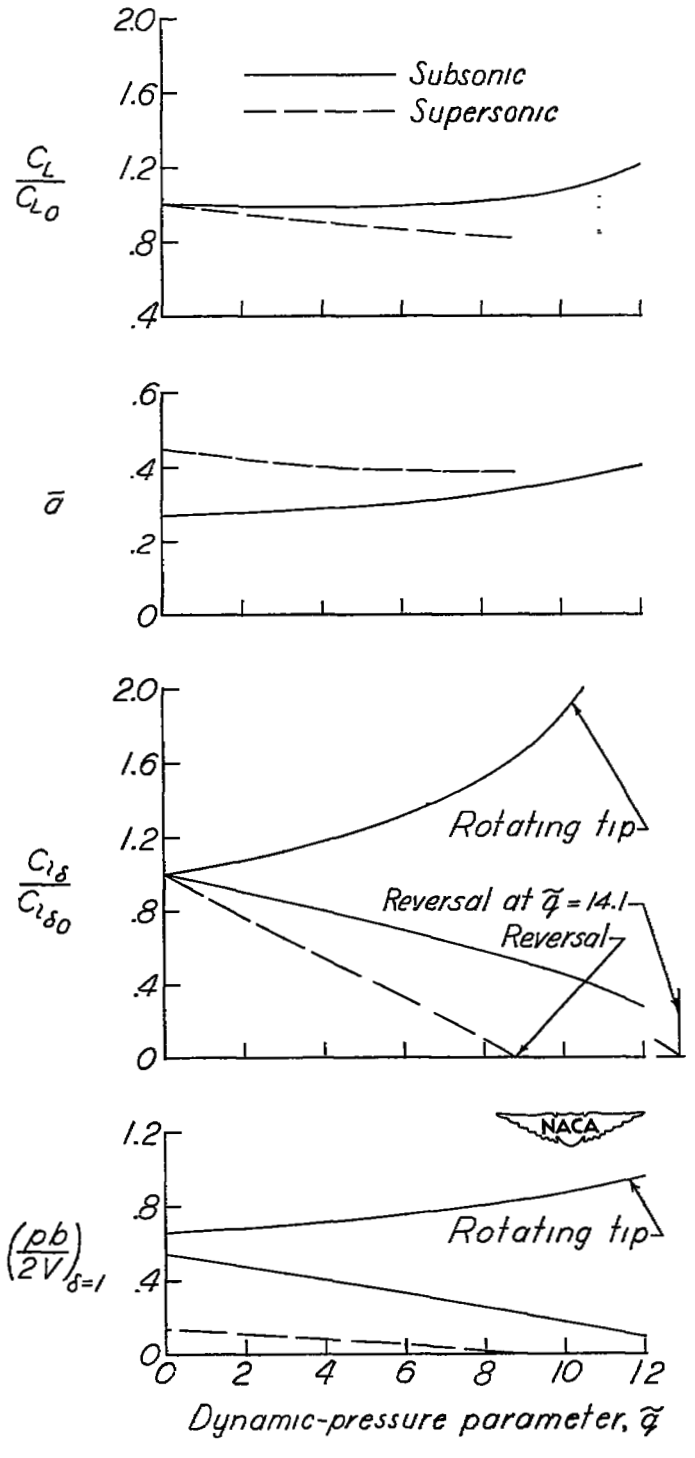

Figure 18.- Aeroelastic characteristics of wing 6. (W-wing; $y^*_B = 0.7$.)

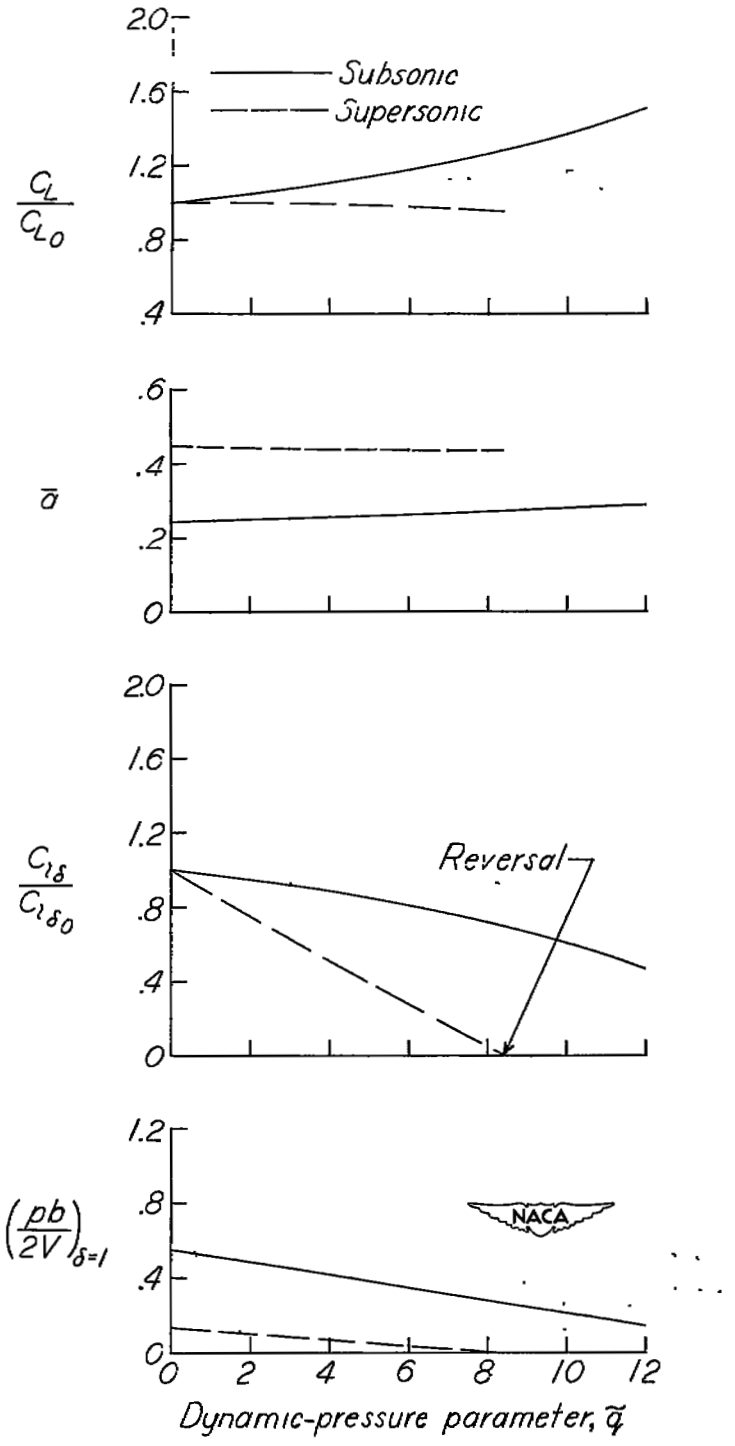

Figure 19.- Aeroelastic characteristics of wing 7. (Λ-wing; $y^*_B = 0.3$.)

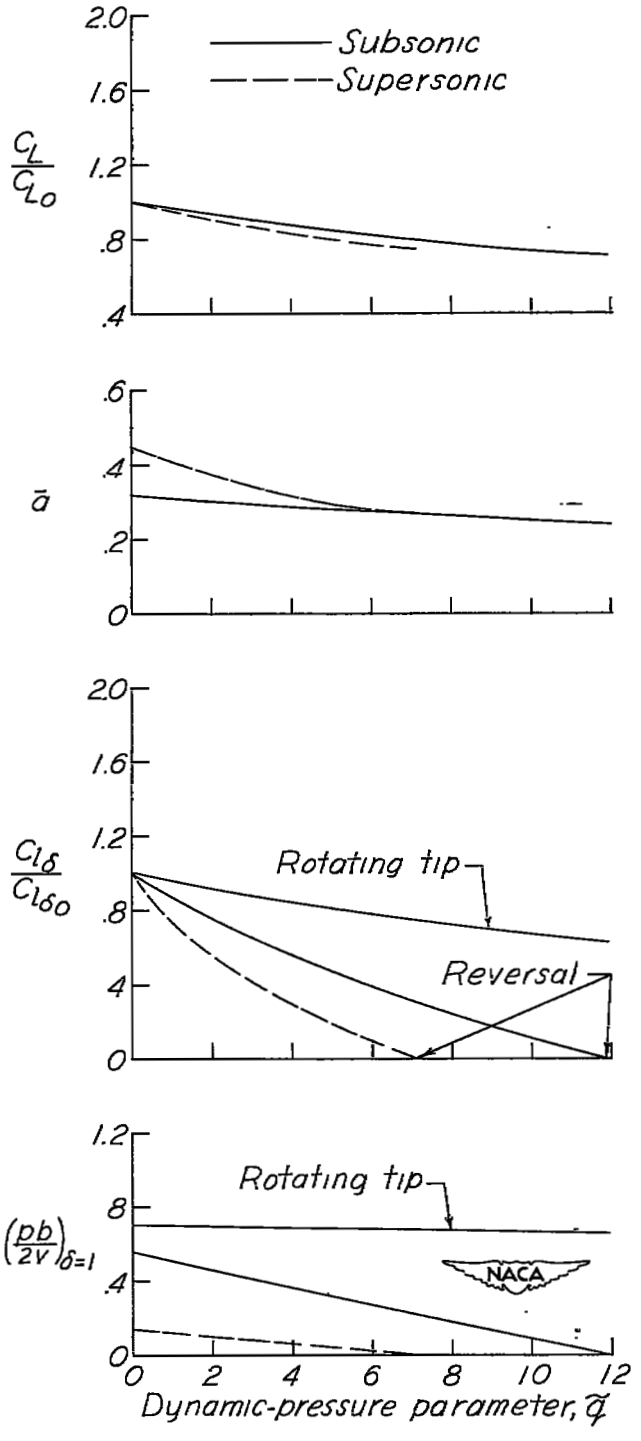

Figure 20.- Aeroelastic characteristics of wing 8. (Λ-wing; $y^*_B = 0.7$.)

[redacted]

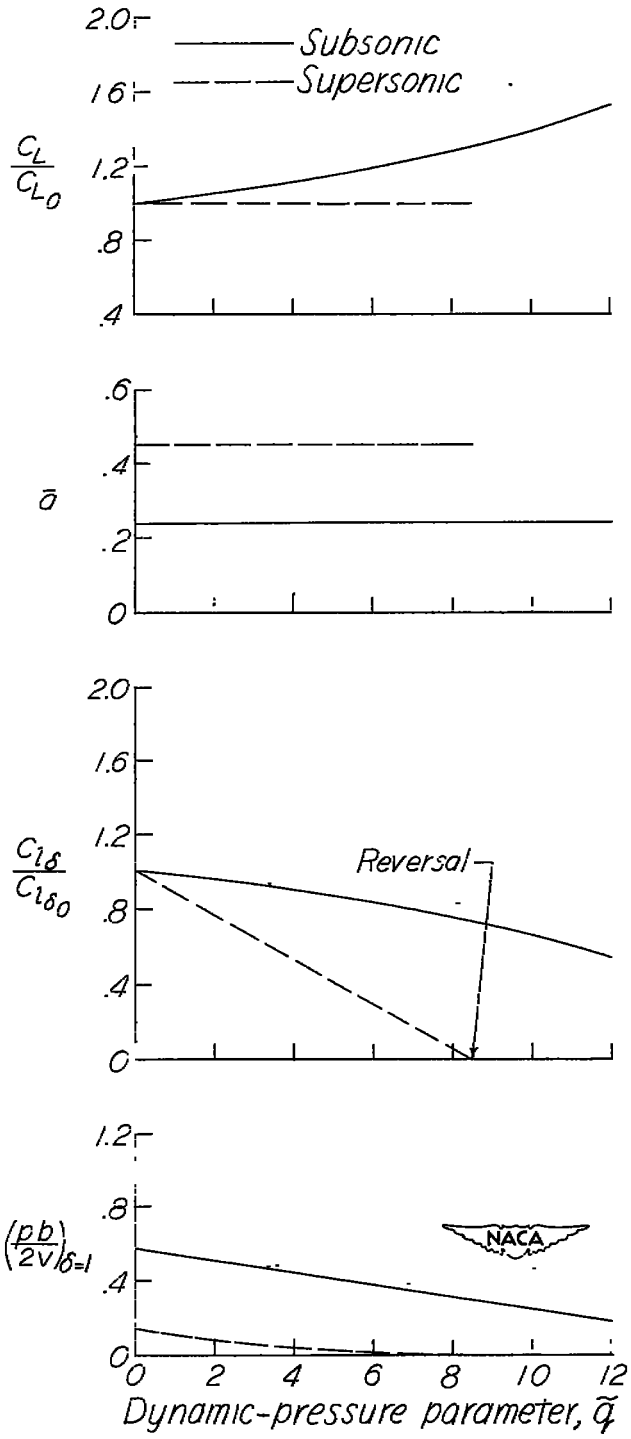

Figure 21.- Aeroelastic characteristics of wing 11. (Unswept wing.)

[redacted]

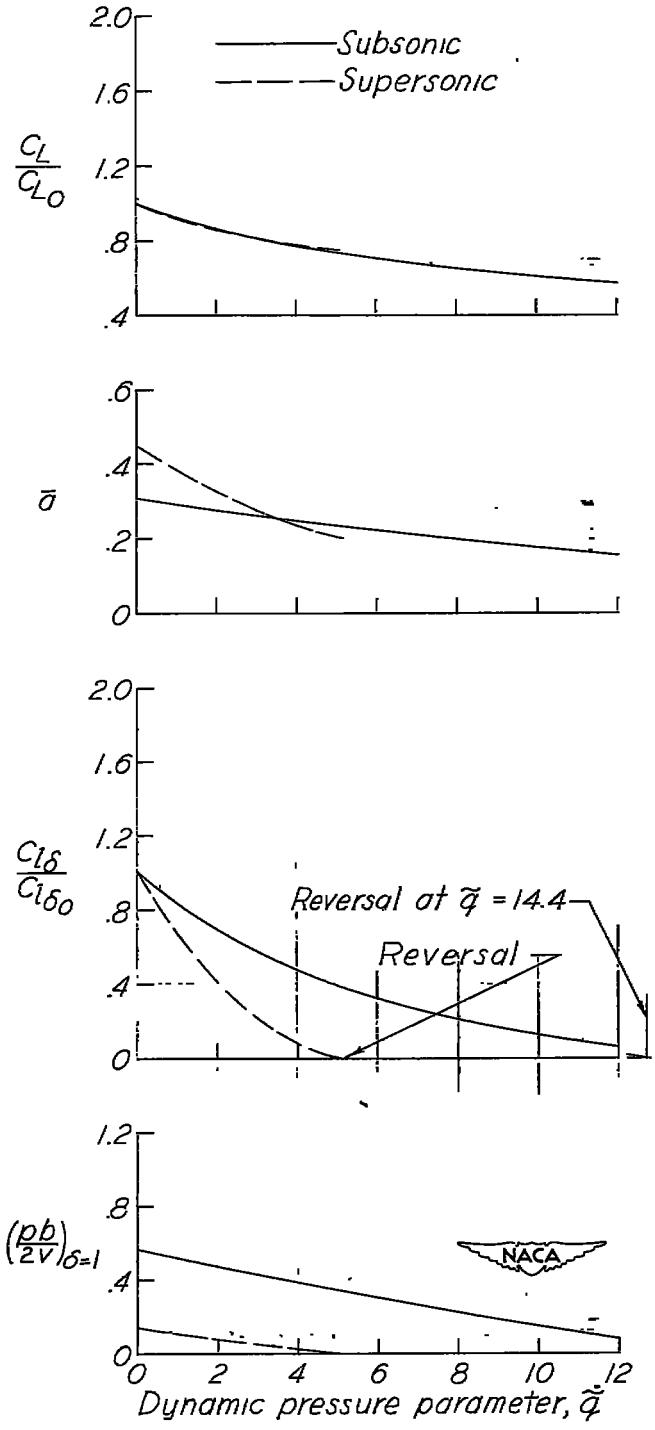

Figure 22.- Aeroelastic characteristics of wing 12. (Sweptback wing.)

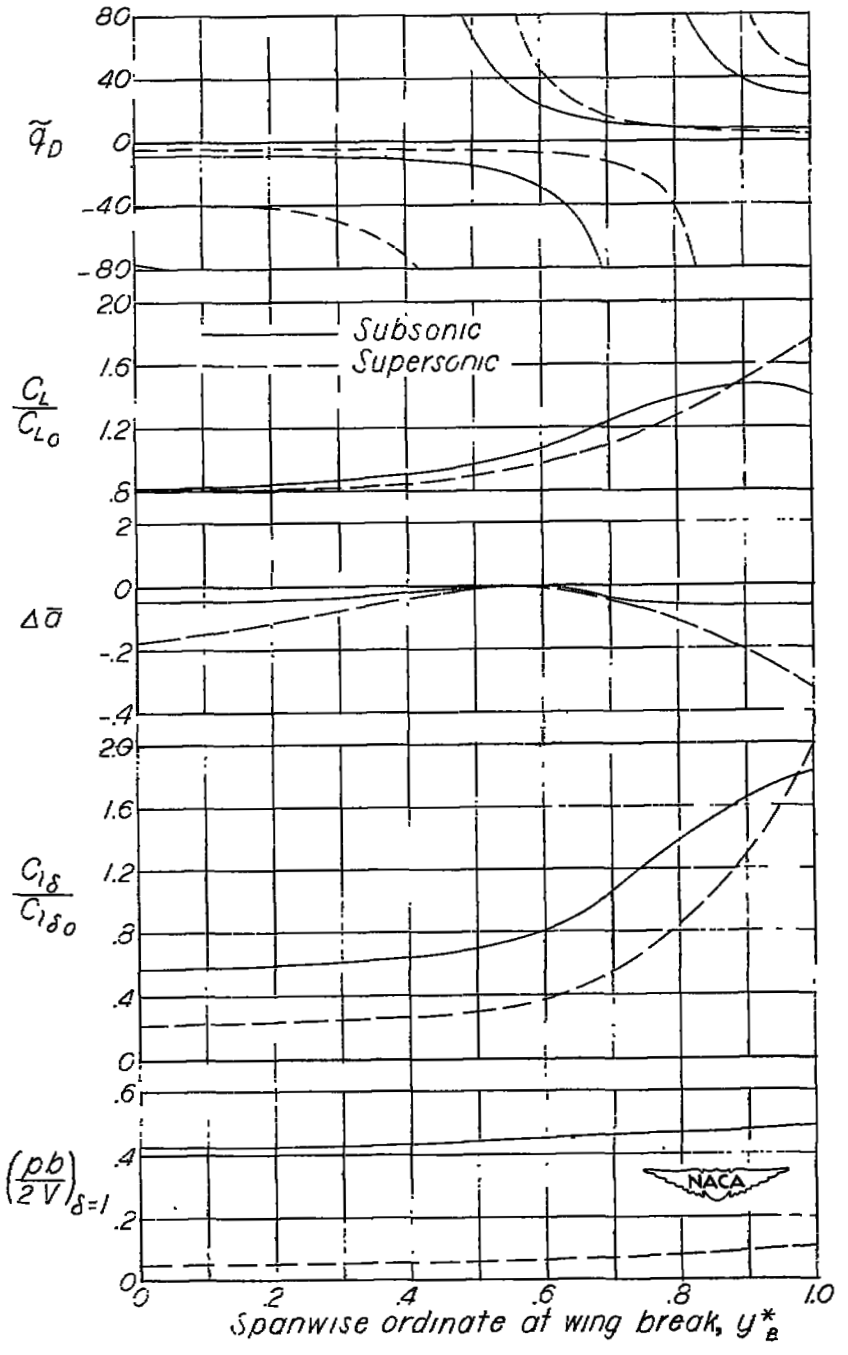

(a) M-wings.

Figure 23.- Variation of aeroelastic characteristics with wing break position; $\tilde{q}$ = 3.0.

[redacted]

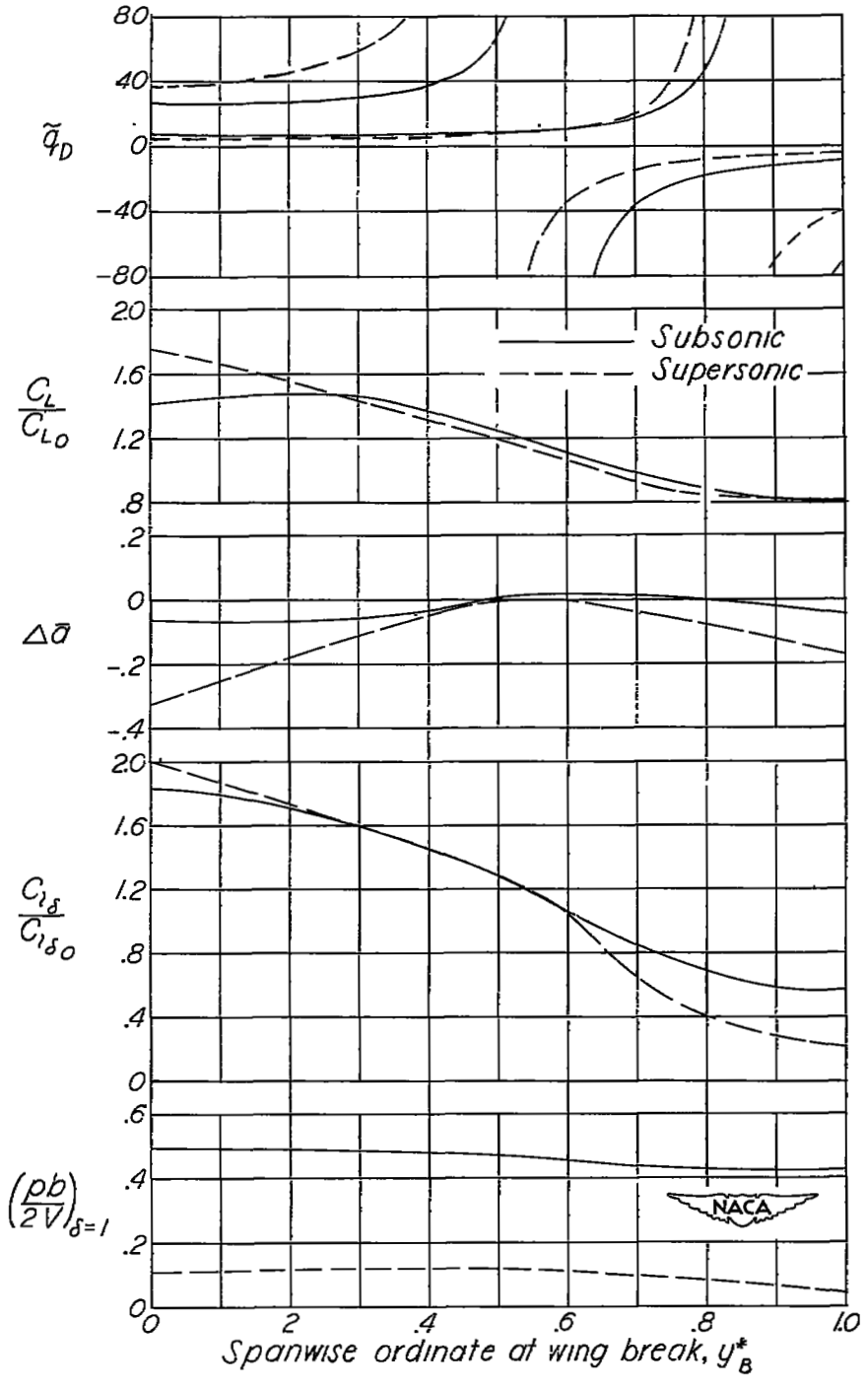

(b) W-wings.

Figure 23.- Continued.

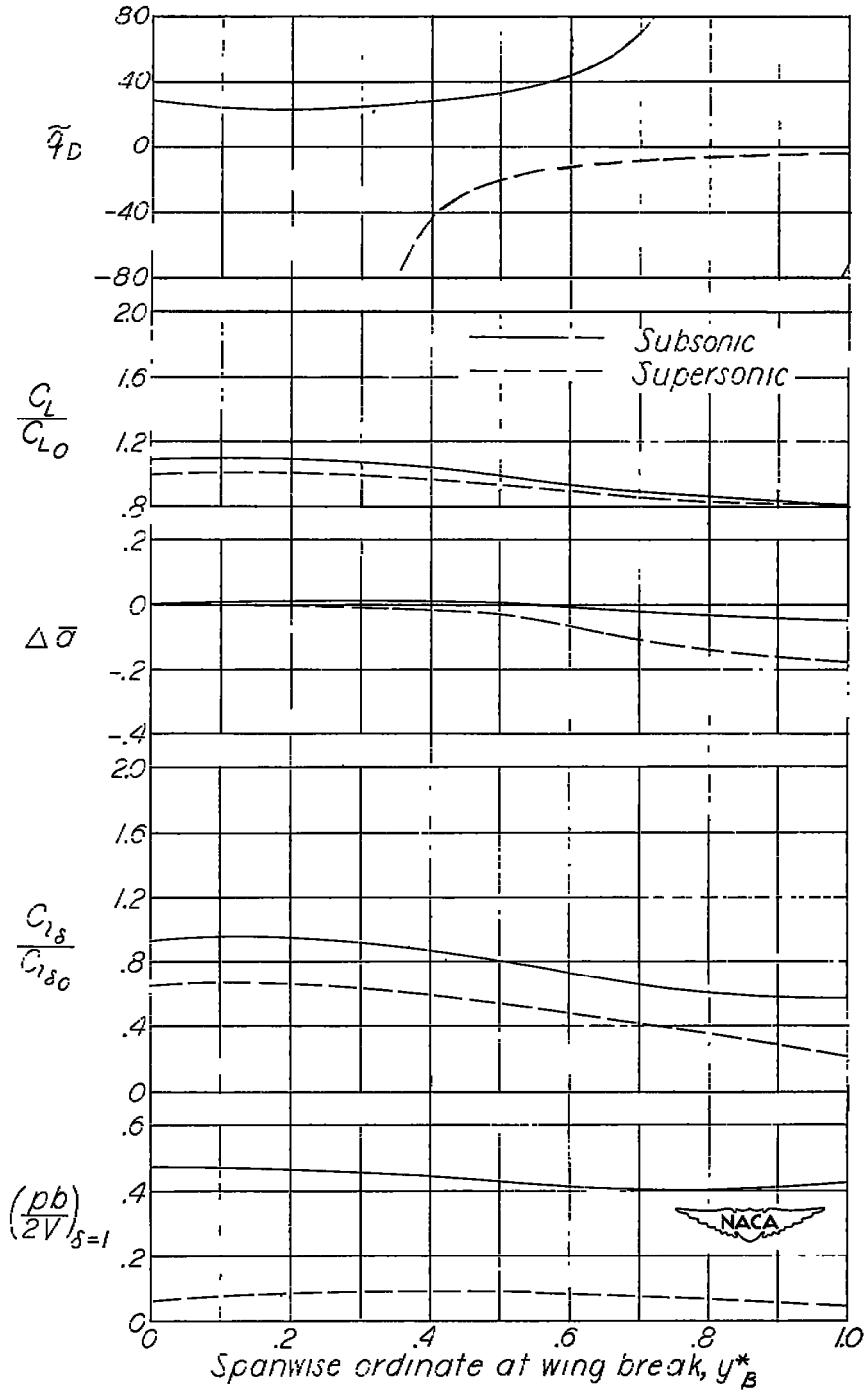

(c) Λ-wings.

Figure 23.- Concluded.

[redacted]

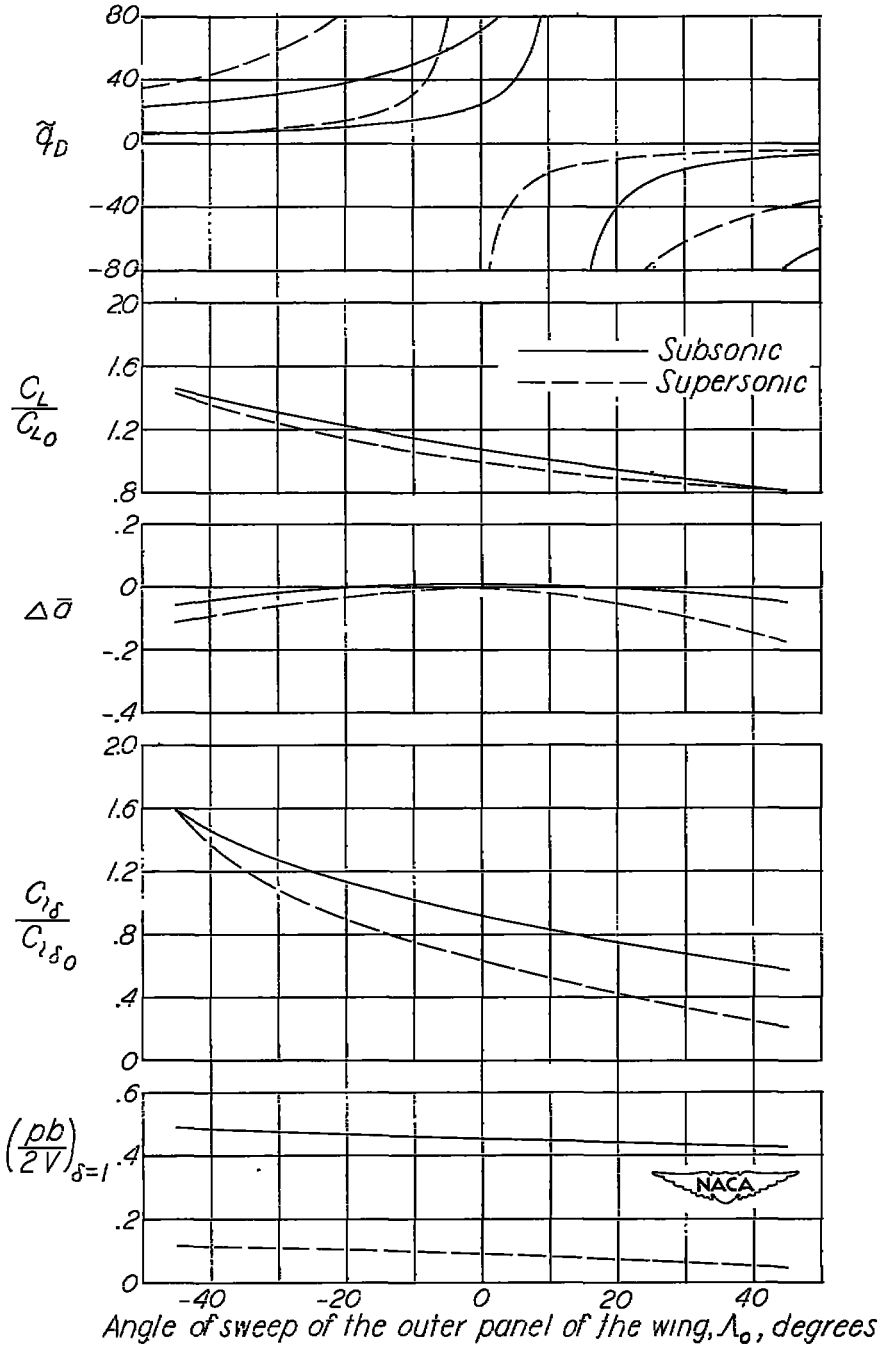

(a) $\Lambda_i = 45°$; $y^*_B = 0.3$.

Figure 24.- Variation of aeroelastic characteristics with sweep of outer wing panel.

[redacted]

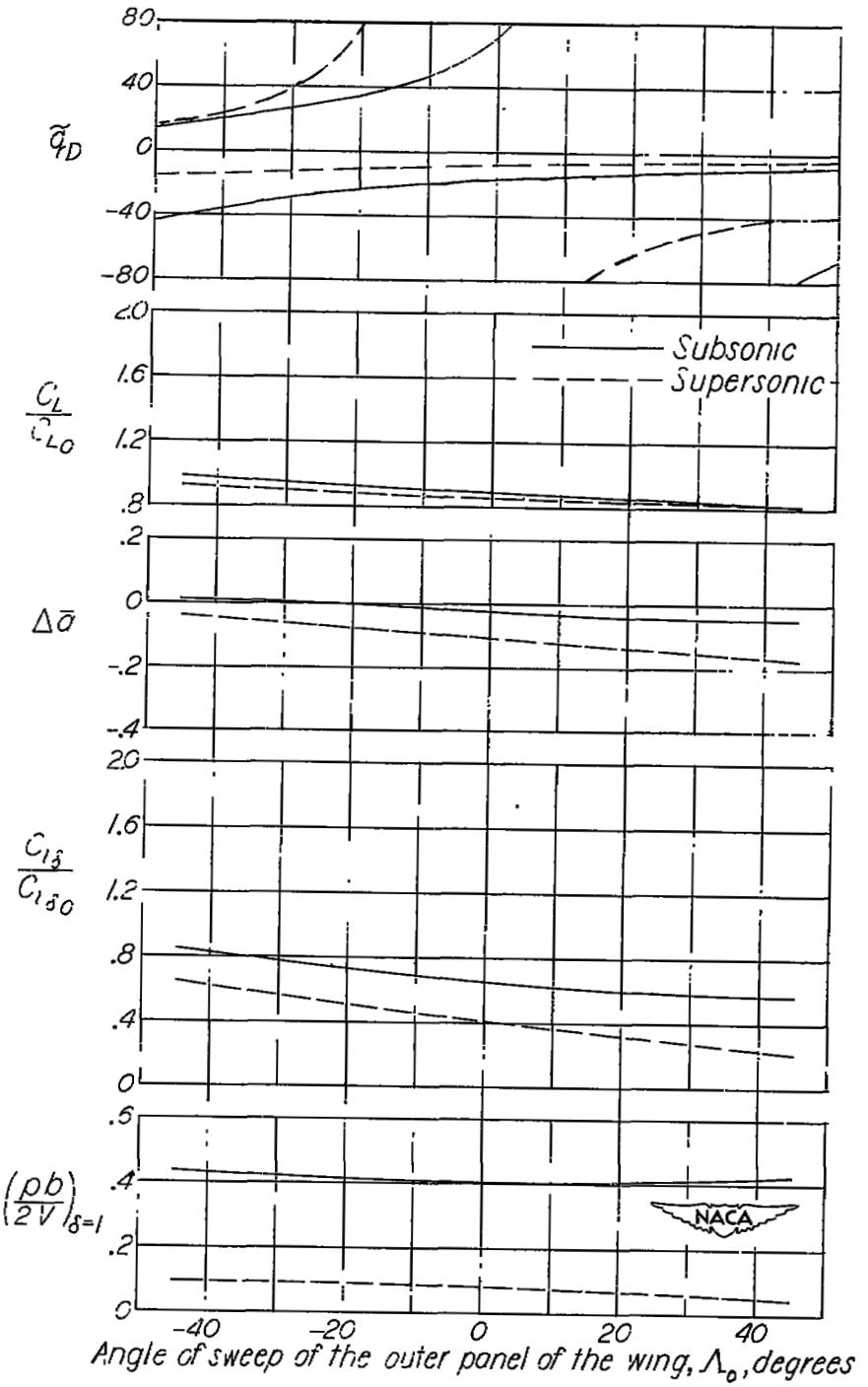

(b) $\Lambda_i = 45°$; $y^*_B = 0.7$

Figure 24.- Continued.

[redacted]

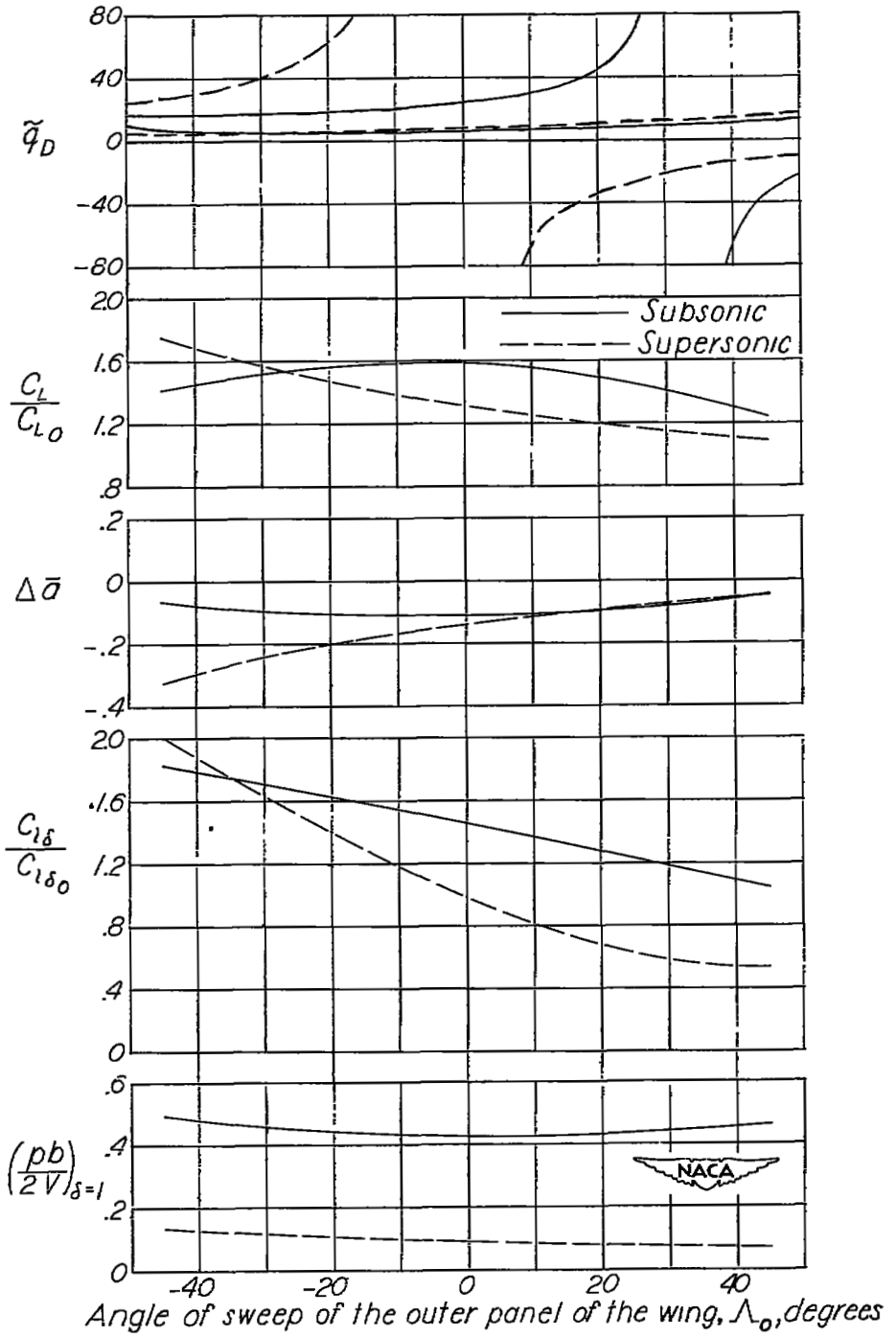

(c) $\Lambda_i = -45°$; $y^*_B = 0.7$.

Figure 24.- Concluded.

[redacted]

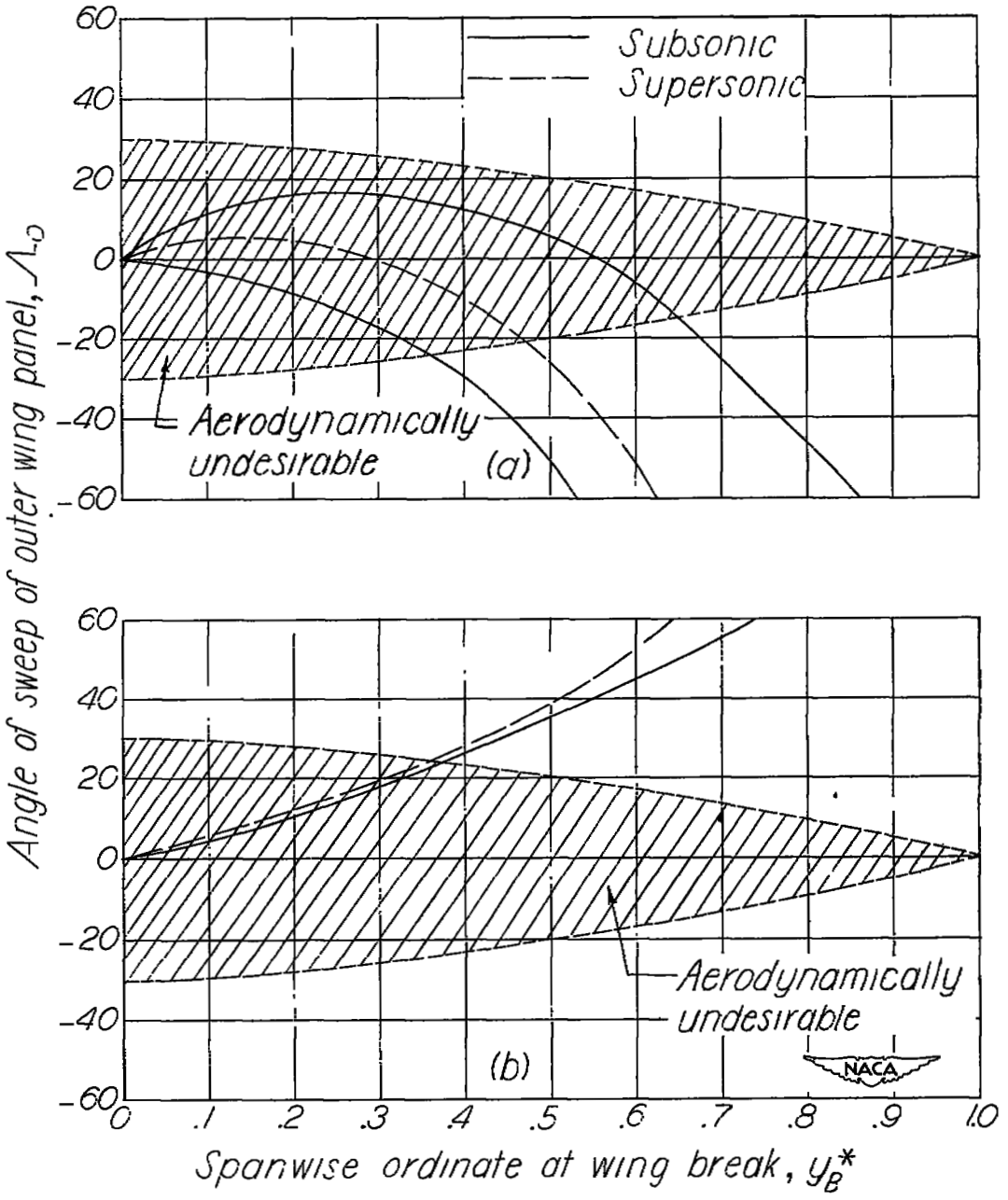

(a) Sweptback inner panel ($\Lambda_i = 45°$).

(b) Sweptforward inner panel ($\Lambda_i = -45°$).

Figure 25.- Combinations of Λ_o and y^*_B for wing configurations having zero aerodynamic-center shift ($\Delta\bar{\alpha} = 0$) at $\tilde{q} = 3.0$.

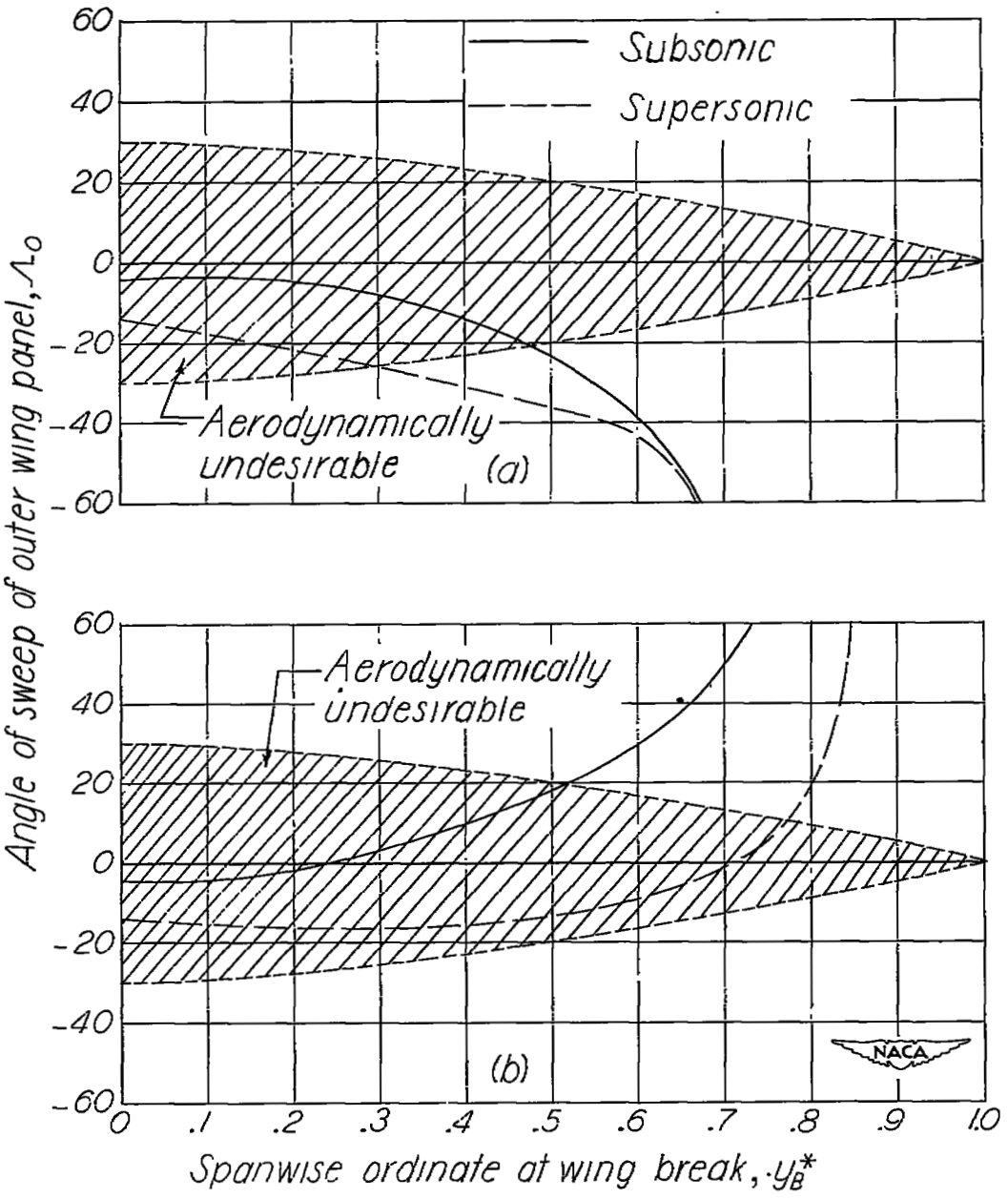

(a) Sweptback inner panel ($\Lambda_i = 45°$).

(b) Sweptforward inner panel ($\Lambda_i = -45°$).

Figure 26.- Combinations of Λ_o and y^*_B for wing configurations having no loss in lateral control $\left(C_{l_\delta} = C_{l_{\delta_o}}\right)$ at $\tilde{q} = 3.0$.

[redacted]